La cosa più bella che possiamo

sperimentare è il mistero,

è la fonte di ogni vera arte

*e di ogni vera scienza***.**

A.Einstein

UNIVERSITÀ DEGLI STUDI DI ROMA "TOR VERGATA"

FACOLTA' DI MEDICINA E CHIRURGIA

DOTTORATO DI RICERCA IN
SCIENZE E BIOTECNOLOGIE DELLA RIPRODUZIONE E DELLO SVILUPPO

CICLO DEL CORSO DI DOTTORATO XXII

A novel nuclear function for the centrosomal serine/threonine kinase Nek2

FEDERICA BARBAGALLO

A.A. 2009/2010

Docente Guida/Tutor: Prof. Claudio Sette

Coordinatore: Prof. Raffele Geremia

INDEX

CHAPTER I

THE SERINE-THREONINE KINASE NEK2

Structure and function of Nek2

Nek2 belongs to the evolutionary conserved family of homologues of the *Aspergillus nidulans* Never in Mitosis A (NIMA) kinase (Schultz et al., 1994). The NIMA family contains 11 mammalian genes (Nek1-11), which are differentially expressed during development and in different tissues of adult organisms (Letwin et al., 1992; Tanaka et Nigg, 1999; Chen et al., 1999; Arama et al., 1998; O'Regan et al., 2007). Nek2 is a centrosomal serine-threonine kinase highly enriched in male germ cells (Rhee & Wolgemuth, 1997). Nek2 displays constitutive catalytic activity, it is able to autophosphorylate, and it phosphorylates several substrates involved in cell cycle regulation (Fry, 2002). In human cultured cells Nek2 is predominantly expressed as two alternative splice variants, named Nek2A and Nek2B, that are differentially expressed during the cell cycle. Nek2B is constitutively expressed in the cell, whereas Nek2A expression and activity show a peak in S- and G2-phase and a decrease in mitosis (Hames RS & Fry AM., 2002). The differential expression is due to their distinct carboxyterminal region, where Nek2A contains a KEN box and a destruction box (D-box), lacking in Nek2B, required for recognition and degradation by the Anaphase Promoting Complex cyclosome (APC/C)-Cdc20 ubiquitin ligase-proteasome system in prometaphase (Hames et al., 2001) (Fig. 1). Recently, a third splice variant was identified by a yeast two hybrid screen using PP1γ1 and PP1γ2 as baits (Wu et al., 2007). This isoform is identical to Nek2A with the exception of a small internal deletion of 8 residues (Δ371-378) (Fig. 1). The deletion starts at the common splice donor (5'-splice site) position of Nek2A and Nek2B, but uses a cryptic downstream splice

acceptor site (3'-splice site) within exon 8. This variant, originally named Nek2A-T, as it was isolated from testicular mRNA, is now referred to as Nek2C because it is not exclusively expressed in testis. Although most biochemical features of Nek2C

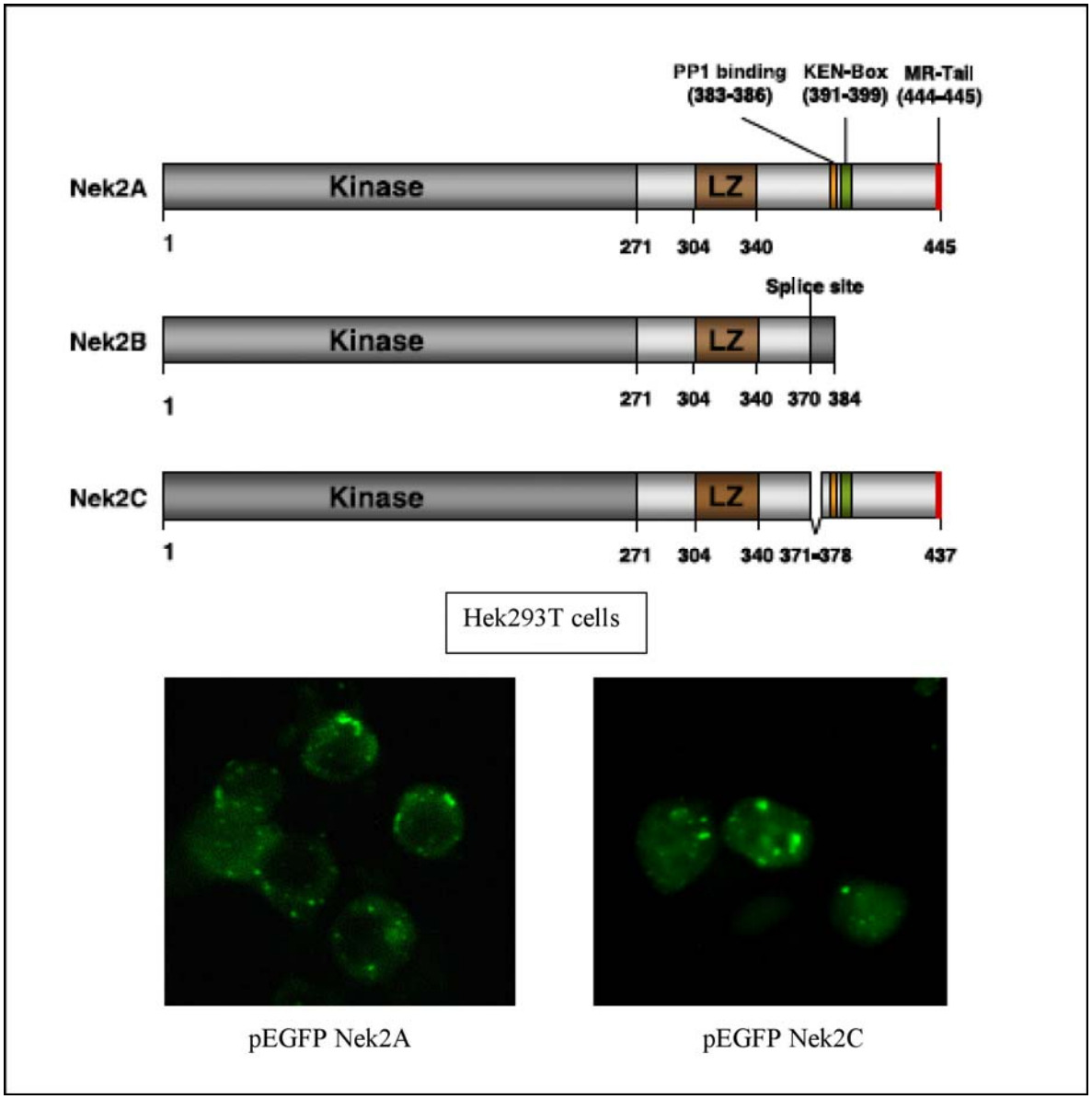

FIGURE 1. *Schematic representation of the Nek2A, Nek2B, and Nek2C proteins highlighting the positions of the catalytic domain (Kinase), leucine zipper motif (LZ), PP1 binding site, KEN-box, and MR-tail. Amino acids numbers are indicated underneath. HEK293T cell images, transfected with GFP Nek2A or GFP Nek2C, show the two variant different localization.*

are undistinguishable from Nek2A, deletion of the 8 amino acid-sequence creates a strong nuclear localization signal (NLS) that allows accumulation of Nek2C in the

nucleus (Fig. 1). Notably, this NLS is much weaker in Nek2A whereas it is absent in Nek2B (Wu et al., 2007).

Nek2A is the best characterized variant in terms of biochemical activity, structural features and biological functions. Nek2A is mainly localized in the cytoplasm, where it binds to microtubules and it is enriched on the centrosome (Fry et al., 1998a). Nek2A binds to C-Nap1, a protein required for centrosome cohesion in interphase (Mayor T., 2000; Fry et al., 1998b), and phosphorylation of C-Nap1 by Nek2A during the G2/M transition contributes to centrosome splitting (Fig.2) (Fry et al., 1998b). Nek2A also has a binding site for the catalytic subunit of PP1, and hyperactivation of Nek2A at the onset of mitosis appears to depend on inactivation of PP1 (Helps et al., 2000). In line with a crucial role of Nek2 in the centrosome cycle, it has been observed that up-regulation of this kinase in human cells causes premature splitting of this organelle (Fry et al., 1998a). On the other hand, overexpression of its kinase-dead derivative induces centrosome abnormalities that result in monopolar spindles and aneuploidy (Faragher & Fry AM., 2003). Hence, a tight regulation of Nek2 abundance and/or activity is essential to insure correct cell cycle progression.

Role of Nek2 in cancer

In support of its crucial role in the regulation of cell division, it has been recently described that Nek2 is overexpressed in both pre-invasive and invasive breast carcinomas (Hayward et al., 2004). These observations suggested that up-regulation of Nek2 is an early event in the neoplastic transformation of breast cells. Indeed, pharmacological inhibition of Nek2, as well as its depletion by RNAi, strongly reduced proliferation and invasiveness of breast cancer cells both in culture and in xenograft models (Wu et al., 2008; Tsunoda et al., 2009). Over-expression of Nek2 in non transformed breast epithelial cells induced centrosome over-duplication (Hayward et al.,

2004), whereas Nek2-dependent phosphorylation of Hec1 was required for correct chromosome segregation (Chen et al., 2002). Thus, it is likely that increased cellular levels of Nek2 directly contribute to generation of aneuploidy. Interestingly, Nek2 also interacts with and phosphorylates Mad2 and Cdc20, two regulators of the spindle check point, thereby enhancing their activity and spindle dynamics in the cell (Liu et al., 2009).

Up-regulation of NEK2 could be due to increased mRNA transcription or decreased protein degradation. In line with the former hypothesis, it has been shown that the transcription factor FoxM1 is upregulated in breast carcinomas and that *NEK2*, together with other genes involved in faithful chromosome segregation like *CENP-A* and *KIF20A*, are among its targets (Wonsey & Follettie, 2005). Moreover, increased Nek*2* transcript levels have been detected in various cancer samples and Nek2 expression levels were proposed to have prognostic value (Landi et al., 2008; Ma et al., 2008; Barbagallo et al., 2009).

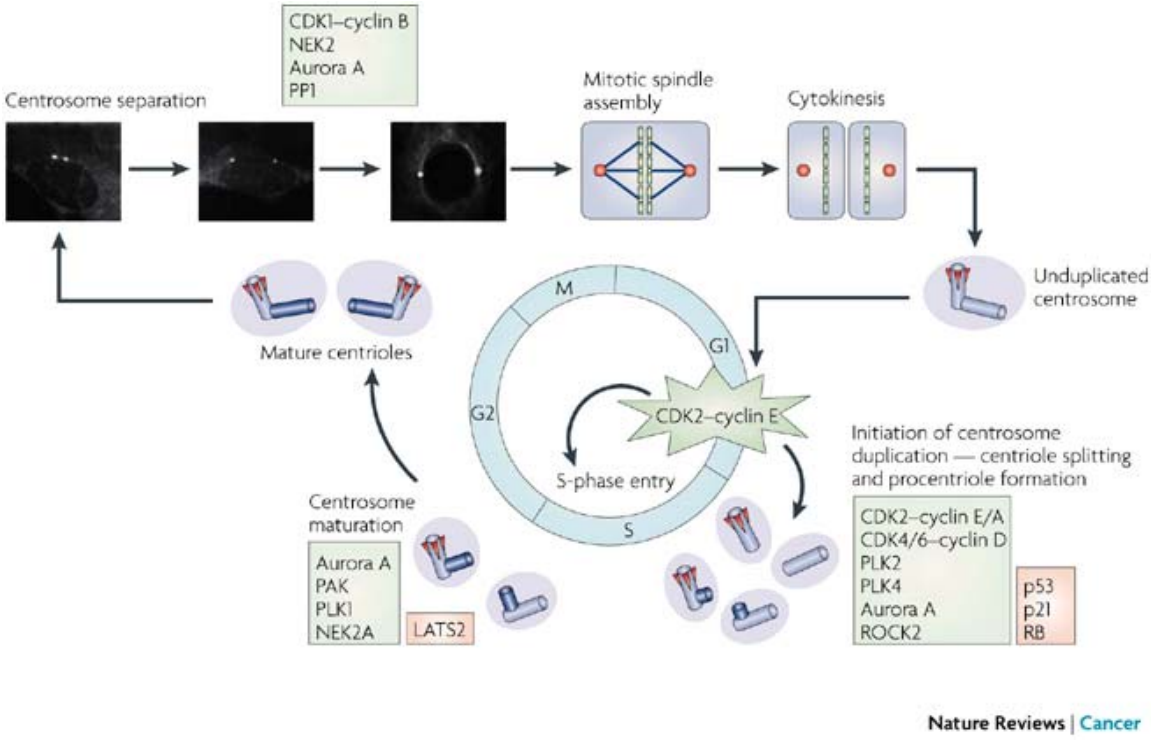

FIGURE 2. *Centrosome duplication begins with the physical splitting of the paired centrioles triggered by CDK2–cyclin E, followed by the formation of procentrioles near the proximal end of each pre-existing centriole. During S and G2 phases, procentrioles elongate, and two centrosomes progressively recruit pericentriolar material (centrosome maturation). In late G2, the daughter centriole of the parental pair acquires subdistal appendages (red wedges), and two mature centrosomes are generated. At late G2 before mitosis, two duplicated centrosomes separate and migrate to opposite ends of the cell (centrosome separation). During mitosis, duplicated centrosomes form spindle poles to direct the formation of bipolar mitotic spindles. On cytokinesis, each daughter cell receives one centrosome along with one half of the duplicated DNA. Some of the oncogenic kinases and phosphatases (green-shaded boxes) as well as tumour-suppressor proteins (red-shaded boxes) that have key roles in each stage of the centrosome duplication cycle are noted: NEK2, NIMA (never in mitosis gene A)-related kinase 2; PAK, p21-activated kinase; PLK, polo-like kinase.*

CHAPTER II

CENTROSOME AND CANCER

The centrosomal localization of Nek2 has suggested its possible involvement in cell cycle events that are aberrantly regulated in cancer. The centrosome is a cytoplasmic organelle strategically placed near the nucleus, where it serves as a nucleation center for microtubules in several phases of the cell cycle. This organelle is composed by two centrioles that are surrounded by a proteinaceus matrix named pericentriolar material. During interphase, the centrosome organizes arrays of microtubules that function as cables for the intracellular traffic of organelles and proteins. At mitosis, the centrosome organizes the spindle and is required for equal distribution of chromosomes between daughter cells (Badano et al., 2005; Nigg, 2001; Saunders, 2005).

In line with its essential role, centrosome duplication and splitting needs to be tightly controlled during the cell cycle (Fig.2) (Nigg, 2001). In the early G1 phase, each cell contains one centrosome and its duplication normally begins in S phase and terminates in G2, before the onset of cell division. During mitosis, the two centrosomes separate and pull in opposite directions to extend the mitotic spindle and maintain tension until all chromosomes are correctly assembled at the equatorial plate and anaphase can take place (Nigg, 2001). In addition to its role in microtubule dynamics, the centrosome serves as a scaffold to recruit many proteins involved in cell cycle related events, such as protein kinases, phosphatases and proteins involved in ubiquitin-proteasome driven protein degradation (Badano et al., 2005; Nigg, 2001; Saunders, 2005).

Several serine-threonine kinases, like cyclinB/cdc2, Polo-like kinase, Aurora A and Nek2, associate with the centrosome during cell cycle progression and regulate the

centrosome cycle and spindle assembly in order to tightly link M-phase progression with chromosome segregation (Nigg, 2001). These kinases are normally ubiquitinated by the APC/C-proteasome system after eliciting their function in mitosis (Nigg, 2001; Barr et al., 2004; Meraldi et al., 2004). However, deregulated expression or hyper-activation of Polo-like kinase, Aurora A and Nek2 has been reported in several neoplastic tissues and it was shown to cause mis-regulation of the centrosome cycle and aneuploidy (Fig.3) (Barr et al., 2004; Meraldi et al., 2004; Hayward et al., 2004). Such abnormalities in centrosome numbers and aneuploidy are a common feature of many human cancer cells, such as breast, prostate, colon, liver and testicular cancers (Mayer et al., 2003; Badano et al., 2005; Saunders, 2005). Moreover, centrosome overduplication can represent an early event in the development of some tumours (D'Assoro et al., 2002; Mayer et al., 2003). In particular, centrosome abnormalities

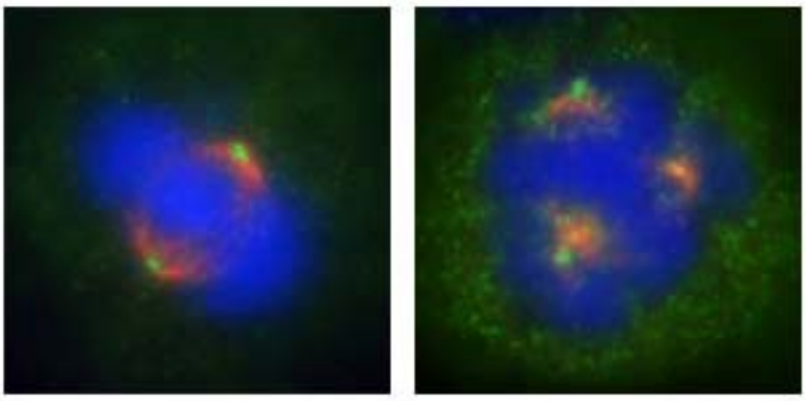

FIGURE 3. *Cells with multiple centrosome form multipolar spindles. left: bipolar mitosis; right: multipolar mitosis*.

appear to play a driving role in testicular germ cells tumours (TGCTs). In this type of tumours, centrosome amplification is often found before neoplastic transformation and it correlates with the earliest steps of tumour development (Mayer et al., 2003). However, the molecular mechanisms that lead to centrosome amplification in TGCTs

are still unknown (Mayer et al., 2003) and investigating the expression of centrosomal kinases in this type of neoplasia could help to unravel the causes of aneuploidy in the early steps of testicular germ cell tumours.

CHAPTER III

TESTICULAR GERM-CELL TUMOURS

Human germ-cell tumours (GCTs) are a heterogeneous group of neoplasms. They develop in the gonads as well as in extragonadal sites along the midline of the body, including the brain (Oosterhuis and Looijenga, 2005). When they develop in the testis, GCTs are named testicular germ cell tumours (TGCTs). It has been suggested that the initiating events in the pathogenenis of TGCTs occur during embryonic development (Chieffi, 2007). TGCTs are classified as seminomatous (SE) and non-seminomatous (NSE) tumours. Distinction between prepuberal TGCTs, represented by Yolk Sac Tumors (YSTs) and teratomas, and postpuberal TGCTs seems to have a great prognostic relevance (Chaganti & Houldsworth, 2000; Ulbright, 1993). Postpuberal TGCTs are the most frequent solid malignant tumours in young men (20-40 years of age), accounting for up to 60% of all malignancies diagnosed in this age group. Despite a high-cure rate, they still represent the most frequent cause of death from solid tumours in young men (Oosterhuis & Looijenga, 2005). SE-TGCTs are radio- and chemo-sensitive tumours, virtually completely curable (Jones & Vasey, 2003). NSE-TGCTs are usually treated with surgery and chemoterapy, with different outcomes depending on the disease stage (Shelley et al., 2002). The cure rate reaches up to 99% in the early stage of the disease. However, this rate decreases to 90% in patients with advanced tumours displaying good prognosis and it drops to 50% in patients with poor prognostic features (Shelley et al., 2002).

The rapid growth and progression of postpuberal TGCTs cause early metastases in lymphnodes and/or distant districts. At the time of diagnosis about of 25% of SE patients and up to 60% of the NSE patients suffers of metastatic lesions and are

refractory to standard therapies (Peckham, 1988; Classen et al., 2001; Al Ghamdi & Jewett, 2005), posing a clinical problem for long-term survival.

Classification of GCTs

The classification systems commonly used are three: a) the British Classification System (BCS), which recognizes all nonseminoma histotypes as teratoma at different stage of differentiation; b) the World Health Classification (WHO), which recapitulates the classical histological entites as seminoma and nonseminoma hystotype; c) a novel classification system that recognizes five entities based on various parameters including cell of origin, histology, genomic imprinting status and chromosomal constitution (Looijenga, & Oosterhuis, 1999).

According to this last classification, Type I is represented by testicular teratomas and YSTs of prepuberal age, type II by postpuberal SE and NSE, type III by spermatocytic seminomas tipically seen only in older patients. The last two groups, dermoid cysts (Type IV) and hydatiform moles (Type V) (see Table 1), are not found in testis.

Type I GCTs

Type I teratomas and Yolk-sac tumour occurs in the ovaries and testes, the sacrococcygeal and retroperitoneal regions, the head and neck, in the pineal and hypothalamic region of the brain. Their incidence is about 0,12 per 100.000, and it has not increased in the last decades. Sacral teratomas are the most frequent, occurring predominantly in newborn females. Clinically, the type I teratomas that occur in sites other than the ovary are virtually all benign, but they can progress to yolk-sac tumours when incompletely removed by surgery. At this advanced stage, these tumours have the potential to metastasize and must be treated by chemotherapy.

Type	Anatomical site	Phenotype	Age	Originating cell	Genomic imprinting	Genotype
I	Testis, ovary, sacral region, retroperitoneum, mediastinum, neck, midline brain	(Immature) Teratoma/ yolk-sac tumour	Neonates and children	Early PGC/ gonocytes	Biparental, partially erased	Diploid (Teratoma). Aneuploid (yolk-sac tumour): + of 1q, 12(p13) and 20q, and loss of 1p, 4, and 6q
II	Testis	Seminoma/ nonseminoma	>15 years (median age 35 and 25 years)	PGC/gonocyte	Erased	Aneuploid (± triploid): + of X, 7, 8, 12p, and 21; loss of Y, 1p, 11, 13, and 18
	Ovary	Dysgerminoma/ nonseminoma	>4 years	PGC/gonocyte	Erased	Aneuploid
	Dysgenetic gonad	Dysgerminoma/ nonseminoma	Congenital	PGC/gonocyte	Erased	Diploid/tetraploid
	Anterior mediastinum	Seminoma/ nonseminoma	Adolescent	PGC/gonocyte	Erased	Diploid/tri-tetraploid
	Midline brain	Germinoma/ nonseminoma	Children (median age 13 years)	PGC/gonocyte	Erased	Diploid/tri-tetraploid
III	Testis	Spermatocytic seminoma	Children/Adults	Spermatogonium/ spermatocyte	Partially complete paternal	Aneuploid: + of 9
IV	Ovary	Dermoid cyst	>50 years	Oogonia/oocite	Partially complete maternal	(Near) Diploid, diploid/ tetraploid, peritriploid (+ of X, 7, 12, and 15)
V	Placenta, uterus	Hydatiform mole	Fertile period	Empty ovum/ spermatozoa	Completely paternal	Diploid (XX and XY)

Note: The classification of TGCTs is based on Looijenga and Oosterhuis (1999).

TABLE 1. Classification of TGCTs (Chieffi et al., 2009)

Type II GCTs

Type II GCTs are histologically and clinically subdivided into seminomatous GCTs (called seminomas when occurring in the testis, dysgerminomas when occurring in the ovary or in dysgenetic gonads) and non-seminomatous GCTs. Type II GCTs occur mainly in the gonads, particularly in the testis (referred to as TGCTs). Seminomas are homogeneous lesions in which the tumour cells have characteristics of embryonic germ cells. By contrast, non-seminomas can be highly heterogeneous, representing the different lineages of differentiation: endoderm, mesoderm, and ectoderm. Therefore, these tumours cannot be classified as carcinomas, because they represent a unique category, with specific characteristics of embryonic (germ) cells (Oosterhuis & Looijenga, 2005).

In the male Caucasian population, type II GCTs are the most frequent testicular

tumours accounting for approximately 1% of all cancers in males of this ethnic background. Interestingly, they account for up to 60% of all malignancies diagnosed in men between 20 and 40 years of age. In spite of intra-European heterogeneity, most countries show a significant rise in the incidence of TGCTs. In Denmark and Switzerland, for example, the lifetime risk of developing a TGCT is up to 1%. Black populations have a significantly lower risk, which does not increase with age, with a similar histology and age distribution. Overall, about 50% of TGCTs are seminomas and 40% non-seminomas; the rest are those containing both components. The median age of patients affected by seminomas is 10 year-higher than that of patients with a non-seminoma (35 years versus 25 years), while the combined tumours are present in patients at an intermediate median age. Therefore, in contrast to most solid human cancers, TGCTs have a peak incidence at the adolescent and young adult age. Human type II GCTs are also different from other solid cancers of adults for their biological features and clinical behaviour. These malignancies can contain all cell lineages, both somatic and extra-embryonic, including the germ cell lineage.

Type III GCTs: the spermatocytic seminomas

The incidence of spermatocytic seminoma is about 0.20 per 100,000, without a clear rise during recent decades. This exclusively testicular tumour, which is bilateral in 5% of cases, occurs predominantly in patients who are over 50 years of age. Spermatocytic seminomas are, for all practical purposes, benign tumours that can be cured by orchidectomy. As an exceptionally rare event, they can progress to give rise to sarcomas. Reports on metastatic spermatocytic seminomas have to be considered with caution because of the pitfall of misdiagnosis as seminoma (Oosterhuis & Looijenga, 2005)

Markers of TGCTs

The most widely accepted model of postpuberal TGCTs development propose an inital tumorigenic events *in utero* and the development of a precursor lesion known as intratubular germ cell neolpasia undifferentiated (ITGCNU) also known as carcinoma *in situ* (CIS) (Skakkebaek, 1972). This is followed by a period of dormancy until after puberty when postpuberal TGCTs emerge. Recently, it has been proposed that these tumours originate from neoplastic cells retaining stem cells properties, such as self–renewal (Wicha et al., 2006). According to the "stem cell" hypothesis, tumours would originate from tissue stem cells or from their immediate progeny. This cellular component drives tumorigenesis and aberrant differentiation, contributing to cellular heterogeneity of the tumour. Thus, preinvasive ITGCNU cells are supposed to be able to develop in different germinal and somatic tissues and are regarded as pluripotent or totipotent cells and, therefore, can be considered as TGCTs stem cells (Wicha et al., 2006).

ITGCNU cells share morphological similarities with gonocytes and it has been proposed that they could be remnants of undifferentiated embryonic/fetal germ cells (Nielsen et al., 1974; Skakkebaek et al., 1987). The embryonic origin is also supported by immunohistochemical studies of proteins present in ITGCNU, also shown to be present in primordial germ cells (PGCs). For instance, two transcription factors, POU5F1 (OCT3/4) and NANOG, known to be associated with pluripotency in embryonic stem (ES) cells, are also expressed in ITGCNU. Moreover a link between ITGCNU cells and ES cells has been further supported by a substantial overlap in their gene expression profile (Almstrup et al., 2004).

In the last few years a large number of proteins have been described as markers of different types of TGCTs. The chromatin- associated proteins HMGA1 and HMGA2, for example, are over-expressed in pluripotent embryonal carcinoma cells but HMGA1

loses its expression in YSTs and both proteins are not expressed in mature adult tissue of teratoma cells. Moreover, only HMGA1 is expressed in seminomas (Franco et al., 2008). Thus, analysis of the differential expression of HMGA isoforms can be useful to distinguish between TGCTs. Another marker used to distinguish different histotype is the mitotic kinase Aurora B. It results overexpressed in all carcinoma *in situ*, seminomas and embryonal carcinomas analysed but it is not detected in teratomas and yolk sac carcinomas (Chieffi et al., 2004; Esposito et al., 2009). Finally, the transcriptional regulatory factor PATZ1 is frequently increased in TGCTs. Interestingly, PATZ1 was aberrantly localized in the cytoplasm of testicular cancer cells, suggesting an impaired function in these tumours (Fedele et al., 2008) (see Appendix 1).

NEK2 AS A NOVEL MARKER OF TGCTs

Most testicular seminomas are polyploid or aneuploid, suggesting aberrant chromosome segregation in the early stages of neoplastic transformation (Oosterhuis & Looijenga, 2005). Aneuploidy also occurs in non-neoplastic germ cells from infertile males and represents a risk factor for the development of GCTs (Oosterhuis & Looijenga, 2005; Mayer et al., 2003). At the molecular level, a recent study has demonstrated that overduplication of the centrosomes is associated with aneuploidy both in seminomas and non-seminomas GCTs and in non neoplastic germ cells from individual with aberrant spermatogenesis (Mayer et al., 2003). However, the molecular mechanism involved in this defect in germ cells undergoing neoplastic transformation remains unknown. A potentially valuable candidate is Nek2, for its central role in centrosome separation (Fry et al., 1998a) and because this kinase is highly expressed in testis (Rhee & Wolgemuth, 1997).

Early studies showed that Nek2 is mainly expressed in mitotic spermatogonia and meiotic spermatocytes of the post-natal testis (Rhee & Wolgemuth, 1997). Our laboratory has previously shown that the activation of Nek2 in meiotic germ cells is under the control of the mitogen activated protein kinase (MAPK) pathway (Di Agostino et al. 2002, Di Agostino et al., 2004). A specific feature of Nek2 in meiotic germ cells was its localization in the nucleus, where it associates with the condensing chromosomes at the pachytene stage (Di Agostino et al., 2002). Moreover, activation of the MAPK/Nek2 pathway appeared to favour chromosome condensation during the meiotic progession of mouse spermatocytes, possibly due to Nek2-mediated phosphorylation of HMGA2 (Di Agostino et al., 2004). Interestingly, activation of MAPKs in male gonocytes (Li et al, 1997) and in meiotic spermatocytes (Vicini et al., 2006) is elicited by estrogens, which have been hypothesized to contribute to the increased incidence of testicular tumours in the recent years (Sharpe, 2003). Hence, it is possible that hyperactivation or up-regulation of Nek2 in germ cells participates to some steps leading to germ cell neoplastic transformation.

The aim of this PhD project is to investigate the role of Nek2 in cancer, with a particular focus to testicular germ cell tumours.

REFERENCES

Al Ghamdi, A. M. and M. A. Jewett (2005). "Stage I nonseminomatous germ cell tumors: the case for management by risk stratification." Can J Urol 12 Suppl 1: 62-5; discussion 103-4.

Almstrup, K., C. E. Hoei-Hansen, et al. (2004). "Embryonic stem cell-like features of testicular carcinoma in situ revealed by genome-wide gene expression profiling." Cancer Res 64(14): 4736-43.

Arama, E., A. Yanai, et al. (1998). "Murine NIMA-related kinases are expressed in patterns suggesting distinct functions in gametogenesis and a role in the nervous system." Oncogene 16(14): 1813-23.

Badano, J. L., T. M. Teslovich, et al. (2005). "The centrosome in human genetic disease." Nat Rev Genet 6(3): 194-205.

Barbagallo, F., M. P. Paronetto, et al. (2009). "Increased expression and nuclear localization of the centrosomal kinase Nek2 in human testicular seminomas." J Pathol 217(3): 431-41.

Barr, F. A., H. H. Sillje, et al. (2004). "Polo-like kinases and the orchestration of cell division." Nat Rev Mol Cell Biol 5(6): 429-40.

Chaganti, R. S. and J. Houldsworth (2000). "Genetics and biology of adult human male germ cell tumors." Cancer Res 60(6): 1475-82.

Chen, A., A. Yanai, et al. (1999). "NIMA-related kinases: isolation and characterization of murine nek3 and nek4 cDNAs, and chromosomal localization of nek1, nek2 and nek3." Gene 234(1): 127-37.

Chen, Y., D. J. Riley, et al. (2002). "Phosphorylation of the mitotic regulator protein Hec1 by Nek2 kinase is essential for faithful chromosome segregation." J Biol Chem 277(51): 49408-16.

Chieffi, P. (2007). "Molecular targets for the treatment of testicular germ cell tumors." Mini Rev Med Chem 7(7): 755-9.

Chieffi, P., G. Troncone, et al. (2004). "Aurora B expression in normal testis and seminomas." J Endocrinol 181(2): 263-70.

Classen, J., R. Souchon, et al. (2001). "Treatment of early stage testicular seminoma." J Cancer Res Clin Oncol 127(8): 475-81.

D'Assoro, A. B., S. L. Barrett, et al. (2002). "Amplified centrosomes in breast cancer: a potential indicator of tumor aggressiveness." Breast Cancer Res Treat 75(1): 25-34.

Di Agostino, S., M. Fedele, et al. (2004). "Phosphorylation of high-mobility group protein A2 by Nek2 kinase during the first meiotic division in mouse spermatocytes." Mol Biol Cell 15(3): 1224-32.

Di Agostino, S., P. Rossi, et al. (2002). "The MAPK pathway triggers activation of Nek2 during chromosome condensation in mouse spermatocytes." Development 129(7): 1715-27.

Esposito, F., S. Libertini, et al. (2009). "Aurora B expression in post-puberal testicular germ cell tumours." J Cell Physiol 221(2): 435-9.

Faragher, A. J. and A. M. Fry (2003). "Nek2A kinase stimulates centrosome disjunction and is required for formation of bipolar mitotic spindles." Mol Biol Cell 14(7): 2876-89.

Fedele, M., R. Franco, et al. (2008). "PATZ1 gene has a critical role in the spermatogenesis and testicular tumours." J Pathol 215(1): 39-47.

Ferrari, S. (2006). "Protein kinases controlling the onset of mitosis." Cell Mol Life Sci 63(7-8): 781-95.

Franco, R., F. Esposito, et al. (2008). "Detection of high-mobility group proteins A1 and A2 represents a valid diagnostic marker in post-pubertal testicular germ cell tumours." J Pathol 214(1): 58-64.

Fry, A. M. (2002). "The Nek2 protein kinase: a novel regulator of centrosome structure." Oncogene 21(40): 6184-94.

Fry, A. M., T. Mayor, et al. (1998b). "C-Nap1, a novel centrosomal coiled-coil protein and candidate substrate of the cell cycle-regulated protein kinase Nek2." J Cell Biol 141(7): 1563-74.

Fry, A. M., P. Meraldi, et al. (1998a). "A centrosomal function for the human Nek2 protein kinase, a member of the NIMA family of cell cycle regulators." Embo J 17(2): 470-81.

Hames, R. S. and A. M. Fry (2002). "Alternative splice variants of the human centrosome kinase Nek2 exhibit distinct patterns of expression in mitosis." Biochem J 361(Pt 1): 77-85.

Hames, R. S., S. L. Wattam, et al. (2001). "APC/C-mediated destruction of the centrosomal kinase Nek2A occurs in early mitosis and depends upon a cyclin A-type D-box." Embo J 20(24): 7117-27.

Hayward, D. G., R. B. Clarke, et al. (2004). "The centrosomal kinase Nek2 displays elevated levels of protein expression in human breast cancer." Cancer Res 64(20): 7370-6.

Hayward, D. G. and A. M. Fry (2006). "Nek2 kinase in chromosome instability and cancer." Cancer Lett 237(2): 155-66.

Helps, N. R., X. Luo, et al. (2000). "NIMA-related kinase 2 (Nek2), a cell-cycle-regulated protein kinase localized to centrosomes, is complexed to protein phosphatase 1." Biochem J 349(Pt 2): 509-18.

Jones, R. H. and P. A. Vasey (2003). "Part II: testicular cancer--management of advanced disease." Lancet Oncol 4(12): 738-47.

Landi, M. T., T. Dracheva, et al. (2008). "Gene expression signature of cigarette smoking and its role in lung adenocarcinoma development and survival." PLoS One 3(2): 1651.

Letwin, K., L. Mizzen, et al. (1992). "A mammalian dual specificity protein kinase, Nek1, is related to the NIMA cell cycle regulator and highly expressed in meiotic germ cells." Embo J 11(10): 3521-31.

Li, H., V. Papadopoulos, et al. (1997). "Regulation of rat testis gonocyte proliferation by platelet-derived growth factor and estradiol: identification of signaling mechanisms involved." Endocrinology 138(3): 1289-98.

Liu, Q., Y. Hirohashi, et al. (2009). "Nek2 targets the mitotic checkpoint proteins Mad2 and Cdc20: A mechanism for aneuploidy in cancer." Exp Mol Pathol.

Looijenga, L. H. and J. W. Oosterhuis (1999). "Pathogenesis of testicular germ cell tumours." Rev Reprod 4(2): 90-100.

Ma, X. J., R. Salunga, et al. (2008). "A five-gene molecular grade index and HOXB13:IL17BR are complementary prognostic factors in early stage breast cancer." Clin Cancer Res 14(9): 2601-8.

Mayer, F., H. Stoop, et al. (2003). "Aneuploidy of human testicular germ cell tumors is associated with amplification of centrosomes." Oncogene 22(25): 3859-66.

Mayor, T., Y. D. Stierhof, et al. (2000). "The centrosomal protein C-Nap1 is required for cell cycle-regulated centrosome cohesion." J Cell Biol 151(4): 837-46.

Meraldi, P., V. M. Draviam, et al. (2004). "Timing and checkpoints in the regulation of mitotic progression." Dev Cell 7(1): 45-60.

Nielsen, H., M. Nielsen, et al. (1974). "The fine structure of possible carcinoma-in-situ in the seminiferous tubules in the testis of four infertile men." Acta Pathol Microbiol Scand A 82(2): 235-48.

Nigg, E. A. (2001). "Mitotic kinases as regulators of cell division and its checkpoints." Nat Rev Mol Cell Biol 2(1): 21-32.

O'Regan, L., J. Blot, et al. (2007). "Mitotic regulation by NIMA-related kinases." Cell Div 2: 25.

Oosterhuis, J. W. and L. H. Looijenga (2005). "Testicular germ-cell tumours in a broader perspective." Nat Rev Cancer 5(3): 210-22.

Peckham, M. (1988). "Testicular cancer." Acta Oncol 27(4): 439-53.

Rhee, K. and D. J. Wolgemuth (1997). "The NIMA-related kinase 2, Nek2, is expressed in specific stages of the meiotic cell cycle and associates with meiotic chromosomes." Development 124(11): 2167-77.

Saunders, W. (2005). "Centrosomal amplification and spindle multipolarity in cancer cells." Sem Cancer Biol 15: 25–32.

Schultz, S. J., A. M. Fry, et al. (1994). "Cell cycle-dependent expression of Nek2, a novel human protein kinase related to the NIMA mitotic regulator of Aspergillus nidulans." Cell Growth Differ 5(6): 625-35.

Sharpe, R. M. (2003). "The 'oestrogen hypothesis'- where do we stand now?" Int J Androl 26(1): 2-15.

Shelley, M. D., K. Burgon, et al. (2002). "Treatment of testicular germ-cell cancer: a cochrane evidence-based systematic review." Cancer Treat Rev 28(5): 237-53.

Skakkebaek, N. E. (1972). "Possible carcinoma-in-situ of the testis." Lancet 2(7776): 516-7.

Skakkebaek, N. E., J. G. Berthelsen, et al. (1987). "Carcinoma-in-situ of the testis: possible origin from gonocytes and precursor of all types of germ cell tumours except spermatocytoma." Int J Androl 10(1): 19-28.

Tanaka, K. and E. Nigg (1999). "Cloning and characterization of the murine Nek3 protein kinase, a novel member of the NIMA family of putative cell cycle regulators." J Biol Chem. 274(19): 13491-7.

Tsunoda, N., T. Kokuryo, et al. (2009). "Nek2 as a novel molecular target for the treatment of breast carcinoma." Cancer Sci 100(1): 111-6.

Ulbright, T. M. (1993). "Germ cell neoplasms of the testis." Am J Surg Pathol 17(11): 1075-91.

Vicini , E., M. Loiarro, et al. (2006). "17-Beta-estradiol elicits genomic and nongenomic responses in mouse male germ cells." J Cell Physiol (206): 238–245.

Wicha, M. S. (2006). "Cancer stem cells and metastasis: lethal seeds." Clin Cancer Res 12(19): 5606-7.

Wonsey, D. R. and M. T. Follettie (2005). "Loss of the forkhead transcription factor FoxM1 causes centrosome amplification and mitotic catastrophe." Cancer Res 65(12): 5181-9.

Wu, G., X. L. Qiu, et al. (2008). "Small molecule targeting the Hec1/Nek2 mitotic pathway suppresses tumor cell growth in culture and in animal." Cancer Res 68(20): 8393-9.

Wu, W., J. E. Baxter, et al. (2007). "Alternative splicing controls nuclear translocation of the cell cycle-regulated Nek2 kinase." J Biol Chem 282(36): 26431-40.

CHAPTER IV

Increased expression and nuclear localization of the centrosomal kinase Nek2 in human testicular seminomas

Protein kinases that regulate the centrosome cycle are often aberrantly regulated in neoplastic cells. Changes in their expression or activity can lead to perturbations in centrosome duplication and aneuploidy. In addition, many centrosomal protein kinases participate to other aspects of cell cycle progression. Testicular germ cell tumors (TGCTs) are characterized by amplification of centrosomes through unknown mechanisms. We have discovered that the centrosomal kinase Nek2 is overexpressed in testicular seminomas and we have characterized its function in neoplastic germ cells.

One unexpected finding of our study was the nuclear localization of Nek2 in germ cells of patients. The same nuclear localization was observed in the seminoma cell line Tcam-2. We found that Nek2 was localized in the nucleus also in undifferentiated embryonal male primordial germ cells (PGCs) and in spermatogonial stem cells from post-natal testis (see the attached article: Barbagallo et al., *Journal of Pathology* 2009). These results suggest that nuclear Nek2 is a novel marker of the undifferentiated stage of male germ cells that is maintained in testicular seminomas, but not in other TGCTs.

Journal of Pathology
J Pathol 2009; **217**: 431–441
Published online 14 October 2008 in Wiley InterScience
(www.interscience.wiley.com) **DOI:** 10.1002/path.2471

Original Paper

Increased expression and nuclear localization of the centrosomal kinase Nek2 in human testicular seminomas

Federica Barbagallo,[1,2] Maria P Paronetto,[1,2] Renato Franco,[3] Paolo Chieffi,[4] Susanna Dolci,[1] Andrew M Fry,[5] Raffaele Geremia[1,2] and Claudio Sette[1,2]*

[1] *Department of Public Health and Cell Biology, University of Rome Tor Vergata, 00133 Rome, Italy*
[2] *Laboratory of Neuroembryology, IRCCS Fondazione Santa Lucia, 00143 Rome, Italy*
[3] *National Cancer Institute 'G Pascale', Section of Pathology, Naples, Italy*
[4] *Department of Experimental Medicine, II University of Naples, Naples, Italy*
[5] *Department of Biochemistry, University of Leicester, Lancaster Road, Leicester LE1 9HN, UK*

**Correspondence to:*
Claudio Sette, Department of Public Health and Cell Biology, University of Rome Tor Vergata, Via Montpellier 1, 00133 Rome, Italy.
E-mail: claudio.sette@uniroma2.it

No conflicts of interest were declared.

Received: 2 July 2008
Revised: 12 September 2008
Accepted: 4 October 2008

Abstract

Protein kinases that regulate the centrosome cycle are often aberrantly controlled in neoplastic cells. Changes in their expression or activity can lead to perturbations in centrosome duplication, potentially leading to chromosome segregation errors and aneuploidy. Testicular germ cell tumours (TGCTs) are characterized by amplification of centrosomes through unknown mechanisms. Herein, we report that Nek2, a centrosomal kinase required for centrosome disjunction and formation of the mitotic spindle, is up-regulated in human testicular seminomas as compared to control testes or other types of testicular germ cell tumours. In addition, Nek2 activity is also increased in human seminomas, as demonstrated by immunokinase assays. Analysis by immunohistochemistry indicated that Nek2 is prevalently localized in the nucleus of neoplastic cells of primary human seminomas. Such nuclear localization and the up-regulation of Nek2 protein were also observed in the Tcam-2 seminoma cell line. We demonstrate that nuclear localization of Nek2 is a feature of the more undifferentiated germ cells of mouse testis and correlates with expression of the stemness markers OCT4 and PLZF. These studies suggest that up-regulation of Nek2 is a frequent event in human seminomas and that this may participate in the onset or progression of neoplastic transformation through deregulation of centrosome duplication and/or nuclear events in germ cells.

Keywords: Nek2; centrosome; neoplastic transformation; germ cells; seminomas; testis

Introduction

Germ cell tumours (GCTs) are a heterogeneous group of neoplastic diseases that occur both in the gonads and in extra-gonadal sites, such as the retroperitoneal district, the mediastinal region, and the brain [1]. Testicular GCTs (TGCTs) can be distinguished in three epidemiologically, clinically, and histologically diverse groups of tumours. The first group includes pre-puberal teratomas and yolk sac tumours and originates from immature germ cells, such as the migrating primordial germ cells (PGCs). The post-puberal testicular germ cell tumours (PTGCTs) include seminomas and non-seminomas (embryonal cell carcinoma, choriocarcinoma, and post-puberal yolk sac tumours and teratomas). They originate from PGCs or gonocytes that have already reached the gonads (group 2), or from more mature mitotic and meiotic germ cells (group 3), such as the spermatocytic seminomas. PTGCTs are the most common form of TGCT, occurring usually between 15 and 40 years of age with an incidence of approximately 6.0 per 100 000 per year [1–3].

Seminomas usually originate from an *in situ* testicular intra-tubular carcinoma and express markers of undifferentiated germ cells, such as the nuclear transcription factors Oct4 and Nanog [4,5], indicating that they derive from PGCs or early gonocytes (prospermatogonia) that fail to enter the spermatogenic differentiation programme [1,6,7]. Most testicular seminomas are polyploid or aneuploid, due to aberrant chromosome segregation in the early stages of the neoplastic transformation [1,8]. Aneuploidy also occurs in non-neoplastic germ cells from infertile males and represents a risk factor for the development of GCTs [1,8]. A recent study has demonstrated that overduplication of centrosomes is associated with aneuploidy both in type II GCTs and in non-neoplastic germ cells from individuals with aberrant spermatogenesis, indicating

that it may precede, and perhaps be causative for, neoplastic transformation [8]. Nevertheless, the molecular basis of centrosome amplification in testicular seminomas is currently unknown.

The centrosome is a cytoplasmic organelle composed of two centrioles surrounded by a proteinaceous matrix, referred to as the pericentriolar material. It serves as a nucleation centre for microtubules throughout the cell cycle. During mitosis, the centrosome organizes the bipolar spindle and is required for equal distribution of replicated chromosomes between daughter cells [9–11]. In line with this role, centrosome duplication and separation need to be tightly coordinated with the cell division cycle [9]. Centrosome duplication begins in the S phase and terminates in G2, before the onset of cell division. At mitosis, the duplicated centrosomes separate to opposite ends of the cell to generate the mitotic spindle and maintain tension until all chromosomes are correctly assembled at the equatorial plate [9–11]. In addition, the centrosome serves as a scaffold to recruit proteins involved in cell cycle-related events, such as protein kinases, phosphatases, and proteins involved in protein degradation by the proteasome [10]. Several serine–threonine kinases, such as Cdk1/cyclin B, Polo-like kinase 1 (Plk1), Aurora A, and Nek2, associate with the centrosome during cell cycle progression and regulate the centrosome cycle and spindle assembly in order to tightly link M-phase progression with chromosome segregation [9–11]. These kinases, or in the case of Cdk1 its regulatory cyclin B subunit, are ubiquitylated and targeted for destruction by the proteasome after eliciting their function in mitosis. Remarkably, deregulated expression or hyperactivation of Plk1 and Aurora A was shown to cause deregulation of the centrosome cycle and aneuploidy in several cancer cells [12,13].

The molecular mechanisms leading to centrosome amplification in GCTs are still unknown [8]. Nek2 is a centrosomal kinase highly enriched in male germ cells [14]. Nek2 promotes centrosome separation at the onset of mitosis through phosphorylation and displacement of proteins involved in centrosome cohesion, including C-Nap1, rootletin, and β-catenin [15–18]. Experimentally, up-regulation of this kinase in human cells causes premature splitting of the centrosome [19], while, in contrast, overexpression of kinase-dead Nek2 induces centrosome abnormalities that result in monopolar spindles and aneuploidy [20]. Hence, tight regulation of Nek2 abundance and activity is essential to ensure the correct centrosome cycle.

Elevated expression of Nek2 protein has been observed in both pre-invasive and invasive breast carcinomas [21], suggesting that it represents an early event in the neoplastic transformation of these cells. We have previously shown that Nek2 is activated during G2/M progression of male germ cells and that Nek2 may contribute to chromatin condensation during the meiotic divisions of spermatocytes [22–24]. Here, we have investigated the expression and regulation of Nek2 in human PTGCTs. Our results indicate that the expression and activity of Nek2 are frequently up-regulated in testicular seminomas. Moreover, Nek2 is prevalently found in the nuclei of seminoma cells. Nuclear localization of Nek2 was also observed in undifferentiated germ cells, but it translocated to the cytoplasm after their commitment to the spermatogenetic programme. Our results suggest that deregulated expression of Nek2 may contribute to the neoplastic transformation of germ cells.

Materials and methods

Tissue samples

The tissue bank of the National Cancer Institute 'G Pascale' provided 42 cases of cryopreserved tissue from two normal testes, 24 seminomas, four mature teratomas, eight embryonal carcinomas, and four selected areas of yolk sac tumours in mixed tumours. The IGCTs were evaluated in the same specimens of human seminomas all the time they were found (16/24 examined seminomas) in the tissue surrounding the tumour as previously described [25,26]. Ethics Committee approval was given in all instances.

Immunohistochemistry

For each case analysed, representative neoplastic and non-neoplastic areas were included. Immunostaining was performed on 5 μm sections of paraffin-embedded tissues as previously described [25,26]. The primary antibodies were as follows: rabbit anti-Nek2 (Abgent AP8074c; 1 : 200); monoclonal anti-PLAP (Cell Marque NB10; 1 : 100); and monoclonal anti-Oct4 (Santa Cruz Biotechnology sc5279; 1 : 100). Immunodetection was performed with biotinylated secondary antibodies and peroxidase-labelled streptavidin (LSAB-DAKO, Glostrup, Denmark). Sections were counterstained with haematoxylin.

Cell culture and transfection

HEK293T, MCF-7, and GC-1 cells were grown at 37 °C in a 5% CO_2 atmosphere in DMEM supplemented with 10% fetal bovine serum (FBS) (Gibco BRL). Tcam-2 cells were grown at 37 °C in a 5% CO_2 atmosphere in RPMI 1640 (LONZA) supplemented with 10% FBS. Transfection of the pCDNA$_3$-myc Nek2 expression plasmid [24] was performed using 3 μl of Lipofectamine 2000 (Invitrogen) and 1 μg of DNA. HEK293T cells were transfected with 300 pmol of small interfering RNA (siRNA) oligonucleotides (MWG Oligo Synthesis), using 6 μl of oligofectamine and Opti-MEM medium (Invitrogen) following the manufacturer's instructions. Nek2 siRNA is 5′-GAAGAGUGAUGGCAAGAUATT-3′; control siRNA is 5′-AGACGAACAAGUCACCGACTT-3′. After transfection, cells were harvested in lysis buffer

and analysed in western blot as previously described [22,24].

Western blot analysis

Proteins were separated on 10% SDS-PAGE gels and transferred to polyvinylidene fluoride Hybond-P membranes (Amersham Biosciences) using a semi-dry blotting apparatus (Bio-Rad). Membranes were incubated with the following primary antibodies overnight at 4 °C: goat anti-Nek2 (1 : 1000), Santa Cruz Biotechnology sc-19; rabbit anti-Erk2 (1 : 1000), Santa Cruz Biotechnology sc-154; mouse anti-myc (1 : 1000), Santa Cruz Biotechnology sc-40; and rabbit anti-Nek2 (1 : 500), Abgent AP8074c. For pre-adsorption of the anti-Nek2 antibody, the pGEX-3X-Nek2$_{295-443}$ construct was transformed in *E. coli* cells (BL21) and the recombinant GST-Nek2$_{295-443}$ protein was purified on glutathione-Sepharose beads (Sigma, G-4510) as previously described [24]. After several washes in PBS, GST-Nek2$_{295-443}$ was incubated overnight with the rabbit anti-Nek2 antibody diluted in PBS containing 5% bovine serum albumin (BSA). The pre-adsorbed antibody was used for subsequent western blot analysis or immunohistochemistry. After incubation with secondary antibodies, immunostained bands were detected by the chemiluminescent method (Santa Cruz Biotechnology) [22,24]. All densitometric analyses were performed using Quantity One (Biorad).

Immunoprecipitation assay

Cells were resuspended in the lysis buffer described above. Tumour tissues were resuspended in homogenization buffer [66 mM Hepes (pH 7.5), 0.2 M NaCl, 1.3% glycerol, 1.3% Triton X-100, 2 mM $MgCl_2$, 6 mM EGTA, 2 mM Na pyrophosphate, 2 mM PMSF, 10 mM Na_2VO_3, 50 mM NaF] and homogenized by ten strokes in a glass Dounce homogenizer. Lysates were kept on ice for 10 min and soluble extracts were separated by centrifugation at 10 000 *g* for 10 min. Tissue or cell extracts (500 μg to 1 mg of total proteins) were pre-cleared for 1 h on a mixture of Protein A- and Protein G-Sepharose beads (Sigma-Aldrich) before incubation with 1 μg of specific antibody for 2 h at 4 °C under constant shaking. Protein A-/Protein G-Sepharose beads were pre-adsorbed with 0.05% BSA before incubation with the immunocomplexes for an additional hour. Hence, beads were washed three times with lysis buffer and absorbed proteins were either eluted in SDS-sample buffer for western blot analysis or used for kinase assay.

Immunokinase assays

Immunocomplexes prepared as described above were rinsed twice with kinase buffer [50 mM Hepes (pH 7.5), 5 mM β-glycerophosphate, 5 mM $MnCl_2$, 5 mM NaF, 0.1 mM Na orthovanadate, 1 mM DTT, protease inhibitor cocktail]. Kinase reactions were carried out in 50 μl for 20 min at 30 °C in kinase buffer supplemented with 10 μM ^{32}P-γ-ATP (0.2 μCi/μl), 4 μM ATP, and MBP as substrate (2 μg), as described before [22–24]. Reactions were stopped by adding SDS-sample buffer and analysed by SDS-PAGE and autoradiography.

Isolation of mouse germ cells

Mouse spermatogonia were obtained from 7-day-old Swiss CD-1 mice, as previously reported [27]. Briefly, germ cell suspensions were obtained by sequential collagenase–hyaluronidase–trypsin digestions of testes. Cells were cultured in E-MEM with 10% FBS for 3 h to allow adhesion of contaminating somatic cells to the dishes. At the end of this pre-plating treatment, enriched germ cell suspensions were rinsed with serum-free medium and cultured in E-MEM supplemented with 2 mM Na pyruvate and 1 mM Na lactate. The purity of spermatogonia after the pre-plating treatment was about 80–90% [28]. Cells were grown in a 32 °C humidified atmosphere of 5% CO_2. Oct4–GFP-positive spermatogonia were sorted from a germ cell suspension obtained from 2 days post-partum (dpp) as previously described [29]. PGCs were isolated and purified from 12.5 dpc (days post-coitum) mouse embryos using the MiniMACS immunomagnetic cell sorter method (PGC purity >90%) [30]. Spermatocytes were isolated by elutriation from testes of 30 dpp CD1 mice as previously described [31].

Immunofluorescence microscopy

Cells were fixed at room temperature for 10 min in 4% paraformaldehyde and permeabilized for 10 min in 0.1% Triton X-100. After 1 h in PBS with 3% BSA, samples were incubated overnight at 4 °C with the following primary antibodies: rabbit anti-Nek2 (1 : 200; Abgent); R31 or R40 rabbit anti-Nek2 antibodies (1 : 100) [21]; and mouse anti-Plzf (1 : 100, Chemicon). Cells were incubated for 1 h at room temperature with secondary antibodies (1 : 300 dilution; Jackson ImmunoResearch Laboratories). Hoechst dye (0.1 mg/ml; Sigma-Aldrich) was added for the last 10 min to stain nuclei. Slides were mounted in Mowiol 4–88 reagent (Calbiochem).

Results

Characterization of Nek2 antibodies

To investigate the expression and activity of Nek2 in human PTGCTs, we tested the specificity of two commercially available polyclonal antibodies. Recombinant myc-Nek2 was expressed in HEK293T cells and immunoprecipitated with the anti-myc antibody. Western blot analysis with the same antibody showed a specific band in the extracts and immunoprecipitates of cells transfected with myc-Nek2 that was absent in cells transfected with empty vector (Mock)

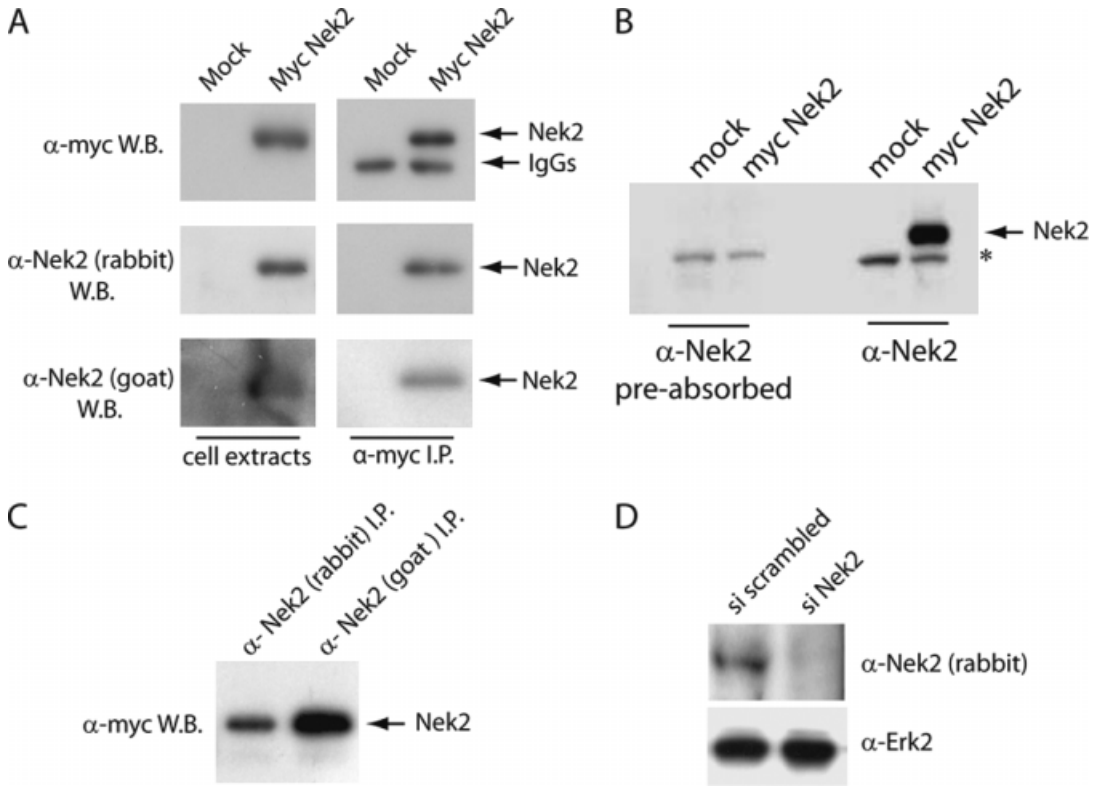

Figure 1. Characterization of Nek2 antibodies. (A) HEK293T cells were transfected with empty vector (mock) or with myc-Nek2 and cell extracts were immunoprecipitated with α-myc antibodies. Western blot analysis of cell extracts and immunoprecipitated proteins using α-myc (upper panel), rabbit α-Nek2 (middle panel), or goat α-Nek2 (lower panel) antibodies. (B) Extracts from HEK293T cells transfected with empty vector (mock) or the myc-Nek2 expression vector were analysed by western blot with rabbit anti-Nek2 antibody pre-absorbed to recombinant GST-Nek2 or with rabbit α-Nek2, as indicated at the bottom. The asterisk indicates a non-specific band. (C) Extracts from HEK293T cells transfected with the myc-Nek2 expression vector were immunoprecipitated with either rabbit or goat α-Nek2 as indicated and analysed by western blot with the α-myc antibody. (D) HEK293T cells were transfected with siRNA for Nek2 or with its scrambled control siRNA and cell extracts were analysed by western blot with rabbit α-Nek2 antibodies

(Figure 1A). Both the rabbit and the goat anti-Nek2 polyclonal antibodies recognized recombinant myc-Nek2, although the rabbit antibody was more efficient in detection of the protein in western blot analysis (Figure 1A). Competition of the rabbit anti-Nek2 antibody by pre-absorption to recombinant GST-Nek2 abolished the Nek2 staining (Figure 1B), indicating the specificity of the band recognized. Both antibodies were also able to immunoprecipitate myc-Nek2, with the goat antibody being more efficient in this assay, demonstrating that they could recognize Nek2 in its native form (Figure 1C). We also determined whether the rabbit anti-Nek2 was capable of recognizing the endogenous Nek2. HEK293T cells were transfected with siRNA for Nek2 or with its scrambled control siRNA and the cell extracts were analysed. As shown in Figure 1D, the band corresponding to endogenous Nek2 was detected in the scrambled siRNA extracts but was absent when Nek2 was silenced by RNAi. These experiments indicate that both commercial antibodies specifically recognize Nek2. For the subsequent experiments, we used the rabbit antibody for western blot analyses and immunohistochemistry, and the goat antibody for immunoprecipitation analyses.

Nek2 is up-regulated in human seminomas

Human PTGCTs ($n = 40$) were analysed for Nek2 expression by immunohistochemistry with the rabbit anti-Nek2 antibody. We observed that Nek2 was highly expressed in the neoplastic cells in all the samples obtained from testicular seminomas (Figures 2C, 2D, and 2G) compared with normal testis (Figure 2A). The staining was specific because no signal was detected after pre-adsorption of the antibody with recombinant GST-Nek2 protein (Figure 2H). We found that Nek2 was already expressed at high levels in the early stages of neoplastic transformation, such as in intratubular germ cell tumours (Figure 2B) in all IGCTs found (in 16 out of 24 seminoma specimens analysed; see Supporting information, Supplementary Table and Figure). Staining of parallel slides for Nek2 (Figure 2I) and the GCT markers PLAP (placenta-like alkaline phosphatase) (Figure 2J) or OCT4 (data not shown) indicated that Nek2-expressing cells were neoplastic cells. Interestingly, Nek2 staining was concentrated in the nucleus of neoplastic cells (Figures 2B–2D, 2G, 2I and Table 1). Up-regulation of Nek2 was a specific feature of testicular seminomas, because other types of PTGCTs, such as embryonal carcinoma (Figure 2E) or teratomas

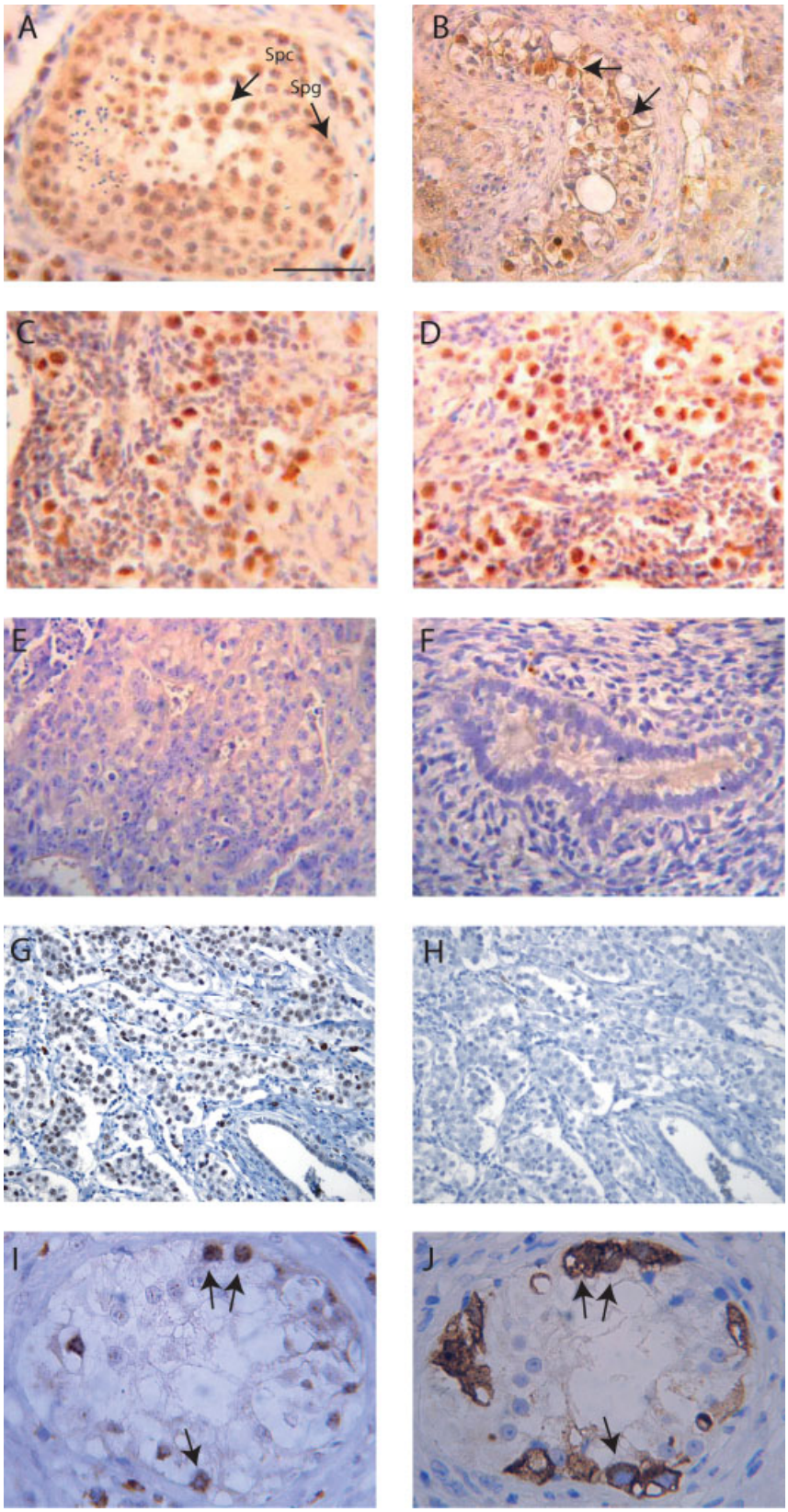

Figure 2. Nek2 expression in human PTGCTs. Immunohistochemistry was performed with a rabbit anti-Nek2 antibody. (A) Normal human testis shows faint Nek2 staining in most cells, with increased expression in pachytene spermatocytes (Spc) and some of the spermatogonia (Spg) at the base of the tubule (arrows). (B) Nek2 expression is up-regulated in cells of *in situ* carcinoma (arrows). Strong nuclear staining of Nek2 is observed. (C, D) Testicular seminomas show intense and nuclear Nek2 staining in most neoplastic cells. (E) Embryonal carcinoma or (F) teratomas show no detectable staining for Nek2. (G, H) Parallel sections of testicular seminomas were stained with anti-Nek2 antibody before (G) or after (H) pre-absorption to recombinant GST-Nek2. (I, J) Parallel sections of testicular seminomas were stained with anti-Nek2 antibody and anti-PLAP antibody. Representative cells positive to both Nek2 and PLAP staining are indicated by arrows. Original magnification: (A–H) 40×; (I, J) 60×. Bar = 25 μm

Table 1. Immunohistochemical analysis of Nek2 in human PTGCTs

	No of cases (40)	Mean age (years)	Nuclear Nek2	Cytoplasmic Nek2
Seminoma	24	27	+++ (24/24)	− (24/24)
EC	8	25	− (8/8)	− (5/8), +/− (3/8)
Mature teratoma	4	17	− (4/4)	− (4/4)
YST	4	19	− (3/4), + (1/4)	− (4/4)

EC = embryonal carcinoma; YST = yolk sac tumour; + + + = intense and diffuse staining; +/− = very focal staining; − = negative staining.

(Figure 2F), did not express detectable levels of Nek2. A detailed description of the samples analysed, with the relative intensity of Nek2 staining and the cellular compartment where the protein was localized, is given in Table 1 and in the Supporting information, Supplementary Table.

To confirm the up-regulation of Nek2 protein in human seminomas by a different technique, we performed western blot analysis on a subset of PTGCTs for which frozen tissue was available. We found that Nek2 protein was more abundant in extracts obtained from seminoma samples than in extracts obtained from teratoma or a sample from a patient affected by chronic epididymitis (Figure 3A). Moreover, in a patient affected by seminoma for which a segment of normal testicular tissue was available, we found higher levels of Nek2 protein in the neoplastic lesion (Figure 3B). Densitometric analysis demonstrated that the increase in Nek2 expression in seminomas ($n = 11$) with respect to non-seminomas ($n = 8$) was statistically significant (Figure 3C). A summary of the results of western blot analyses in all patients available is shown in Table 2. These results indicate that up-regulation of Nek2 protein is a frequent event in human seminomas but not in other types of PTGCTs.

Nek2 activity is increased in human seminomas

Nek2 activity is modulated during cell cycle progression, with a peak of activity in the G2 phase when its activity is required for centrosome separation [32]. To determine whether Nek2 activity was also increased in human seminomas, we performed an immunokinase assay with an exogenous substrate. Nek2 was immunoprecipitated with the goat anti-Nek2 antibody, which gave a better yield than the rabbit antibody in this assay (Figure 1C), and the activity of Nek2 was assayed using myelin basic protein (MBP) as substrate [22–24]. We observed that Nek2 activity was increased in three of the four human seminomas (lanes 4–6 in Figure 3D) with respect to non-neoplastic testis (lane 1) or teratoma (lane 2), likely due to its up-regulated levels in these patients. Since active Nek2 efficiently autophosphorylates [32], we tested the specificity of our assay by checking the autophosphorylation of Nek2 after its immunoprecipitation from different TGCT samples. With respect to pre-immune IgGs (Figure 3E, lanes 1–5), the anti-Nek2 antibody could immunoprecipitate higher Nek2 activity from seminoma samples (lanes 6, 7, and 10) but not from embryonal carcinomas (lanes 8 and 9) or teratomas (data not shown). These assays indicate that Nek2 activity is increased in human seminomas but not in other PTGCTs.

Nuclear localization of Nek2 is maintained in the Tcam-2 human seminoma cell line

A peculiar feature of the expression of Nek2 in human seminoma cells was its predominantly nuclear localization. Nek2 is a centrosomal kinase involved in centrosome separation in the late G2 phase/prophase [19,20]. To investigate further the localization of Nek2 in human seminomas, we used Tcam-2 cells, the only available cell line that maintains the features of the original seminoma cells [33]. First, western blot analysis confirmed that Nek2 protein was up-regulated in Tcam-2 cells with respect to non-transformed NIH3T3 cells, the GC1 spermatogonial cell line [34,35], or primary mouse spermatocytes (Figure 4A). The levels of Nek2 in Tcam-2 cells were comparable to those expressed by MCF-7, a breast cancer cell line previously shown to have up-regulated levels of Nek2 [21]. Moreover, the nuclear localization of Nek2 was also maintained in Tcam-2 cells, as shown by immunofluorescence analysis (Figure 4B). The same results were observed using two previously validated anti-Nek2 antibodies, R31 and R40 [21] (data not shown). These data indicate that Tcam-2 cells behave as primary seminoma cells also with respect to Nek2 up-regulation and nuclear localization.

Nuclear localization of Nek2 in mouse undifferentiated male germ cells

Human seminoma cells derive from undifferentiated and pluripotent PGCs or post-natal gonocytes and maintain markers of this undifferentiated state, such as the transcription factor Oct4 [1,4]. Thus, we asked whether nuclear localization of Nek2 was a feature of undifferentiated male germ cells. First, we isolated PGCs from 12.5 dpc mouse embryos and analysed these cells by immunofluorescence microscopy. As shown in Figure 5A, we observed that Nek2 was equally distributed in the nucleus and in the cytoplasm of these cells. Undifferentiated germ cells are also found in the luminal pole of 1–4 dpp of seminiferous tubules, whereas most of these cells enter the differentiation programme once they reach the basal lamina at 5–7 days post-partum [36]. Remarkably, the presence of Nek2 in the nuclei of germ cells correlated strongly with their position in the tubules: nuclear localization

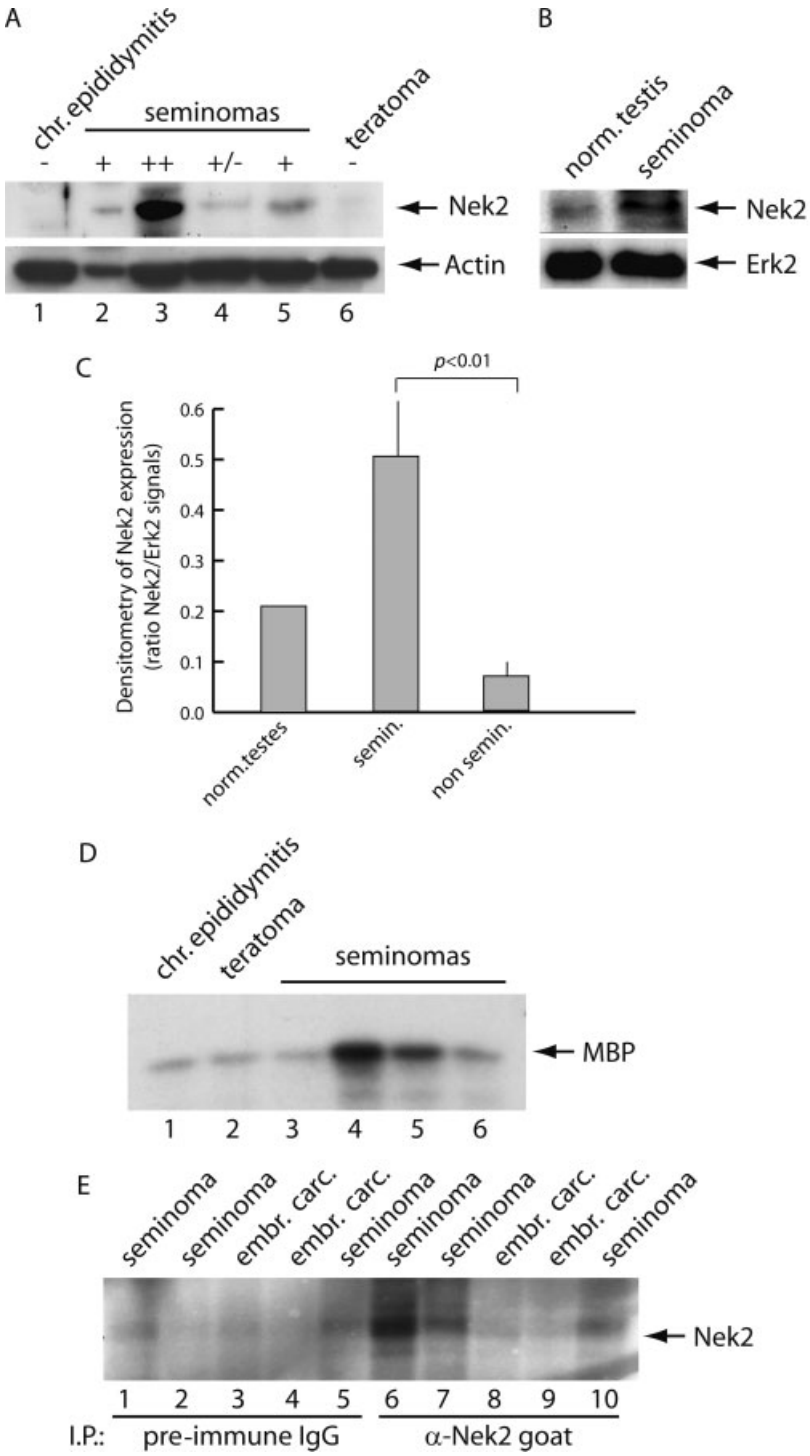

Figure 3. Nek2 is overexpressed and activated in human testicular seminomas. (A) Western blot analysis of Nek2 in representative human PTGCTs. Extracts from tumour tissues were analysed with the rabbit α-Nek2 (upper panel) antibody. Lane 1: testicular tissue from a patient affected by chronic epididymitis; lanes 2–5: tissues from testicular seminoma patients; lane 6: tissue from a teratoma patient. Western blot analysis for actin was used as loading control (bottom panel). The intensity of the Nek2 signal was evaluated as $-$ (absent), $+/-$ (faint), $+$ (readily detected), or $++$ (strong) according to the representative examples shown in the western blot (symbols above the gel). The same standards were applied to all samples analysed in Table 2. (B) Western blot analysis of Nek2 in normal testicular (norm. testis) tissue and a neoplastic lesion (seminoma) of a patient. Erk2 staining was performed for normalization. (C) Densitometric analysis of Nek2 expression in normal testes ($n = 2$), seminomas ($n = 11$), and non-seminomas ($n = 8$). Values are expressed as the ratio between Nek2 and Erk2 signal for each sample analysed. Average values $\pm$ standard deviation are shown for seminomas and non-seminomas. Statistical analysis was performed using the unpaired *T*-test ($p < 0.01$). (D) Nek2 activity was assayed in human PTGCT tissues using an immunokinase assay. Nek2 was immunoprecipitated with the goat anti-Nek2 antibody and its activity was assayed using myelin basic protein (MBP) as substrate [22–24]. Samples were separated by SDS-PGE and the dried gel was analysed by autoradiography. Nek2 activity was increased in three of the four human seminomas (lanes 4–6) with respect to non-neoplastic testis (lane 1) or teratoma (lane 2). (E) Nek2 autophosphorylation was measured by an immunokinase assay as described in D but without the addition of MBP. The anti-Nek2 antibody immunoprecipitated higher Nek2 activity, compared with pre-immune IgGs (lanes 1–5), from seminoma tissues (lanes 6, 7, and 10) than from embryonal carcinomas (lanes 8 and 9)

Table 2. Western blot analysis of Nek2 expression in human TGCTs

Type of TGCT	Nek2 signal in western blot
Normal testis	+/−
Normal testis	+/−
Chronic epididymitis	−
Seminoma	+
Seminoma	++
Seminoma	+/−
Seminoma	+
Seminoma	++
Seminoma	++
Seminoma	++
Seminoma	+
Seminoma	++
Seminoma	++
Seminoma	+
Seminoma	+
Embryonal carcinoma	+/−
Embryonal carcinoma	+/−
Embryonal carcinoma	−
Teratoma	−
Teratoma	−
Yolk sac	−
Teratoma/yolk sac	−
Teratoma/yolk sac	−
Mixed tumour	+/−

++ = strong signal; + = readily detected signal; +/− = weak signal; − = undetectable signal. Representative examples are shown in Figure 3A.

was observed at 1 dpp when gonocytes are localized in the luminal pole (Figure 5B, indicated by an arrow in the left panel), whereas the protein was predominantly in the cytoplasm after they reached the basal lamina at 7 dpp (Figure 5B, indicated by an arrow in the right panel).

To confirm that the nuclear localization of Nek2 correlated with the more undifferentiated state of germ cells, we used two approaches. First, by using flow cytometry, we isolated the undifferentiated germ cells from neonatal testes of mice expressing the fluorescent protein GFP under the control of the OCT4 promoter [37]. Immunofluorescence analysis of Nek2 localization in these cells indicated that the protein was equally distributed in the nuclei and cytoplasm, as in PGCs (Figure 5C). Next, we purified germ cells from 7 dpp testes of wild-type mice. At this age, most of the undifferentiated spermatogonia do not express Oct4 anymore but they express PLZF, another marker of their undifferentiated state [38,39]. Co-staining experiments showed that Nek2 was localized in the nuclei of PLZF-positive spermatogonia, whereas it was enriched in the cytoplasmic rim of PLZF-negative spermatogonia (Figure 5D). These results indicate that nuclear localization of Nek2 is a feature of undifferentiated germ cells and neoplastic germ cells.

Discussion

Regulation of the centrosome cycle is crucial to maintain genome stability and needs to be finely coordinated with cell cycle progression [10–12,40]. In

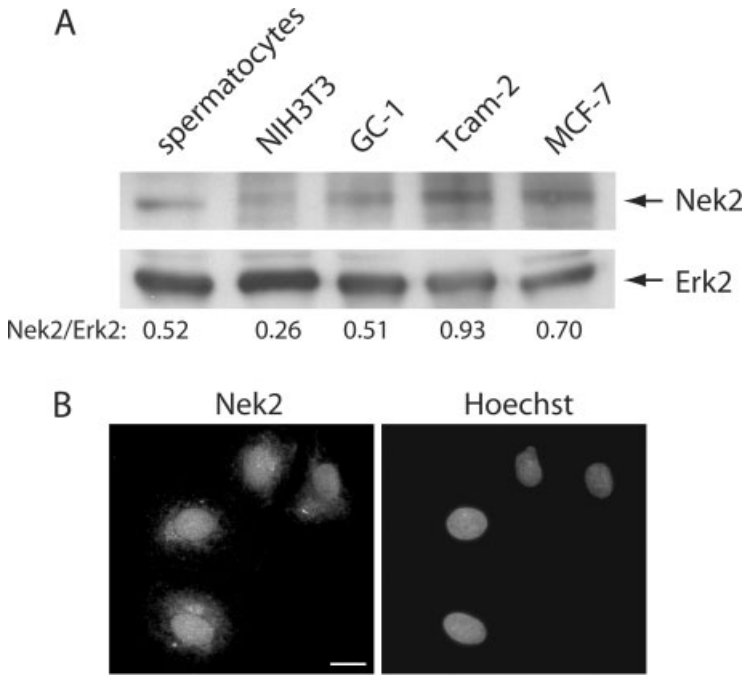

Figure 4. Nek2 expression in the Tcam-2 seminoma cell line. (A) Western blot analysis of cell extracts from purified mouse spermatocytes [31], NIH3T3, GC-1, Tcam-2 or MCF-7, as indicated, using the rabbit anti-Nek2 (upper panel) antibody. Western blot analysis for Erk2 was used as a loading control (bottom panel). Values obtained by densitometric analysis of the ratio between Nek2 and Erk2 signals for each cell line are indicated below the panel. (B) Immunofluorescence analysis of Nek2 (left panel) expression in Tcam-2 cells using the rabbit anti-Nek2 antibody. Nek2 is predominantly localized in the nuclei of these cells. Hoechst staining of nuclei is shown in the right panel. Bar = 10 μm

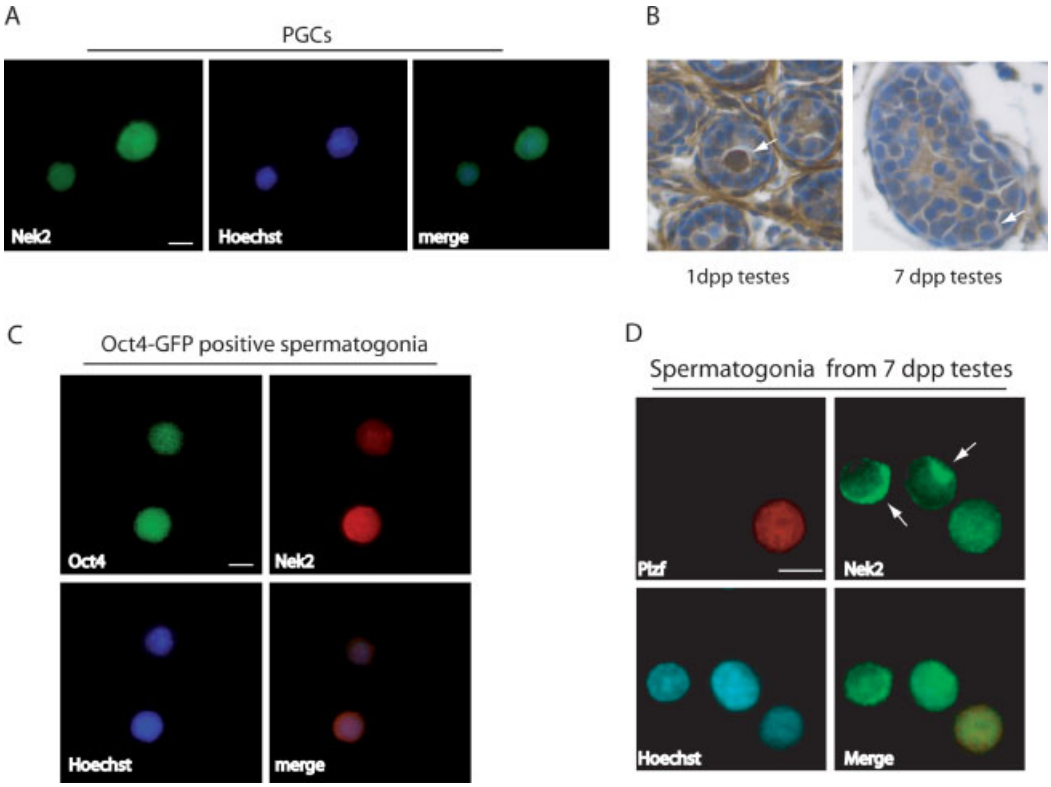

Figure 5. Nek2 is localized in the nuclei of mouse undifferentiated male germ cells. (A) Immunofluorescence analysis of Nek2 expression in PGCs from 12.5 dpc embryos. Cells were stained with rabbit anti-Nek2 (green) antibody and Hoechst (blue) for DNA. Nek2 is equally distributed between the nucleus and cytoplasm in PGCs. (B) Immunohistochemistry of Nek2 expression in postnatal testes. Undifferentiated germ cells, localized in the luminal pole of 1 dpp seminiferous tubules, are indicated by an arrow in the left panel and show both nuclear and cytoplasmic localization of Nek2. At 7 dpp, spermatogonia have reached the basal lamina and begin spermatogenic differentiation. At this age, Nek2 is retained in the cytoplasm of the majority of spermatogonia (indicated by an arrow in the right panel). (C) Undifferentiated germ cells from neonatal testes of mice expressing the fluorescent protein GFP under the control of the OCT4 promoter were analysed by immunofluorescence microscopy. Nek2 (red) localization in these cells indicated that the protein is equally distributed in the nuclei and cytoplasm. (D) Spermatogonia obtained from 7 dpp mice were stained for Nek2 (green), PLZF (red), and Hoechst. As indicated by arrows, Nek2 is distributed in a cytoplasmic ring in PLZF-negative cells, whereas its localization is both nuclear and cytoplasmic in PLZF-positive cells. Bars = 10 μm

many cancers, defects in centrosome regulation have been associated with aneuploidy [11,40–42]. In most TGCTs, aberrant centrosome duplication precedes aneuploidy but the mechanisms leading to this defect are still unknown [8]. Nek2 is a centrosomal kinase highly expressed in testis [14] and it has been previously shown to regulate centrosome separation in late G2/early mitosis [19,20]. Here, we have demonstrated that Nek2 protein levels and kinase activity are up-regulated in human testicular seminomas, but not in other types of PTGCTs. Moreover, our results indicate that Nek2 is prevalently localized in the nucleus of seminoma cells and that its nuclear localization is a marker of the more undifferentiated state of germ cell development. Hence, our data suggest an additional role of the centrosomal kinase Nek2 in the regulation of nuclear events in testicular neoplastic cells.

Nek2 is a core protein of the centrosome and is required for centrosome separation at the onset of mitosis. Aberrant expression of Nek2 has been described in Ewing tumour cell lines, diffuse large B-cell lymphomas, breast cancer cells, and cholangiocarcinoma cells [21,43–45]. In breast cells, up-regulation of Nek2 protein was sufficient to cause amplification of the centrosomes and aneuploidy [21]. Our work indicates that up-regulation of Nek2 also occurs in human seminomas and it might account in part for the amplification of centrosomes and aneuploidy frequently observed in this cancer [8]. Indeed, we found that increased levels of Nek2 protein are already present in intratubular germ cell tumours, at the early steps of the neoplastic transformation. Hence, since centrosome amplification is associated with aneuploidy both in normal germ cells of infertile patients and in TGCTs [8], the increased levels of Nek2 might be part of the alterations that lead to this defect. Remarkably, we observed that up-regulation of Nek2 protein and activity was a specific feature of seminomas and it was not observed in other types of PTGCTs. Since aneuploidy is also a feature of non-seminomas, it is likely that other proteins regulating the centrosome duplication cycle, such as Plk1, Cdk1/cyclin B, and Cdk2/cyclin E [10], are involved in these other neoplastic cells.

An interesting observation of our study is the nuclear localization of Nek2 in human seminoma cells. A recent study suggested that nuclear localization of Nek2 could be due to alternative splicing

of its pre-mRNA [46]. The *NEK2* gene encodes for two major alternatively spliced isoforms, Nek2A and Nek2B, which differ in their non-catalytic C-termini [47]. These isoforms share similar enzymatic activity, dimerization, and localization within the cells; however, while Nek2A is rapidly degraded in mitosis, the lack of a destruction box in the Nek2B isoform protects the protein from ubiquitination-dependent proteolysis [47]. A third splice variant, named Nek2C, was recently described as resulting from an alternative splicing event that excises eight amino acids within the C-terminal domain of Nek2A. The resulting protein contains a novel nuclear localization sequence that is lacking in Nek2A and Nek2B. Although experiments with recombinant proteins showed that Nek2A also partially accumulates in the nuclei, the non-centrosomal pool of Nek2C accumulated in the nuclei much more efficiently [46]. Due to the similar size and the lack of specific antibodies, endogenous Nek2A and Nek2C cannot be distinguished at the protein level. Moreover, specific RT-PCR conditions need to be used to detect the Nek2C transcript [46]. We have attempted to detect the Nek2C isoform by RT-PCR in both human PTGCT tissues and Tcam-2 cells without success (data not shown). The main isoform detected in both tissue and cellular specimens was Nek2A; however, due to the difficulties in the detection of Nek2C, we cannot rule out that this isoform is present in human testicular seminomas.

In addition to seminoma cells, we found that nuclear localization of Nek2 was a feature of undifferentiated germ cells, such as migrating primordial germ cells and testicular gonocytes. Interestingly, in the postnatal testis, nuclear localization of Nek2 correlated with the expression of markers for the stemness of germ cells, such as the transcriptional regulators Oct4 and PLZF [48,49]. By contrast, Nek2 localized predominantly in the cytoplasm of germ cells that have lost these markers and have begun the spermatogenetic differentiation programme. Since human seminomas also continue to express Oct4 protein, it is possible to speculate that the localization of Nek2 in the nucleus is an additional marker of the undifferentiated state of seminoma cells. On the other hand, the observation that Nek2 is not expressed in the nucleus of other PTGCTs suggests that its presence in seminomas correlates with the pathogenesis of this particular PTGCT and it is not merely a reflection of the undifferentiated state of these neoplastic cells. Nevertheless, functional analysis of the role of Nek2 in seminoma cells will be required to determine its role in neoplastic transformation of germ cells.

For other protein kinases, such as the Cdk1/cyclin B1 or cyclin E complexes [50–52], it has been previously shown that centrosomal localization precedes their translocation to the nucleus and modifies their activity. Thus, the nuclear and centrosomal pools of Nek2 might also be coordinately regulated during the cell cycle and it is possible that this equilibrium is modulated to account for specific features of undifferentiated germ cells and/or neoplastic germ cells. Nek2 was observed in the nuclei of mouse meiotic spermatocytes [14]. Moreover, we have shown that Nek2 is activated during the meiotic progression of pachytene spermatocytes induced by okadaic acid or microgravity [22,23] and that the transcriptional regulators HMGA1 and HMGA2 are substrates of Nek2 in meiotic cells [24]. Interestingly, HMGA1 is also highly expressed in human seminomas [26], indicating that regulation of its activity by the nuclear pool of Nek2 might play a role in human seminoma cells. Future studies will address the specific function of Nek2 in undifferentiated and neoplastic germ cells.

Acknowledgements

We thank Drs Massimo De Felici, Enrica Bianchi, and Alessia Di Florio for their helpful suggestions during this study; Dr Maria Loiarro for purification of the GST-Nek2 protein; Drs Marianna Tedesco, Francesca Lolicato, and Paola Grimaldi for assistance with purification of PGCs and OCT4-GFP spermatogonia; Drs Sohei Kitazawa and Leendert Looijenga for the gift of Tcam-2 cells; and Dr Hans Scholer for the generous gift of the OCT4-GFP mouse strain. This work was supported by grants to CS from the Lance Armstrong Foundation, Telethon Grant GGP04118, AIRC, and Italian Ministry of Education (PRIN2004 and 2006). AMF acknowledges support from Cancer Research UK, the Association for International Cancer Research, and the Wellcome Trust.

Supporting information

Supporting information may be found in the online version of this article.

References

1. Oosterhuis JW, Looijenga LH. Testicular germ-cell tumors in a broader perspective. *Nature Rev Cancer* 2005;**5:**210–222.
2. Ulbright TM. Germ cell neoplasms of the testis. *Am J Surg Pathol* 1993;**17:**1075–1091.
3. Swerdlow AJ. In *Germ Cell Tumors IV*, John WG, Appleyard I, Harnden P, Joffe JK (eds). John Libbey: London, 1998; 3–8.
4. Looijenga LH, Stoop H, de Leeuw HP, de Gouveia Brazao CA, Gillis AJ, van Roozendaal KE, *et al*. POU5F1 (OCT3/4) identifies cells with pluripotent potential in human germ cell tumors. *Cancer Res* 2003;**63:**2244–2250.
5. Hart AH, Hartley L, Parker K, Ibrahim M, Looijenga LH, Pauchnik M, *et al*. The pluripotency homeobox gene NANOG is expressed in human germ cell tumors. *Cancer* 2005;**104:**2092–2098.
6. Zhao GQ, Garbers DL. Male germ cell specification and differentiation. *Dev Cell* 2002;**2:**537–547.
7. Schneider DT, Schuster AE, Fritsch MK, Hu J, Olson T, Lauer S, *et al*. Multipoint imprinting analysis indicates a common precursor cell for gonadal and nongonadal pediatric germ cell tumors. *Cancer Res* 2001;**61:**7268–7276.
8. Mayer F, Stoop H, Sen S, Bokemeyer C, Oosterhuis JW, Looijenga LH. Aneuploidy of human testicular germ cell tumors is associated with amplification of centrosomes. *Oncogene* 2003;**22:**3859–3866.
9. Bettencourt-Dias M, Glover DM. Centrosome biogenesis and function: centrosomics brings new understanding. *Nature Rev Mol Cell Biol* 2007;**8:**451–463.

10. Doxsey S, McCollum D, Theurkauf W. Centrosomes in cellular regulation. *Annu Rev Cell Dev Biol* 2005;**21:**411–434.
11. Saunders W. Centrosomal amplification and spindle multipolarity in cancer cells. *Sem Cancer Biol* 2005;**15:**25–32.
12. Barr FA, Sillje HH, Nigg EA. Polo-like kinases and the orchestration of cell division. *Nature Rev Mol Cell Biol* 2004;**5:**429–440.
13. Meraldi P, Honda R, Nigg EA. Aurora kinases link chromosome segregation and cell division to cancer susceptibility. *Curr Opin Genet Dev* 2004;**4:**29–36.
14. Rhee K, Wolgemuth DJ. The NIMA-related kinase 2, Nek2, is expressed in specific stages of the meiotic cell cycle and associates with meiotic chromosomes. *Development* 1997;**124:**2167–2177.
15. Fry AM, Mayor T, Meraldi P, Stierhof YD, Tanaka K, Nigg EA. C-Nap1, a novel centrosomal coiled-coil protein and candidate substrate of the cell cycle-regulated protein kinase Nek2. *J Cell Biol* 1998;**141:**1563–1574.
16. Mayor T, Stierhof YD, Tanaka K, Fry AM, Nigg EA. The centrosomal protein C-Nap1 is required for cell cycle-regulated centrosome cohesion. *J Cell Biol* 2000;**151:**837–846.
17. Bahe S, Stierhof YD, Wilkinson CJ, Leiss F, Nigg EA. Rootletin forms centriole-associated filaments and functions in centrosome cohesion. *J Cell Biol* 2005;**171:**27–33.
18. Bahmanyar S, Kaplan DD, Deluca JG, Giddings TH Jr, O'Toole ET, Winey M, *et al*. Beta-catenin is a Nek2 substrate involved in centrosome separation. *Genes Dev* 2008;**22:**91–105.
19. Fry AM, Meraldi P, Nigg EA. A centrosomal function for the human Nek2 protein kinase, a member of the NIMA family of cell cycle regulators. *EMBO J* 1998;**17:**470–481.
20. Faragher AJ, Fry AM. Nek2A kinase stimulates centrosome disjunction and is required for formation of bipolar mitotic spindles. *Mol Biol Cell* 2003;**14:**2876–2889.
21. Hayward DG, Clarke RB, Faragher AJ, Pillai RM, Hagan IM, Fry AM. The centrosomal kinase Nek2 displays elevated levels of protein expression in human breast cancer. *Cancer Res* 2004;**64:**7370–7376.
22. Di Agostino S, Rossi P, Geremia R, Sette C. The MAPK pathway triggers activation of Nek2 during chromosome condensation in mouse spermatocytes. *Development* 2002;**129:**1715–1727.
23. Di Agostino S, Botti F, Di Carlo A, Sette C, Geremia R. Meiotic progression of isolated mouse spermatocytes under simulated microgravity. *Reproduction* 2004;**128:**25–32.
24. Di Agostino S, Fedele M, Chieffi P, Fusco A, Rossi P, Geremia R, *et al*. Phosphorylation of high-mobility group protein A2 by Nek2 kinase during the first meiotic division in mouse spermatocytes. *Mol Biol Cell* 2004;**15:**1224–1232.
25. Fedele M, Franco R, Salvatore G, Paronetto MP, Barbagallo F, Pero R, *et al*. *PATZ1* gene has a critical role in the spermatogenesis and testicular tumours. *J Pathol* 2008;**215:**39–47.
26. Franco R, Esposito F, Fedele M, Liguori G, Pierantoni GM, Botti G, *et al*. Detection of high-mobility group proteins A1 and A2 represents a valid diagnostic marker in post-pubertal testicular germ cell tumours. *J Pathol* 2008;**214:**58–64.
27. Rossi P, Dolci S, Albanesi C, Grimaldi P, Ricca R, Geremia R. Follicle-stimulating hormone induction of steel factor (SLF) mRNA in mouse Sertoli cells and stimulation of DNA synthesis in spermatogonia by soluble SLF. *Dev Biol* 1993;**155:**68–74.
28. Rossi P, Lolicato F, Grimaldi P, Dolci S, Di Sauro A, Filipponi D, *et al*. Transcriptome analysis of differentiating spermatogonia stimulated with kit ligand. *Gene Expr Patterns* 2007;**8:**58–70.
29. Lolicato F, Marino R, Paronetto MP, Pellegrini M, Dolci S, Geremia R, *et al*. Potential role of Nanos3 in maintaining the undifferentiated spermatogonia population. *Dev Biol* 2008;**313:**725–738.
30. Pesce M, De Felici M. Purification of mouse primordial germ cells by MiniMACS magnetic separation system. *Dev Biol* 1995;**170:**722–727.
31. Sette C, Barchi M, Bianchini A, Conti M, Rossi P, Geremia R. Activation of the mitogen-activated protein kinase ERK1 during meiotic progression of mouse pachytene spermatocytes. *J Biol Chem* 1999;**274:**33571–33579.
32. Fry AM, Schultz SJ, Bartek J, Nigg EA. Substrate specificity and cell cycle regulation of the Nek2 protein kinase, a potential human homolog of the mitotic regulator NIMA of *Aspergillus nidulans*. *J Biol Chem* 1995;**270:**12899–12905.
33. De Jong J, Stoop H, Gillis AJ, Hersmus R, van Gurp RJ, van de Geijn GJ, *et al*. Further characterization of the first seminoma cell line TCam-2. *Genes Chromosomes Cancer* 2008;**47:**185–196.
34. Hofmann MC, Narisawa S, Hess RA, Millan JL. Immortalization of germ cells and somatic testicular cells using the SV40 large T antigen. *Exp Cell Res* 1992;**201:**417–435.
35. Vicini E, Loiarro M, Di Agostino S, Corallini S, Capolunghi F, Carsetti R, *et al*. 17-Beta-estradiol elicits genomic and non-genomic responses in mouse male germ cells. *J Cell Physiol* 2006;**206:**238–245.
36. Lacham-Kaplan O. *In vivo* and *in vitro* differentiation of male germ cells in the mouse. *Reproduction* 2004;**128:**147–152.
37. Boiani M, Eckardt S, Schöler HR, McLaughlin KJ. Oct4 distribution and level in mouse clones: consequences for pluripotency. *Genes Dev* 2002;**16:**1209–1219.
38. Buaas FW, Kirsh AL, Sharma M, McLean DJ, Morris JL, Griswold MD, *et al*. Plzf is required in adult male germ cells for stem cell self-renewal. *Nature Genet* 2004;**36:**647–652.
39. Costoya JA, Hobbs RM, Barna M, Cattoretti G, Manova K, Sukhwani M, *et al*. Essential role of Plzf in maintenance of spermatogonial stem cells. *Nature Genet* 2004;**36:**653–659.
40. Nigg EA. Origins and consequences of centrosome aberrations in human cancers. *Int J Cancer* 2006;**119:**2717–2723.
41. Ghadimi BM, Sackett DL, Difilippantonio MJ, Schröck E, Neumann T, Jauho A, *et al*. Centrosome amplification and instability occurs exclusively in aneuploid, but not in diploid colorectal cancer cell lines, and correlates with numerical chromosomal aberrations. *Genes Chromosomes Cancer* 2000;**27:**183–190.
42. Pihan GA, Wallace J, Zhou Y, Doxsey SJ. Centrosome abnormalities and chromosome instability occur together in pre-invasive carcinomas. *Cancer Res* 2003;**63:**1398–1404.
43. Kokuryo T, Senga T, Yokoyama Y, Nagino M, Nimura Y, Hamaguchi M. Nek2 as an effective target for inhibition of tumorigenic growth and peritoneal dissemination of cholangiocarcinoma. *Cancer Res* 2007;**67:**9637–9642.
44. de Vos S, Hofmann WK, Grogan TM, Krug U, Schrage M, Miller TP, *et al*. Gene expression profile of serial samples of transformed B-cell lymphomas. *Lab Invest* 2003;**83:**271–285.
45. Wai DH, Schaefer KL, Schramm A, Korsching E, Van Valen F, Ozaki T, *et al*. Expression analysis of pediatric solid tumor cell lines using oligonucleotide microarrays. *Int J Oncol* 2002;**20:**441–451.
46. Wu W, Baxter JE, Wattam SL, Hayward DG, Fardilha M, Knebel A, *et al*. Alternative splicing controls nuclear translocation of the cell cycle-regulated Nek2 kinase. *J Biol Chem* 2007;**282:**26431–26440.
47. Fry AM. The Nek2 protein kinase: a novel regulator of centrosome structure. *Oncogene* 2002;**21:**6184–6194.
48. Brinster RL. Male germline stem cells: from mice to men. *Science* 2007;**316:**404–405.
49. Hess RA, Cooke PS, Hofmann MC, Murphy KM. Mechanistic insights into the regulation of the spermatogonial stem cell niche. *Cell Cycle* 2006;**5:**1164–1170.
50. Jackman M, Lindon C, Nigg EA, Pines J. Active cyclin B1–Cdk1 first appears on centrosomes in prophase. *Nature Cell Biol* 2003;**5:**143–148.
51. Lindqvist A, van Zon W, Karlsson Rosenthal C, Wolthuis RM. Cyclin B1–Cdk1 activation continues after centrosome separation to control mitotic progression. *PLoS Biol* 2007;**5:**e123.
52. Matsumoto Y, Maller JL. A centrosomal localization signal in cyclin E required for Cdk2-independent S phase entry. *Science* 2004;**306:**885–888.

CHAPTER V

The centrosomal kinase Nek2 associates with splicing factors in the nucleus and modulates alternative splicing in cancer cells

The nuclear localization of Nek2 is not a unique feature of testicular seminomas. In this study, we show that Nek2 is mainly distributed in the nucleus of cancer cells from other tissues, including breast, prostate and colon cancer cells. The subnuclear distribution of Nek2 in speckles closely resembled that of many regulators of pre-mRNA splicing. We found that Nek2 physically associates with several splicing factors, such as SR proteins (ASF/SF2), hnRNPs (A1, F and H), and the STAR protein Sam68. We focused our study on Sam68 because this splicing regulator is also up-regulated in breast and prostate carcinomas like Nek2. Our study shows that Sam68 is also overexpressed in testicular seminomas but not in other TGCTs, like Nek2. Moreover, Nek2 phosphorylates Sam68 and affects Sam68-dependent splicing of CD44v5 pre-mRNA, an alternatively spliced form of the receptor, frequently altered in cancer cells, that promotes cell proliferation and invasiveness. These results identify a novel nuclear function of Nek2 and suggest that modulation of alternative splicing events by this kinase can contribute to neoplastic transformation.

The centrosomal kinase Nek2 associates with splicing factors in the nucleus and modulates alternative splicing in cancer cells

Federica Barbagallo[1,2], Maria Paola Paronetto[1,2], Renato Franco[3], Paolo Chieffi[4], Raffaele Geremia[1] and Claudio Sette[1,2]

[1]Department of Public Health and Cell Biology, Section of Anatomy, University of Rome "Tor Vergata," 00133 Rome, Italy; and [2]Laboratory of Neuroembryology, Fondazione Santa Lucia IRCCS, 00143 Rome, Italy; [3] National Cancer Institute "G. Pascale", Section of Pathology, Naples, Italy; [4]Department of Experimental Medicine, II University of Naples, Naples, Italy;

Keywords: Sam68, spermatogenesis, meiosis, RNA metabolism, alternative splicing, transcription.

Running title: Nek2 regulates alternative splicing

Corresponding Author: Claudio Sette
Department of Public Health and Cell Biology
University of Rome "Tor Vergata"
Via Montpellier, 1
00133, Rome
Italy
Telephone: 3906 72596260
Fax: 3906 72596268
Email: claudio.sette@uniroma2.it

INTRODUCTION

The mitotic kinase Nek2 is frequently overexpressed in various human cancers, such as testicular seminoma (Barbagallo et al., 2009), breast and prostate cancer (Hayward et al., 2004) and cholangiocarcinoma (Kokuryo et al., 2007). The specific function of Nek2 in neoplastic cells is still largely unknown. In the cytoplasm, Nek2 might contribute to cell transformation by altering the centrosome duplication cycle and favouring aneuploidy (Hayward & Fry, 2006). However, this function of Nek2 might not fully explain its oncogenic features, as recent observations have highlighted a potential new role of Nek2 in the nucleus. For instance, this kinase is predominantly localized in the nucleus at specific stages of male germ cell differentiation (Rhee & Wolgemuth, 1997; Di Agostino et al., 2002; Barbagallo et al., 2009). In particular, nuclear distribution was observed in undifferentiated gonocytes (Barbagallo et al., 2009), which retain pluripotent features that also characterize tumour germ cells. Moreover, Nek2 was also enriched in the nucleus of neoplastic germ cells, suggesting that its nuclear functions affect cell transformation.

The nucleus is the site of storage of genetic information, which is maintained through duplication of the genome at each cell division. Correct chromosome segregation is required to maintain cellular properties and this process is frequently altered in cancer cells, thus contributing to their neoplastic phenotype. Transcription and processing of mRNAs also occurs in the nucleus and cancer cells often display an altered regulation of these processes. Many transcriptional regulators are up- or down-regulated in cancer, thereby directly causing changes in gene expression (Devarajan & Huang, 2009; Villagra et al., 2010; Ruggero, 2009). Furthermore, recent data have demonstrated that post-transcriptional events can also contribute to neoplastic transformation. In particular, alternative splicing of many exons is often aberrant in

cancer cells and leads to the expression of tumour-specific isoforms with unique functions (Venables, 2004; Venables, 2006; Ghigna & Biamonti, 2008).

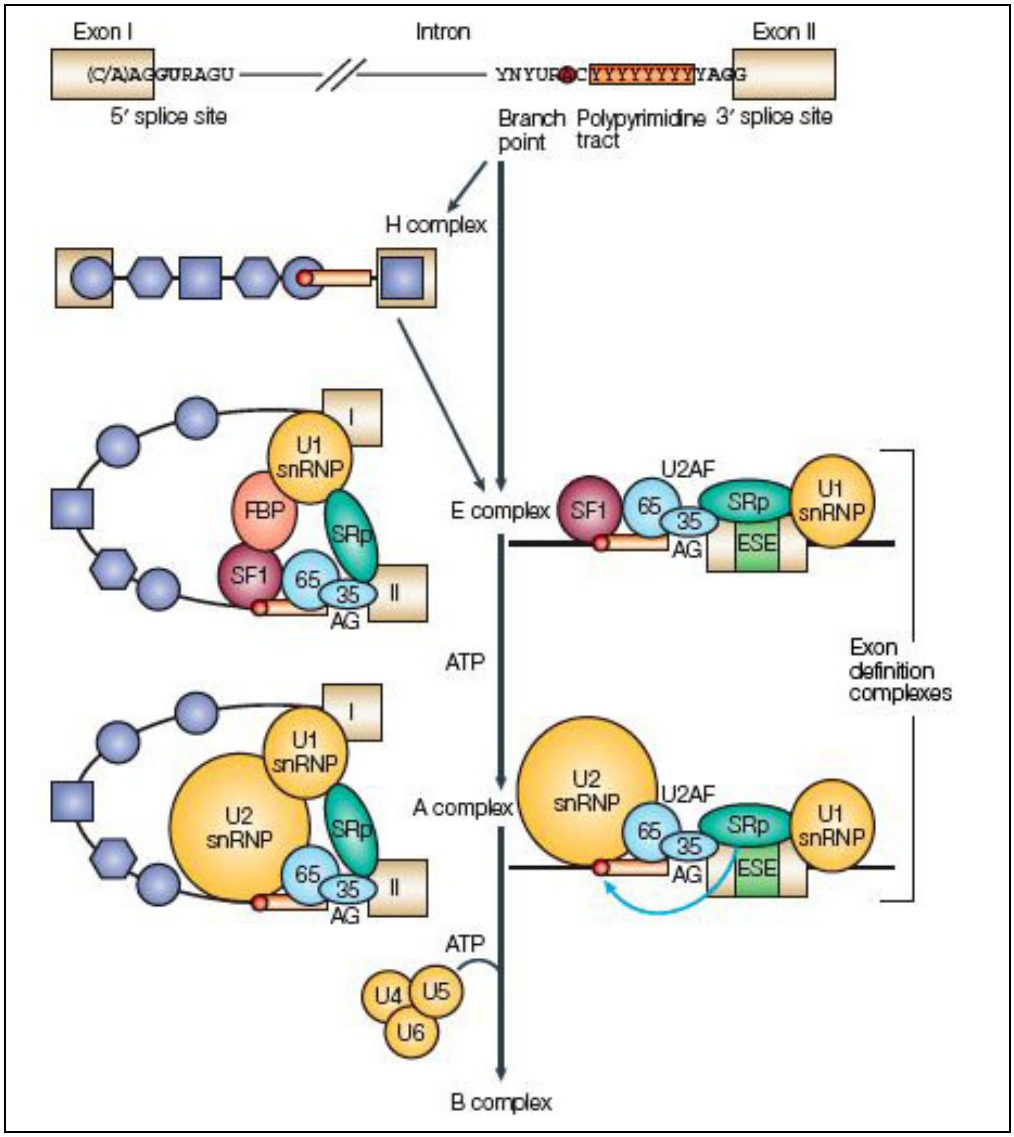

FIGURE 1. Spliceosoma assembly (Matlin et al, 2005). *The removal of introns is catalysed by the spliceosome, an assembly of five small nuclear ribonucleoprotein (snRNP) particles (U1, U2, U4, U5 and U6) that are associated with a large number of additional proteins. The spliceosome assembles onto the pre-mRNA through a series of complexes. Pre-mRNAs become incorporated together with heterogeneous nuclear ribonucleoproteins (hnRNPs); the precise complement of proteins might antagonize or promote the subsequent interaction of spliceosomal components with alternative splice sites.*

In eukaryotes, the vast majority of pre-mRNA transcripts are alternatively spliced to yield at least two mRNA variants from the same gene. This process is thought to increase the transcriptome potential and proteome diversity (Sharp, 2004). Eukaryotic

genes are characterized by large non-coding intronic sequences that separate the protein-coding exons. Splicing of the introns and ligation of the exons is operated by the spliceosome, a large processing machine consisting of 5 small nuclear ribonucleoproteins (U1, U2, U4, U5, and U6 snRNPs) and more than one hundred constitutive and ancillary proteins (Fig. 1) (Black, 2003). Assortment of different exons in the mature mRNA through alternative splicing often generates protein isoforms with different biological properties in terms of protein-protein interactions, subcellular localization, or catalytic activity (Tazi et al., 2009). Although general splicing machinery defects are likely to be incompatible with life, changes in alternative splicing can be tolerated by an organism, but they often manifest in disease (Tazi et al., 2009).

Alternative splicing occurs because the information in splice sites at the exon-intron junction is generally not sufficient for their recognition by the spliceosome. A large number of RNA binding proteins (RBPs) recognize sequences in exons and introns that promote (Splicing Enhancers) or repress (Splicing Silencers) splice site recognition (Fig. 2). The majority of these splicing regulatory RBPs belong to two classes: heterogeneous nuclear ribonucleoproteins (hnRNPs) and serine-arginine rich (SR)-proteins (Matlin et al., 2005). These RBPs contain RNA-binding domains and sites for protein-protein interactions. They bind with low specificity to accessible, mostly single-stranded stretches of the pre-mRNA. To overcome their low RNA-binding specificity, splicing regulatory proteins use their protein-interaction domains to bind to each other. SR proteins generally promote exon recognition by the spliceosome, whereas hnRNPs often play an antagonistic role (Matlin et al, 2005). Ultimately, the high fidelity of exon recognition is achieved by the combination of multiple weak protein:protein, protein:RNA and RNA:RNA interactions (Fig. 2), which can also be influenced by the phosphorylation status of the splicing factors (Stamm, 2008).

In response to external stimuli, cells can regulate alternative splicing events through the activation of signal transduction cascades (Stamm., 2002; Shin & Manley, 2004; Blaustein et al., 2007; Stamm, 2008). For instance, SR-proteins are phosphorylated by several kinases, including the Clk/Sty kinase family (cdc2 like kinases, Clk1-4) and the SRPK family (SRPK1,2) (Long & Caceres, 2009). A change in phosphorylation of the arginine and serine rich domain (RS domain) influences its ability to interact with other proteins, as demonstrated by the increased binding of phosphorylated SF2/ASF, a prototypical SR protein, to the U1-70K protein of the U1snRNP (Xiao & Manley, 1997). However, in most cases the molecular mechanisms affecting regulation of alternative splicing, and in particular their aberrant control in cancer cells, remain unknown, suggesting that additional regulators might be involved.

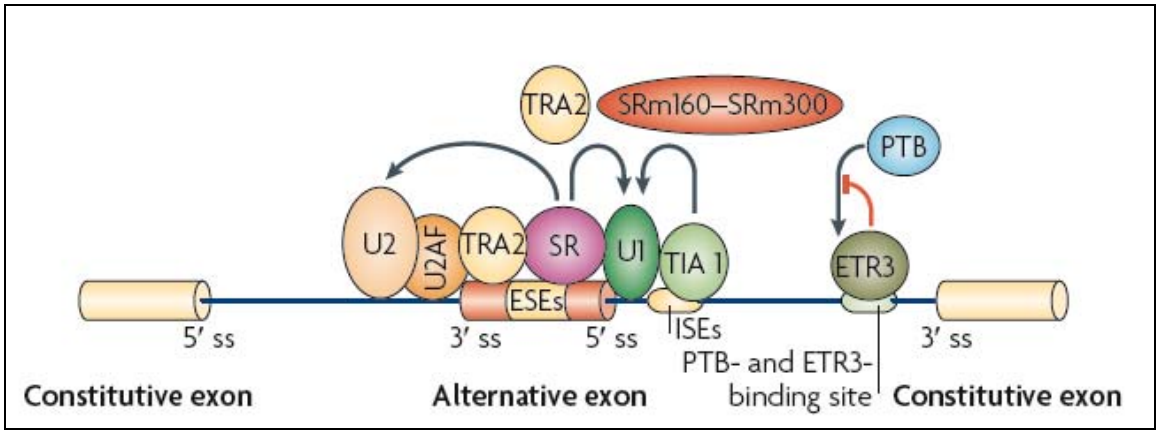

FIGURE 2. Diagram depicting mechanisms of splicing activation. *(Manle, 2009) SR (Ser–Arg) proteins bind to exonic splicing enhancers (ESEs) to stimulate the binding of U2AF to the upstream 3′ splice site(ss) or the binding of the U1 small nuclear ribonucleoprotein (snRNP) to the downstream5′ ss. SR proteins function with other splicing co-activators, such as transformer 2(TRA2) and the SR-related nuclear matrix proteins SRm160–SRm300.*

In this study, we have identified a new function of Nek2 in the regulation of alternative splicing. Our work shows that nuclear localization of Nek2 is a frequent feature of cancer cells obtained from different tissues. Nek2 physically interacts with several splicing regulators and its up-regulation can affect splicing decisions in live cells. Thus, our results suggest that Nek2 can contribute to aberrant expression of

specific splicing variants in cancer through phosphorylation of splicing factors and modulation of their activity.

RESULTS

Nuclear localization of Nek2 is a common feature of neoplastic cells

To determine whether the nuclear localization of Nek2 was a unique feature of seminoma cells or, rather, it was shared by other cancer cells, we analysed Nek2 localization in different tumours. Using a previously validated polyclonal anti-Nek2 antibody (Barbagallo et al., 2009), we performed immunohistochemical staining of tissue sections derived from cancer patients (Fig. 3). We observed that Nek2 was mainly localized in the nucleus of breast (Fig. 3A) and lung (Fig. 3B) cancer cells. In colon cancer cells, although Nek2 staining was enriched in nuclei, it was also detected in the cytoplasm (Fig. 3C). Seminoma cells were used as positive control, as we previously reported the nuclear localization of Nek2 in this tumour cells (Fig. 3D); see also Barbagallo et al., 2009 in Chapter IV). These results indicate that nuclear localization of Nek2 is a common feature of neoplastic cells.

To further investigate the tumour specific nuclear localization of Nek2 we analysed its distribution in cancer cell lines where the kinase was shown to be overexpressed: Tcam-2 (seminoma), PC3 (prostate) and MCF7 (breast) cells (Fig. 4A-C, respectively). Immunofluorescence analyses confirmed that Nek2 is predominantly nuclear in all these tumour cell lines. Moreover, the distribution of the kinase was not diffused within the nucleoplasm, but it was compartmentalized in granules of variable size and irregular shape (indicated by arrows in Fig. 4A-C) that resembled the speckles formed by several splicing regulatory proteins.

The splicing speckles are dynamic subnuclear structures located in the interchromatin region of the nucleoplasm of mammalian cells (Lamond & Spector, 2003). These structures are enriched in pre-mRNA splicing factors, like snRNPs proteins and SR proteins, as well as in kinases and phosphatases that modify them. For

FIGURE 3. Nek2 protein localization in human cancers. *Immunohistochemistry of rabbit anti-Nek2 antibody showing strong nuclear staining in breast (A) and lung (B) cancer cells, although Nek2 staining was enriched in nuclei, it was also detected in the cytoplasm. Seminoma cells (D) were used as positive control.*

this reason, it has been suggested that nuclear speckles function in the storage, assembly and modification of splicing factors (Lamond & Spector, 2003). To test whether Nek2 also localizes to nuclear speckles, we co-stained MCF7 cells with antibodies specific for Nek2 and for two SR proteins commonly used as markers of the splicing speckles: ASF/SF2 and SC35 (Fig. 5). Confocal immunfluorescence analysis demonstrated that Nek2 partially co-localizes with ASF/SF2 (Fig. 5A) whereas it perfectly co-localizes with SC35 (Fig. 5B). These results indicate that Nek2 localizes to nuclear speckles in cancer cells and suggest that it could take part to regulation of splicing events in these cells.

FIGURE 4. Localization of Nek2 in human cancer cell lines. *Immunofluorescence analysis of Nek2 expression derived from different human cancers. Cells were stained with rabbit anti-Nek2 (green) antibody and Hoechst (blue) for DNA and analysed by confocal microscope. Nek2 is mainly nuclear in TCam-2 (seminoma)(A) in PC3 (prostate)(B) and in MCF7(breast)(C) cancer cell lines. Arrows indicate Nek2 nuclear granules.*

Nek2 associates with the nuclear matrix-attached insoluble fraction

It has been reported that, when they are hyperphosphorylated, splicing factors are mostly retained in the nuclear matrix-attached insoluble fraction, whereas they are found in the nuclear soluble fraction in their hypophosphorylated status (Lin et al., 2005). To test whether Nek2 cofractionated with the splicing factors, HEK293T cells were transfected with a plasmid encoding Myc-tagged Nek2C, or an empty vector as control, and cell extract fractionation was performed as reported in the scheme in Figure

6. This protocol allows separation of the cell lysate in three fractions: cytosolic (S), nuclear soluble (NS), and nuclear matrix-attached insoluble (NI) fractions. Consistent with previous characterization (Lin et al., 2005), all splicing factors tested were enriched in the NI fraction (Fig. 7). Interestingly, Western Blot analysis demonstrated that Nek2C is present in both the NS and the NI fraction, in addition to the expected localization in the cytosolic fraction (Fig. 7). This result suggests that Nek2 might physically associate with splicing factors within the nucleus.

FIGURE 5. Nek2 localizes to splicing speckles in cancer cells. MCF7 cells were stained with Nek2 (green), ASF/SF2 (A) or SC35 (B) (red) and analysed with confocal microscope. Magnification of nuclei is shown in the panel. Arrows in the merge photos, indicate co-localization granules.

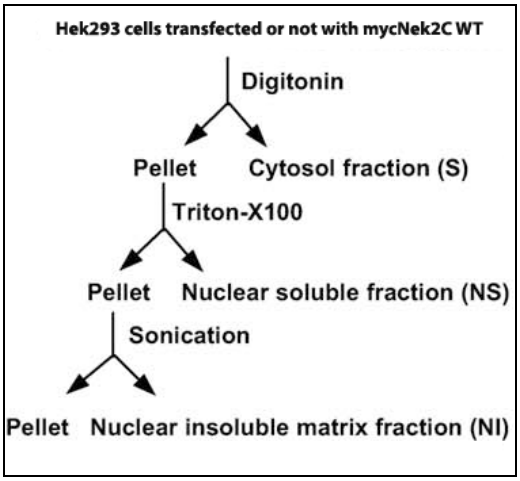

FIGURE 6. **Scheme of cell fractionation**

FIGURE 7. **Nek2 associates with the nuclear matrix-attached insoluble fraction** *Fractionation of Hek293 cells transfected with an empty vector (mock) or with MycNek2C. C, cytosolic; NS, nuclear soluble; NI, nuclear insoluble matrix-associated protein. Tubulin and transcription factor TAFIID p90 were detected on the same extracts as marker of C fraction and NI fraction respectively.*

Identification of new potential nuclear substrate for Nek2

Nek2 is known to interact with substrates and activators through the C-terminal regulatory region. Thus, we have used purified GST-Nek2 C-terminal protein as bait in

affinity chromatography to identify interacting proteins in HEK293T nuclear extracts. The proteins bound to GST-Nek2-Cterm, or GST used as control, were eluted, resolved on SDS-PAGE and analysed by Western blot using antibodies for the splicing factors.

As illustrated in Figure 8, GST-Nek2-Cterm selectively associates with hnRNPA1 and hnRNPF/H but not with hnRNPC1/C2, or with the SR protein ASF/SF2 but not with SRp20. Moreover, Nek2 also specifically interacted with the splicing regulators TIA1 and Sam68 (Fig. 8). These results further suggested that Nek2 plays a novel role in post-transciptional RNA processing events.

FIGURE 8. Nek2 interacts with splicing factors in vitro. *HEK293T nuclear extract were incubated with GST-Nek2 or GST (used as control). Eluted proteins were separated on SDS-PAGE and analyzed by Western blot.*

Nek2 phosphorylates Sam68 in vitro and in vivo

Next, we set out to determine whether Nek2 affected the function of some splicing factors. We focused our attention of Sam68 for the following reasons: Sam68 is upregulated in prostate carcinoma (Busà et al., 2007) and in breast carcinoma (Aubele et al., 2008) like Nek2 (Hayward et al., 2004); Sam68 modulates alternative splicing events that regulate cancer cell proliferation and survival (Matter et al., 2002; Paronetto et al., 2007; Paronetto et al., 2010); Sam68 is abundantly expressed in the testis (Paronetto et al., 2006) like Nek2. Moreover, we found that Sam68 is also up-regulated in human testicular seminomas (Fig. 9A), but not in other types of TGCTs (Fig. 9B).

FIGURE 9. Sam68 expression is elevated in testicular seminomas but not in other type of TGCTs. *Testicular seminoma or normal testis sections were stained with polyclonal anti-Sam68. Immunohystochemical analyses are shown (A). Testicular seminoma cells show highly elevated Sam68 expression (right panel) as compared with*

normal testis tissue (left panel). (B) Western blot analysis of Sam68 in representative human PTGCTs. Extracts from tumour tissues were analysed with the rabbit α-Sam68 (upper panel) and anti-Erk2 (used as loading control) antibodies.

Since the same pattern of selected upregulation in seminomas is typical of Nek2 (Barbagallo et al., 2009), these observations suggest that these proteins might cooperate in cancer cells.

FIGURE 10. Nek2 phosphorylates Sam68 in vitro and in vivo. (A) *Immunoprecipitated Nek2 was incubated with GSTSam68 N-terminal or GSTSam68 C-terminal (underlined in B) as substrates. Proteins were eluted and resolved in SDS-PAGE. The level of phosphorylation was detected by autoradiography. B) Human Sam68 sequence and putative Nek2 phosphorylation sites. C) HEK293 cells treated with 0.1 uM Okadaic Acid (OA). Cell extracts were separeted on SDS-PAGE and analyzed by Western blot. OA induces a Nek2-dependent shift in the electrophoretic mobility of Sam68 (indicated as p-Sam68).*

As first step, we determined if Sam68 was a direct substrate of Nek2 by in vitro kinase assays. Nek2 was immunoprecipitated from HEK293T cells and incubated with recombinant GST-Sam68 fusion proteins encoding the N- or C-terminal regulatory regions in the presence of labelled ATP ([γ-^{32}P]ATP). Autoradiographic analysis of the assay showed that Nek2 efficiently phosphorylates Sam68 in vitro, with a preference for the C-terminal region (Fig. 10A). This result is consistent with the higher abundance of putative Nek2 consensus sites (L/V/AxxS/T) in this region of Sam68 (Fig. 10B).

Although the signalling pathways impinging on Nek2 are still largely unknown, it was previously shown that treatment of cells with the PP1/PP2A phosphatase inhibitor Okadaic Acid (OA) caused activation of the kinase (Rhee & Wolgemuth 1997). Thus, we used OA to verify the ability of Nek2 to phosphorylate Sam68 also in live cells. We co-transfected HEK293T cells with plasmids encoding GFP-Nek2C, either wild type (WT) or kinase-dead (KD), and Myc-Sam68. After 24h, cells were treated with OA and cell extracts were separated by SDS-PAGE. Western blot analysis demonstrated that

OA induces a Nek2-dependent shift in the electrophoretic mobility of Sam68 (Fig. 10C indicated as p-Sam68), which is a hallmark of its phosphorylation in serine/threonine residues (Paronetto et al., 2006). Indeed, the slower migrating form of Sam68 was observed only in cells co-transfected with Nek2 WT, but not with the catalytically inactive KD derivative. These results identify Sam68 as a novel substrate of the Nek2 kinase.

Nek2 modulates the splicing activity of Sam68

A well characterized function of Sam68 is regulation of alternative splicing. Notably, serine/threonine or tyrosine phosphorylation have been previously reported to regulate the splicing activity of Sam68 (Matter et al., 2002; Paronetto et al., 2007, Paronetto et al., 2010). Thus, we asked whether Nek2-dependent phosphorylation of Sam68 also affected its splicing activity. The best characterized splicing target of Sam68 is CD44. Sam68 induces inclusion of the variable exon v5 in the CD44 mRNA. Activation of Ras in response to phorbol ester triggered MAPK-dependent phosphorylation of Sam68 and enhanced this splicing event in mouse T-lymphoma cells (Matter et al., 2002).

FIGURE 11. Overexpression of Nek2 enhances inclusion of CD44 variable exon v5. *A) Schematic representation of CD44 minigene. Diagram shows the minigene with insulin exons (open boxes), introns (black lines), CD44 exon v5 (black box), splicing alternatives (grey lines) and PCR primer positions (arrows) B-C) HEK293 cells were co-transfected with the CD44 minigene and the indicated proteins. After 24 hours, splicing assays were evaluated by RT-PCR. The levels of transfected proteins were analysed by Western blot. Densitometric analyses for all experiment were performed, ratio between CD44(+V5) and CD44(-V5) is represented by histogram bars. Error bars indicate standard deviations based on three independent transfections.*

FIGURE 12. Overexpression of Nek2 is sufficient to enhance the inclusion of CD44 variable exon v5. *(A-B)HEK293T cells were co-transfected with the indicated protein.*

After 24 hours, splicing assays were evaluated by RT-PCR. Co-expression of an active Nek2C is sufficient to promote the inclusion of CD44 variable exon v5. Transfected protein levels were analysed by Western blot. Densitometric analyses were performed and ratio between CD44(+V5) and CD44(-V5) is represented by histogram bars. Error bars indicate standard deviations based on three independent transfections. C) The diagram shows the splice-reporter gene with insulin exon sequences (open boxes), CD44 exon v5 (black box), luciferase (Luc) coding sequence (grey box) and introns (black lines); v5-exon skipping (grey) and inclusion (black) modes are indicated. HEK293 transfected with the splice reporter gene pETv5lu were analyzed using a biocounter luminometer according to dual-luciferase reporter assay system. Data from three experiments were normalized for transfection efficiency and ratio between Firefly and Renilla luciferase activity is shown in the histogram bars.

To investigate if Nek2-dependent phosphorylation of Sam68 could influence CD44v5 splicing, we performed splicing assays in live cells. A minigene encoding the CD44 variable exon v5, flanked by constitutive exons, was used as reporter system (Fig. 11A). HEK293T were co-transfected with the CD44 minigene and suboptimal amounts of Myc-Sam68 plasmid, in the presence or absence of GFP-Nek2C plasmid. This construct encodes for the predominantly nuclear Nek2C splicing variant (Wu et al., 2007), thereby recapitulating the localization of endogenous Nek2 observed in cancer cells (Fig. 3 and 4). After 24h, cell extracts were prepared for RT-PCR and Western blot analyses. As expected, Sam68 promoted the inclusion of CD44 variable exon v5 (Fig. 11B; lane 2). Remarkably, co-expression of Nek2C strongly enhanced this splicing event and v5 inclusion was almost doubled with respect to cells transfected with Sam68 alone (Fig 11B; lane 3). The effect of Nek2 was likely mediated by phosphorylation, because the KD mutant did not affect CD44v5 inclusion (Fig. 11C).

Interestingly we found that transfection of Nek2CWT alone, but not its KD mutant, was sufficient to induce inclusion of the variable exon v5 (Fig. 12A). This effect was dose-dependent and could be appreciated already at low concentrations of Nek2C (Fig. 12B). The same results were obtained using a luciferase reporter vector containing the v5 variable exon upstream luciferase (Fig. 12C), which allows more quantitative analysis of the splicing event (Matter et al., 2002). These results indicate

that Nek2 can affect alternative splicing in the nucleus.

The splicing activity of Nek2 requires Sam68

To test whether the effect of Nek2 on CD44 v5 splicing was mediated by the endogenous Sam68, we performed RNAi-depletion experiments. PC3 cells stably transfected with a plasmid encoding control- (pLKO) or Sam68-siRNA (pLKO si-Sam68) were transfected with the CD44 minigene and GFP-tagged Nek2C WT and KD vectors. After 24h, cell lysates were analysed by Western blot and RT-PCR. As shown in Figure 13A, Sam68 was efficiently depleted in PC3 pLKO si-Sam68 cells with respect to the pLKO control cells (~90% reduction). Similarly to what observed in HEK293 cells, Nek2 WT induced exon v5 inclusion in PC3 pLKO cells, whereas Nek2 KD was much less effective (Fig. 13A,B). However, the effect of Nek2 on v5 splicing was almost completely abolished in cell silenced for Sam68 (Fig. 13A,B), indicating that the effect of Nek2 on CD44 exon v5 was mediated by the endogenous Sam68. These results suggest that phosphorylation of Sam68 by Nek2 increases its splicing activity in cancer cells.

FIGURE 10 Nek2 requires Sam68 to induce CD44 variable exon v5 inclusion. *Control pLKO and pLKO-si-Sam68 (stably interfered for Sam68 expression) PC3 cells were transfected with CD44 minigene and indicated protein. A) After 24h the cell lysate were analyzed by RT-PCR and Western Blot. B) CD44 v5 levels in empty vector transfected cells were set as 100 in the histogram, in the transfected cells v5 inclusion was calculated as fold increase. Data are expressed as meanfold induction ± SD from three separate experiments.*

DISCUSSION

Nek2 is aberrantly expressed in human testicular seminomas (Barbagallo et al., 2009) and in various other cancers like Ewing tumour, diffuse large B-cell lymphoma, breast cancer, and cholangiocarcinoma (Hayward, et al., 2004; Kokuryo, et al., 2007; Wai, et al., 2002). Interestingly, despite its well described role in centrosome dynamics, our study indicates that Nek2 is prevalently localized in the nucleus of cancer cells in which it is up-regulated (Barbagallo, et al., 2009 and Fig. 1 and 2 in this study). This observation led us to hypothesize that Nek2 might also play a role in the nucleus, perhaps related to tumour progression.

A recent study suggested that nuclear localization of Nek2 could be due to alternative splicing of its pre-mRNA (Wu et al., 2007). In addition to the well described Nek2A and Nek2B proteins (Fry, 2002), the *NEK2* gene encodes a third variant, named Nek2C, deriving from a splicing event that excises eight amino acids in the C-terminal domain of Nek2A. This internal deletion creates a strong nuclear localization signal (NLS) that is lacking in the other variants (Wu et al., 2007). Since the available antibodies cannot distinguish between Nek2A and Nek2C, it was possible that the increased nuclear localization of the kinase in cancer cells was due to up-regulation of the Nek2C splicing variant. However, our RT-PCR analyses have shown that the main isoform detected in both cancer tissue and cell lines was Nek2A (data not shown). Nevertheless, due to the difficulties in the detection of Nek2C by PCR amplification (Wu et al., 2007), we cannot rule out that this isoform is present in human cancers. On the other hand, up-regulation of Nek2A also leads to increased nuclear localization (data not shown), suggesting that its higher levels in cancer cells might explain the increased Nek2 signal observed in the nucleus.

Remarkably, we found that Nek2 accumulates in nuclear granules. We identified

these structures as splicing speckles, in which Nek2 might interact with several factors involved in alternative splicing such as Sam68, ASF/SF2 and hnRNPA1. Alternative splicing often allows cells to decipher external signals conveyed by environmental cues (Lee et al., 2009). This regulation is guided by the activation of signal transduction cascades through phosphorylation/dephosphorylation of specific splicing factors (Chen & Manley, 2009; Stamm, 2008). Thus, we hypothesized that Nek2 participates to fine-tuning regulation of post-transcriptional events through its interaction with splicing factors in the nucleus. Among the Nek2-interacting proteins, a well-suited candidate is Sam68, an RBP known to integrate signal transduction pathways with RNA metabolism (Lukong & Richard, 2003; Sette et al., 2009). Sam68 belongs to the evolutionary conserved STAR (Signal Transduction Activator of RNA) family of RBPs, which play key roles during cell differentiation and development (Sette et al., 2009). Sam68 contains a GSG (GRP33/Sam68/GLD-1) RNA binding domain flanked by regulatory regions that allow its interaction with protein partners and are sites for post-translational modifications (Lukong & Richard, 2003). Sam68 acts as a scaffold protein recruited during activation of various signal transduction pathways in different cellular settings (Lukong & Richard, 2003; Najib et al., 2005). Serine-threonine and tyrosine phoshorylation of Sam68 in response to such pathways modulate its affinity for RNA, and results in changes of Sam68 activity. For instance, Sam68 was shown to regulate alternative splicing (Matter et al., 2002; Paronetto et al., 2007; Chawla et al., 2009) and this activity was enhanced by serine-threonine phosphorylation (Matter et al., 2002; Paronetto et al., 2010) and repressed by tyrosine phosphorylation (Paronetto et al., 2007, Paronetto et al., 2010). Moreover, Sam68 cooperates with the splicing activator SRm160 (Cheng and Sharp, 2006) and Brm, a component of the SWI/SNF chromatin remodeling complex (Batsché et al., 2006) in the regulation of CD44 alternative splicing. Thus, Nek2 could regulate Sam68 activity through protein-protein interaction

and/or direct phosphorylation.

Our results strongly suggest that Nek2 regulates Sam68 splicing activity through phosphorylation. First, we observed that Sam68 is a substrate of Nek2 in vitro and in vivo. Second, co-expression of Nek2 and Sam68 enhanced splicing of the CD44 v5 exon, a known Sam68 target, whereas a kinase-inactive form of Nek2 did not exert significant effects. Finally, up-regulation of Nek2 alone was sufficient to affect exon v5 inclusion, but this effect relied on the expression of endogenous Sam68. Thus, our results identify a novel function of Nek2 in the regulation of alternative splicing. In normal cells Nek2 localizes preferentially in the cytoplasm and is enriched on the centrosome. Since Sam68 is instead predominantly localized in the nucleus, its association with Nek2 is likely prevented in non transformed cells (Fig. 14). On the other hand, we propose that in cancer cells, where Nek2 is up-regulated and mainly localizes in the nucleus, the kinase can physically associate with Sam68. This interaction would lead to phosphorylation of Sam68 and to increased inclusion of the CD44 variable exon v5 (Fig. 14). Importantly, through alternative splicing, the CD44 gene encodes a large family of proteins showing considerable structural and functional diversity. Overexpression of CD44 variant isoforms (CD44v1-10), including v5-containing isoforms, leads to increased proliferation and invasiveness of cancer cells (Ponta et al., 2003). Thus, the functional interaction between Sam68 and Nek2 might favour the expression of oncogenic variants of CD44. Moreover, since Sam68 regulates alternative splicing of other genes involved in neoplastic transformation, such as Bcl-x (Paronetto et al., 2007) and Cyclin D1 (Paronetto et al., 2010), it is possible that Nek2 more generally affects post-transcriptional events in cancer cells. In this regard, it also remains to be established if Nek2 regulates the splicing activity of other RBPs that interact with it (i.e. ASF/SF2, hnRNP A1, TIA1, hnRNP F/H), and whether or not this regulation participates to oncogenic transformation of cells in which Nek2 is up-

regulated.

FIGURE 11. Proposed model. *In normal cells (left panel) Nek2 localizes preferentially in the cytoplasm and is enriched on the centrosome. Since Sam68 is instead predominantly localized in the nucleus, its association with Nek2 is likely prevented. In neoplastic cells (right panel) where Nek2 is up-regulated and localizes in the nucleus, can physically associates with Sam68. This association leads to Sam68 phosphorylation that enhances the inclusion of CD44 variable exon v5.* Overexpression of CD44 variant isoforms (CD44v1-10), *including v5-containing isoforms, leads to increased proliferation and invasiveness of cancer cells.*

MATERIAL AND METHODS

Histological analysis and immunohistochemistry

As source of neoplastic tissues, tissue Bank of National Cancer Institute "G. Pascale" provided 14 cases of cryopreserved tissue from seminoma, breast cancer, lung cancer and colon cancer.. Ethical Committee approval was given in all instances.

For light microscopy, tissues were fixed by immersion in 10% formalin and embedded in paraffin by standard procedures. Five micrometer sections were processed for immunohistochemistry. For each paraffin-embedded sample a 5-μm serial section mounted on slides pretreated for immunohistochemistry were dewaxed in xylene and brought through ethanols to deionized distilled water. Before staining for immunohistochemistry, sections were incubated in a 750 W microwave oven for 15 min in 10 mM, 6.0 pH buffered citrate to complete antigen unmasking. The classical Avidin-Biotin peroxidase Complex (ABC) procedure was used for immunohistochemistry. In the ABC system, endogenous peroxidase was quenched by incubation of the sections in 0.1% sodium azide with 0.3% hydrogen peroxide for 30 min at room temperature. Non-specific binding was blocked by incubation with non-immune serum (1% TRIS-bovine albumin for 15 min at room temperature). Sections were incubated overnight with antibodies against Nek2 (Abgent AP8074c) and Sam68 (Santa Cruz Biotechnology sc-33) at a dilution 1:200. Peroxidase activity was developed with the use of a filtered solution of 5 mg of 3-3'-diaminobenzideine tetrahydrochloride (dissolved in 10 ml of 0.05 M tris buffer, pH 7.6) and 0.03 %

H_2O_2. We used Mayer's hematoxylin for nuclear counterstaining. Sections were mounted with a synthetic medium.

Cell culture and transfection

HEK293T, MCF-7, PC3 cells were grown at 37 ◦C in a 5% CO2 atmosphere in DMEM supplemented with 10% fetal bovine serum (FBS) (BioWhittaker Cambrex Bioscience Gibco). Tcam-2 cells were grown at 37 ◦C in a 5% CO2 atmosphere in RPMI 1640 (LONZA), gentamycin, penicillin and streptomycin. pLKO and pLKO-si-Sam68 PC3 cells stable clones were mantained with 1 μg/ml puromycin (Sigma).

PC3 cells were transfected either with pLKO (control pLKO) or PLKO.1-KHDRBS1_527 (pLKO-si-Sam68) (MISSION shRNA, Sigma Aldrich) in a 12 multiwell plate using Lipofectamine 2000 reagent (Invitrogen) according to manufacturer's instructions. The puromycin resistance marker was used for stable selection of PC3 colonies. Puromycin (Sigma-Aldrich) was added at a concentration of 1 μg/ml in fresh medium every two days. Sam68 knockdown was verified by RT-PCR and western blot analyses. Transfection of all the expression plasmids was performed using Lipofectamine 2000 (Invitrogen) using manufacturer's instruction.

Plasmid vectors

The expression vector pcDNA3N2Myc-Nek2C WT was a generous gift of Prof A. Fry; catalytically inactive mutant of Nek2KD ($Nek2_{K37R}$) was created by site-directed mutagenesis of pCDNA3N2myc-Nek2C WT. Mutagenic oligonucleotides were as follows: forward, 5'AGATATTAGTTTGGAGAGAACTTGACTATGGC3'; and reverse, with the underlined codon corresponding to residue 37 in wild-type Nek2C. The sequence of wild-type and mutant Nek2 were confirmed by sequence analysis. The expression vectors pEGFP Nek2C WT or KD were sublcloned from pcDNA3N2Myc into pEGFPc1. pGEX-3X–$Nek2_{273–444}$ encoding the regulatory domain of Nek2 fused to

glutathione *S*-transferase (GST) has been described previously (Di Agostino *et al*., 2002). CD44 minigene and pETv5luc were a kind gift of prof Matter.

Western blot analysis

HEK293T cells were homogenized directly into lysis buffer (50 mM HEPES, 10 mM $MgCl_2$,100 mM NaCl, 10 mM β-glicerophosphate , 2 mM EGTA, 10% glycerol, 1%Triton-X-100, 1 mM phenylmethylsulfonyl fluoride, 10 μg/ml aprotinin, 10 μg/ml pepstatin, 10 μg/ml leupeptin, 0,1 mM sodium orthovanadate,). The lysates were clarified by centrifugation at 12,000 rpm x 10 min. Protein concentrations were estimated by a Bio-Rad assay (Bio-Rad, München, Germany), and boiled in Laemmli buffer (Tris-HCl ph 6.8 0,125 M, SDS 4%, glycerol 20%, 2-mercaptoethanol 10%, bromophenol blue 0.002%) for 5 min before electrophoresis. Proteins were separated on 10% or 8% SDS-PAGE gels and transferred to polyvinylidene fluoride Hybond-P membranes (Amersham Biosciences) using a semi-dry blotting apparatus (Bio-Rad). Membranes were incubated with the following primary antibodies overnight at 4 ◦C:, rabbit anti-Erk2 (1 : 1000), Santa Cruz Biotechnology sc-154; mouse anti-myc (1 : 1000), Santa Cruz Biotechnology sc-40; rabbit anti-GFP (1:1000); rabbit anti-Nek2 (1 : 500); goat anti-Nek2 Santa Cruz Biotechnology; rabbit anti-Erk2 (1:1000); rabbit anti-Sam68 (1:1000) Santa Cruz Biotechnology; mouse anti-hnRNP A1 (1:500) Sigma-Aldrich; goat anti-TIA-1 (1:200) Santa Cruz Biotechnology; mouse anti-ASF/SF2 (1:1000); mouse anti-hnRNP F/H and hnRNP C1/C2 (1:500) Santa Cruz Biotechnology; mouse anti-tubulin (1:1000); goat anti-U170k (1:500) mouse anti-SC35 Santa Cruz Biotechnology; rabbit anti-TAFIIDp90 (1:1000) Santa Cruz Biotechnology. After incubation with secondary antibodies, immunostained bands were detected by the chemiluminescent method (Santa Cruz Biotechnology).

Nuclear extract and cellular fractionation

Briefly, cells were collected in 1.0 ml isotonic RSB-100 (10 mM Tris-HCl [pH 7.4], 140 mM NaCl, 2.5 mM MgCl2). Digitonin (Calbiochem) was added at a final concentration of 40 mg/ml, and cells were incubated on ice for 5 min. After centrifugation at 2000 3 g for 8 min, the supernatant was collected as the soluble cytosolic fraction. The pellet was resuspended in RSB-100 containing 0.5% Triton X-100 and incubated on ice for 5 min. The soluble nuclear fraction was then collected after centrifugation at 2000 3 g for 8 min. The pellet was finally resuspended in the same buffer and disrupted by sonication twice, 5 s each time. The sonicated material was layered onto a 30% sucrose cushion in RSB-100 and centrifuged at 4000 3 g for 15 min. The supernatant was collected as the nuclear insoluble fraction. The extracts obtained were bolied in SDS loading buffer and analyzed in a 8%-10% SDS-PAGE gel.

Immunofluorescence microscopy

Cells were fixed at room temperature for 10 min in 4% paraformaldehyde and permeabilized for 10 min in 0.1% Triton X-100. After 1 h in PBS with 3% BSA, samples were incubated overnight at 4 ◦C with the following primary antibodies: rabbit anti-Nek2 (1 : 200; Abgent); mouse anti-SF2/ASF (1:200; Santa Cruz Biotechnology sc-); mouse anti-SC35 (1 : 400; Santa Cruz Biotechnology sc-) Cells were incubated for 1 h at room temperature with secondary antibodies FITC-coniugated donkey anti-rabbit; cy3-coniugated donkey anti-mouse 1:400 (Jackson Immunoresearch) Hoechst dye (0.1 mg/ml; Sigma- Aldrich) was added for the last 10 min to stain nuclei. Slides were mounted in Mowiol 4–88 reagent (Calbiochem) and cells analysed by confocal microscope.

Bacterial protein expression and purification

Escherichia coli cells (BL21-DE3) were transformed with the appropriate plasmid, grown at 37°C in LB medium to an optical density (600 nm) of 0.4, and induced with 0.5 mM isopropyl-1-thio--galactopyranoside for 3 h at the same temperature. Cells were harvested by centrifugation and lysed in ice-cold phosphate-buffered saline (PBS) containing 0.1% Triton X-100, 1 mM dithiothreitol (DTT), protease inhibitors, by probe sonication (3 cycles of 1 min). After centrifugation at 12,000 x *g*, supernatant fractions were incubated with either glutathione-Sepharose beads (G 4510; Sigma-Aldrich, St. Louis, MO), for 2 h at 4°C under constant shaking. After washes in PBS, GST-Sam68 were eluted with either 100 mM Tris-HCl, pH 8, 250 mM NaCl containing 10 mM glutathione (G 4251; Sigma-Aldrich), wherease GST-Nek2C-terminal was used for pull-down assay. Purified protein was stored at -80°C in the same buffer also containing 10% glycerol.

Immunoprecipitation Experiments

HEK293T were collected by centrifugation at 1000 x *g* for 10 min, and washed twice in ice-cold 1x PBS. Cells were homogenized in lysis buffer. For immunoprecipitation, 1 µg goat anti-Nek2 was incubated for 60 min with a mixture of protein A/G-Sepharose beads (Sigma-Aldrich) in PBS containing 0.05% BSA under constant shaking at 4°C. At the end of the incubation, the beads were washed twice with PBS/0.05% BSA, twice with lysis buffer, and then incubated for 90 min at 4°C with the HEK293 cell-extracts (0.5 mg of protein) under constant shaking. Sepharose bead-bound immunocomplexes were rinsed three times with lysis buffer and washed twice with the appropriate kinase buffer for immunokinase assays.

Immunokinase Assays

Immunocomplexes bound to Sepharose beads obtained from immunoprecipitation of cell extracts were rinsed twice with Nek2-kinase buffer (50 mM HEPES pH 7.5, 5 mM -glycerophosphate, 5 mM $MnCl_2$, 5 mM NaF, 0.1 mM sodium orthovanadate, 1 mM DTT, 10 µg/ml leupeptin, and 10 µg/ml aprotinin). Kinase reactions were carried out in 50 µl for 20 min at 30°C in kinase buffer supplemented with 10 µM [^{32}P]-ATP (0.2 µCi/µl), 4 µM ATP, 1 µg of cAMP-dependent protein kinase inhibitor, and the appropriate substrate (GST-Sam68 N-term or C-term) . Reactions were stopped by adding SDS-sample buffer and analyzed by SDS-PAGE and autoradiography.

Pull-Down Assay

HEK293T nuclear extract obtained as described above were added to GST Nek2 C-terminal adsorbed on glutathione-agarose (Sigma-Aldrich) for 2 h at 4°C under constant shaking. Beads were washed three times with PBS. Adsorbed proteins were analyzed by Western blot .

Transfections , CD44v5-luciferase (v5-Luc) or CD44 minigene splicing assay

HEK293T or PC3 cells were seeded the day before transfection (3.5x105) in 35 mm plates and then transfected with myc-tagged or GFP-tagged protein expression vectors using Lipofectamine 2000 (Invitrogen) according to manufacturer's instructions. For Luciferase assay, control pLKO and pLKO-si-Sam68PC3 cells were cultured in 12-well plates (~ 10 x 10^5/well). Cells were transfected with the minigene pETv5luc , GFPNek2C WT or KD and the Renilla luciferase reporter gene as an internal control using Lipofectamine 2000 (Invitrogen), according to the manufacturer's instructions.

Twenty-four hours after transfection, cells were harvested, lysed, and analyzed

using a biocounter luminometer according to dual-luciferase reporter assay system (Promega). Data from three experiments were normalized for transfection efficiency, ratio between Firefly and Renilla luciferase activity.

For minigene CD44 v5 alternative splicing analysis, transfected Hek293 cell were harvested in TRIzol reagent (Invitrogen) for total RNA extraction according to the manufacturer's instructions. After digestion with RNase-free DNase (Roche), 1 μg of total RNA was used for RT using M-MLV reverse transcriptase (Invitrogen). Semi-quantitative PCRs were carried out and analysed on agarose gel. Densitometry was performed using Quantity one program (Biorad)

REFERENCES

Aubele, M., A. K. Walch, et al. (2008). "Prognostic value of protein tyrosine kinase 6 (PTK6) for long-term survival of breast cancer patients." Br J Cancer 99(7): 1089-95.

Barbagallo, F., M. P. Paronetto, et al. (2009). "Increased expression and nuclear localization of the centrosomal kinase Nek2 in human testicular seminomas." J Pathol 217(3): 431-41.

Batsché, E., M. Yaniv, et al. (2006). "The human SWI/SNF subunit Brm is a regulator of alternative splicing." Nat Struct Mol Biol. 13(1): 22-29.

Black, D. L. (2003). "Mechanisms of alternative pre-messenger RNA splicing." Annu Rev Biochem 72: 291-336.

Blaustein, M., F. Pelisch, et al. (2007). "Signals, pathways and splicing regulation." Int J Biochem Cell Biol 39(11): 2031-48.

Busa, R., M. P. Paronetto, et al. (2007). "The RNA-binding protein Sam68 contributes to proliferation and survival of human prostate cancer cells." Oncogene 26(30): 4372-82.

Chawla, G., C. H. Lin, et al. (2009). "Sam68 regulates a set of alternatively spliced exons during neurogenesis." Mol Cell Biol 29(1): 201-13.

Chen, M. and J. L. Manley (2009). "Mechanisms of alternative splicing regulation: insights from molecular and genomics approaches." Nat Rev Mol Cell Biol 10(11): 741-54.

Cheng, C. and P. A. Sharp (2006). "Regulation of CD44 alternative splicing by SRm160 and its potential role in tumor cell invasion." Mol Cell Biol 26(1): 362-70.

Devarajan, E. and S. Huang (2009). "STAT3 as a central regulator of tumor metastases." Curr Mol Med 9(5): 626-33.

Di Agostino, S., M. Fedele, et al. (2004). "Phosphorylation of high-mobility group protein A2 by Nek2 kinase during the first meiotic division in mouse spermatocytes." Mol Biol Cell 15(3): 1224-32.

Di Agostino, S., P. Rossi, et al. (2002). "The MAPK pathway triggers activation of Nek2 during chromosome condensation in mouse spermatocytes." Development 129(7): 1715-27.

Fry, A. M. (2002). "The Nek2 protein kinase: a novel regulator of centrosome structure." Oncogene 21(40): 6184-94.

Ghigna, C., C. Valacca, et al. (2008). "Alternative splicing and tumor progression." Curr Genomics 9(8): 556-70.

Hayward, D. G., R. B. Clarke, et al. (2004). "The centrosomal kinase Nek2 displays elevated levels of protein expression in human breast cancer." Cancer Res 64(20): 7370-6.

Hayward, D. G. and A. M. Fry (2006). "Nek2 kinase in chromosome instability and cancer." Cancer Lett 237(2): 155-66.

Kokuryo, T., T. Senga, et al. (2007). "Nek2 as an effective target for inhibition of tumorigenic growth and peritoneal dissemination of cholangiocarcinoma." Cancer Res 67(20): 9637-42.

Lamond, A. and D. Spector (2003). "Nuclear speckles: a model for nuclear organelles." Nat Rev Mol Cell Biol 4(8): 605-12.

Lee, J. A., Z. Z. Tang, et al. (2009). "An inducible change in Fox-1/A2BP1 splicing modulates the alternative splicing of downstream neuronal target exons." Genes Dev 23(19): 2284-93.

Lin, S., R. Xiao, et al. (2005). "Dephosphorylation-dependent sorting of SR splicing factors during mRNP maturation." Mol Cell 20(3): 413-25.

Long, J. C. and J. F. Caceres (2009). "The SR protein family of splicing factors: master regulators of gene expression." Biochem J 417(1): 15-27.

Lukong, K. E. and S. Richard (2003). "Sam68, the KH domain-containing superSTAR." Biochim Biophys Acta 1653(2): 73-86.

Matlin, A. J., F. Clark, et al. (2005). "Understanding alternative splicing: towards a cellular code." Nat Rev Mol Cell Biol 6(5): 386-98.

Matter, N., P. Herrlich, et al. (2002). "Signal-dependent regulation of splicing via phosphorylation of Sam68." Nature 420(6916): 691-5.

Najib, S., C. Martin-Romero, et al. (2005). "Role of Sam68 as an adaptor protein in signal transduction." Cell Mol Life Sci 62(1): 36-43.

Paronetto, M., M. Cappellari, et al. (2010). "Alternative splicing of the cyclin D1 proto-oncogene is regulated by the RNA-binding protein Sam68." Cancer Res 70(1): 229-39.

Paronetto, M. P., T. Achsel, et al. (2007). "The RNA-binding protein Sam68 modulates the alternative splicing of Bcl-x." J Cell Biol 176(7): 929-39.

Paronetto, M. P., F. Zalfa, et al. (2006). "The nuclear RNA-binding protein Sam68 translocates to the cytoplasm and associates with the polysomes in mouse spermatocytes." Mol Biol Cell 17(1): 14-24.

Ponta, H., L. Sherman, et al. (2003). "CD44: from adhesion molecules to signalling regulators." Nat Rev Mol Cell Biol 4(1): 33-45.

Rhee, K. and D. J. Wolgemuth (1997). "The NIMA-related kinase 2, Nek2, is expressed in specific stages of the meiotic cell cycle and associates with meiotic chromosomes." Development 124(11): 2167-77.

Ruggero, D. (2009). "The role of Myc-induced protein synthesis in cancer." Cancer Res 69(23): 8839-43.

Sette, C., V. Messina, et al. (2009). "Sam68: A New STAR in the Male Fertility Firmament." J Androl.

Sharp, P. A. (1994). "Split genes and RNA splicing." Cell 77(6): 805-15.

Shin, C., Y. Feng, et al. (2004). "Dephosphorylated SRp38 acts as a splicing repressor in response to heat shock." Nature 427(6974): 553-8.

Stamm, S. (2002). "Signals and their transduction pathways regulating alternative splicing: a new dimension of the human genome." Hum Mol Genet 11(20): 2409-16.

Stamm, S. (2008). "Regulation of alternative splicing by reversible protein phosphorylation." J Biol Chem 283(3): 1223-7.

Tazi, J., N. Bakkour, et al. (2009). "Alternative splicing and disease." Biochim Biophys Acta 1792(1): 14-26.

Venables, J. P. (2004). "Aberrant and alternative splicing in cancer." Cancer Res 64(21): 7647-54.

Venables, J. P. (2006). "Unbalanced alternative splicing and its significance in cancer." Bioessays 28(4): 378-86.

Villagra, A., E. M. Sotomayor, et al. (2010). "Histone deacetylases and the immunological network: implications in cancer and inflammation." Oncogene 29(2): 157-73.

Wai, D. H., K. L. Schaefer, et al. (2002). "Expression analysis of pediatric solid tumor cell lines using oligonucleotide microarrays." Int J Oncol 20(3): 441-51.

Wu, W., J. E. Baxter, et al. (2007). "Alternative splicing controls nuclear translocation of the cell cycle-regulated Nek2 kinase." J Biol Chem 282(36): 26431-40.

Xiao, S. H. and J. L. Manley (1997). "Phosphorylation of the ASF/SF2 RS domain affects both protein-protein and protein-RNA interactions and is necessary for splicing." Genes Dev 11(3): 334-44.

APPENDIX I

PATZ1 is a ubiquitously expressed transcriptional regulator that binds to the RING finger protein RNF4 that, in turn, associates with a variety of transcription factors involved in chromatin remodeling (HMGA1, gscl, SPBP). By virtue of the POZ domain, PATZ1 acts as a transcriptional repressor on different promoters. Recently, it has been shown that PATZ1 is a coregulator of the androgen receptor (AR) acting on the coactivator RNF4, a protein expressed in normal germ cell but not in human testicular tumours. No information on PATZ1 function in normal or neoplastic germ cells was available. In collaboration with the group of Prof. Paolo Chieffi (*Dipartimento di Medicina Sperimentale, II Universita' di Napoli)* we studied the role of PATZ1 in testicular germ cells. Since PATZ1 has been indicated as a potential tumour suppressor gene, we also looked at its expression in tumours deriving from testicular germ cells (TGCTs). Although expression of PATZ1 protein was increased in these tumours, it was delocalized in the cytoplasm, suggesting an impaired function. These results indicate that PATZ1 up-regulation and mis-localization could be associated to the development of TGCTs.

Journal of Pathology
J Pathol 2008; **215**: 39–47
Published online 10 January 2008 in Wiley InterScience
(www.interscience.wiley.com) **DOI:** 10.1002/path.2323

Original Paper

PATZ1 gene has a critical role in the spermatogenesis and testicular tumours

M Fedele,[1] R Franco,[2] G Salvatore,[3] MP Paronetto,[4,5] F Barbagallo,[4,5] R Pero,[1] L Chiariotti,[1,6] C Sette,[4,5] D Tramontano,[1] G Chieffi,[7] A Fusco[1,6] and P Chieffi[1,7]*

[1] *IEOS, CNR and Dipartimento di Biologia e Patologia Cellulare e Molecolare, Università di Napoli 'Federico II, 80131 Naples, Italy*
[2] *Istituto Nazionale dei Tumori 'Fondazione G. Pascale', 80131 Naples, Italy*
[3] *Dipartimento di Medicina Clinica e Sperimentale, Università di Napoli 'Federico II', 80131 Naples, Italy*
[4] *Dipartimento di Sanità Pubblica e Biologia Cellulare, Università di Roma Tor Vergata, 00133 Rome, Italy*
[5] *IRCCS Fondazione Santa Lucia, 00143 Rome, Italy*
[6] *NOGEC, Naples Oncogenomic Center, CEINGE Biotecnologie Avanzate, 80131 Naples, Italy*
[7] *Dipartimento di Medicina Sperimentale, II Università di Napoli, 80138 Naples, Italy*

**Correspondence to:*
P Chieffi, Dipartimento di Medicina Sperimentale, Via Costantinopoli 16, 80138 Naples, Italy.
E-mail: Paolo.Chieffi@unina2.it

No conflicts of interest were declared.

Received: 20 October 2007
Revised: 19 December 2007
Accepted: 28 December 2007

Abstract

PATZ1 is a recently discovered zinc finger protein that, due to the presence of the POZ domain, acts as a transcriptional repressor affecting the basal activity of different promoters. To gain insights into its biological role, we generated mice lacking the *PATZ1* gene. Male *PATZ1*$^{-/-}$ mice were unfertile, suggesting a crucial role of this gene in spermatogenesis. Consistently, most of adult testes from these mice showed only few spermatocytes, associated with increased apoptosis, and complete absence of spermatids and spermatozoa, with the subsequent loss of tubular structure. The analysis of *PATZ1* expression, by northern blot, western blot and immunohistochemistry, revealed its presence in Sertoli cells and, among the germ cells, exclusively in the spermatogonia. Since *PATZ1* has been indicated as a potential tumour suppressor gene, we also looked at its expression in tumours deriving from testicular germ cells (TGCTs). Although expression of PATZ1 protein was increased in these tumours, it was delocalized in the cytoplasm, suggesting an impaired function. These results indicate that PATZ1 plays a crucial role in normal male gametogenesis and that its up-regulation and mis-localization could be associated to the development of TGCTs.

Keywords: MAZR; ZSG; spermatogenesis; testicular cancer; tumour suppressor

Introduction

PATZ1, also named *MAZR* or *ZSG*, is a recently discovered ubiquitously expressed transcriptional regulatory factor gene whose product binds to the RING finger protein RNF4 that, in turn, associates with a variety of transcription regulators (HMGA1, gscl, SPBP) [1–4]. By virtue of the POZ domain, PATZ1 acts as a transcriptional repressor on different promoters [1–5], even though it has been also shown to function as a strong activator of the c-myc promoter [6]. Indeed, PATZ1 is able to bind proteins involved in chromatin remodeling such as HMGA1 and the above-mentioned RNF4 [1]. Interestingly, it has been found rearranged through a paracentric inversion of 22q12 with the *EWS* gene, in small round cell sarcoma, suggesting a potential tumour suppressor role [4]. Recently, it has been shown that PATZ1 is an androgen receptor (AR) coregulator that acts by modulating the effect of the AR coactivator RNF4 [7], a protein expressed in normal germ cell but not in human testicular tumours [8]. In addition, it has been described its function in mast cells [9] and in brain [10]. However, no information is currently available on the expression or involvement of PATZ1 in human germ cell tumours. Testicular germ cell tumours (TGCTs) are a heterogeneous group of neoplasms seen mainly in young men [11]. They are classified as seminomatous (SE-TGCT) and non-seminomatous (NSE-TGCT) tumours, both of which appear to arise from intratubular germ cell neoplasias (ITGCN) [11]. The former is constituted by neoplastic germ cells that retain the morphology of primordial germ cells or gonocytes, whereas NSE-TGCT display primitive zygotic (embryonal carcinomas), embryonal-like somatically differentiated (teratomas) and extra-embrionally differentiated (choriocarcinomas, yolk sac tumours) patterns [11]. TGCTs are frequently associated with ITGCN that, often, progresses to invasive cancer [11].

The molecular basis of germ cell malignant transformation is poorly understood. The most common genetic alterations detected in TGCTs and ITGCN are

a triploid/tetraploid chromosomal complement and an increased copy number of 12p, which results in over-expression of the product of the *CCND2* gene, viz. G_1 cyclin D2 [12,13]. In addition, deficiencies in the short arms of chromosomes 1, 3 and 11 are associated with TGCTs [14,15], suggesting the presence of a TGCT specific suppressor genes in these regions. It is important to note that high frequency of allelic imbalance was observed also at chromosome arm 22q [16,17]. TGCTs are often accompanied by the over-expression of autocrine and/or paracrine growth and angiogenic factors such as glial cell line-derived neurotrophic factor (GDNF), and vascular endothelial growth factor (VEGF) [18,19]. It was recently shown that the loss of the tumour suppressor gene *PTEN* plays a crucial role in the pathogenesis of TGCTs [20].

Due to the impairment of the male fertility shown by *PATZ1* $^{-/-}$ mice, we analysed the role of this gene in the spermatogenesis. Interestingly, gene transcript and protein analysis revealed the presence of PATZ1 exclusively in the spermatogonia and Sertoli cells. Moreover, we found that the disrupted spermatogenesis in *PATZ1*-null mice is associated with an increased apoptosis and subsequent loss of tubule structure. PATZ1 expression in TGCTs was also analysed. In contrast to its suggested tumour suppressor role, PATZ1 was found over-expressed in TGCTs compared to normal human testis. Nevertheless, immunohistochemical studies followed by Western blot performed on cytoplasmic/nucleic fractionated samples showed a cytoplasmic delocalization of the PATZ1 protein, suggesting an impairment of its function. Taken together these results indicate that PATZ1 could play a key role in normal male gametogenesis and TGCTs.

Materials and methods

Tissue samples

As a source of normal tissue, 10 CD1 adult mice (Charles River Italia) were killed and the testes removed and stored at −80 °C until being processed or quickly prepared for histological examination. The animals used in the present study were maintained at the Department of Biology and Pathology Animal Facility. The study was approved by our institutional committee on animal care. As a source of neoplastic tissues, the tissue Bank of National Cancer Institute 'G. Pascale' provided 14 cases of cryopreserved tissue from seminomas and 16 non-seminomas (eight embryonal carcinomas, eight teratomas). To analyse the *in situ* germ cell tumours, we evaluated six *in situ* carcinomas areas in six of 14 examined seminomas. Ethical Committee approval was given in all instances.

Testicular cells isolation

Spermatogonia and Sertoli cells were prepared from 7dpp testes as previously described [21]. Testes from 40–60 day-old CD1 mice (Charles River, Como, Italy) were used to obtain pachytene spermatocytes and spermatids by elutriation technique as previously described [22,23]. Mature spermatozoa were obtained from the cauda of the epididymus of mature mice [23].

Histological analysis and immunohistochemistry

For light microscopy, tissues were fixed by immersion in 10% formalin and embedded in paraffin by standard procedures; 5 μm sections were stained with haematoxylin and eosin (H&E) or processed for immunohistochemistry. The classical avidin–biotin peroxidase complex (ABC) procedure was used for immunohistochemistry. The sections were incubated overnight with antibodies against PATZ1 at 1 : 200 dilution and against PCNA (Dako Corp., Denmark) at 1 : 200 dilution. The following controls were performed: (a) omission of the primary antibody; (b) substitution of the primary antiserum with non-immune serum diluted 1 : 500 in blocking buffer; (c) addition of the target peptide used to produce the antibody (10^{-6} M); no immunostaining was observed after any of the control procedures. The antibodies against the PATZ1 proteins are described elsewhere [1].

TUNEL and apoptotic assays

Testes were dissected and fixed in 4% paraformaldehyde overnight, dehydrated, and embedded in paraffin, then subjected to TUNEL assay, which was performed according to Boehringer-Mannheim's *in situ* cell death detection instructions, as described previously [24]. For quantitation of apoptosis in testes, sections of testes derived from mice with different genotypes and from the same litter were subjected to TUNEL assay. The number of both TUNEL-positive and TUNEL-negative tubules was determined, and TUNEL-positive cells per each tubule were counted.

RNA extraction and northern blot analysis

Total RNA was extracted from cells and tissues using the RNAzol kit (Tel-Test Inc., Friendswood, TX, USA) according to standard procedures; 20 μm total RNA were fractionated on a 1.2% agarose/formaldehyde gel and blotted onto a nylon membrane (Hybond-N, Amersham, UK). Northern blot hybridization was performed as described previously [25]. The *PATZ1* cDNA were radiolabelled with a random prime synthesis kit (Amersham, Milan, Italy).

Protein extraction and western blot analysis

Total proteins were prepared as described [26]. Differential extraction of nuclear or cytoplasmic proteins was obtained as previously described [20]. Mouse tissues and TGCT extracts (40 μm) were analysed by western blot, using either rabbit anti-PATZ1 antibody (1 : 400) or rabbit anti-Bak (1 : 1000; Santa Cruz, CA, USA), or rabbit anti-caspase 3 (1 : 1000; Santa Cruz), or rabbit anti-ERK1/2 (1 : 1000; Santa Cruz), or mouse

anti-β-Actin (1 : 1000; Sigma, Italy), or mouse anti-β-tubulin (1 : 1000, Sigma), or rabbit anti-SP1 (1 : 1000, Santa Cruz), and chemiluminescence detection (Amersham, UK) as previously described [26].

Results

Defective spermatogenesis in *PATZ1*$^{-/-}$ male mice

In order to define the *PATZ1* function *in vivo*, we have recently generated *PATZ1*$^{-/-}$ showing a variety of phenotypic alterations (Fedele *et al*., manuscript in preparation). In this work we have focused on the analysis of testis functions. We have observed that all the knockout of both alleles of the *PATZ1* gene are unfertile. *PATZ1*$^{-/-}$ testes mean size and weight were reduced in comparison with those of wild-type mice. Histological examination revealed seminiferous tubules with a small diameter and relatively abundant interstitial tissue, containing hyperplastic Leydig cells, in all *PATZ1*$^{-/-}$ analysed compared to the wild-type mice (Figure 1A, B). The most striking feature was the block of spermatogenesis. Moreover, we observed that most tubules showed cystic dilation with lack of a cellular component. In fact, many tubules had only a few spermatogonia and Sertoli cells, whereas other tubules contained Sertoli cells and degenerating spermatogonia and only a few spermatocytes (Figure 1B). In particular, spermatogonia and spermatocytes had large clear cytoplasms, indicating cell damage. These *PATZ1*-deficient mice were not fertile because they lacked spermatids and spermatozoa (Figure 1B). We also examined the testes of the heterozygote male mice and found no differences from wild-type mice (data not shown). To further define the defective spermatogenesis, we used proliferating cell nuclear antigen (PCNA) as a marker for the proliferative status of spermatogonia. As shown in Figure 1C, D, many tubules of *PATZ1*$^{-/-}$ mice lacked PCNA-positive cells, whereas they were present in wild-type mice.

In addition, to determine whether apoptosis contributes to the abnormality in testes, we carried out terminal dUTP nick-end labeling (TUNEL) assays on testis sections (Figure 2A–C). Apoptotic cells, identified by TUNEL-positive nuclei, were found in the peripheral region near the basement of seminiferous tubule confined only in spermatogonia (Figure 2B). We also evaluated the expression of the apoptotic molecular markers Bak and caspase 3. As shown in Figure 2D, Bak and caspase 3 expression (cleaved isoform) was higher in *PATZ1*$^{-/-}$ testes than in those of wild-type mice.

PATZ1 expression in mouse testicular cells

The presence of testis defects in *PATZ1* knockout mice hampered a detailed analysis of *PATZ1* expression in the testis. Therefore, to define better the cells in which PATZ1 is expressed in normal testis, we examined wild-type testes by immunohistochemistry. PATZ1 protein was found in the germinal epithelium only in the nuclei of some spermatogonia, in Sertoli cells and in a few Leydig cells, but not in spermatocytes, spermatids and spermatozoa (Figure 3A). No staining was observed when the same samples were stained with the antibody pre-incubated with the peptide against which antibody was raised or in the absence of the primary antibodies (data not shown).

We confirmed the differential expression of *PATZ1* in the different cell types in the mouse testis by northern blot hybridization and western blot analysis. *PATZ1* mRNA was expressed as a single band of about 3.0 kb only in the spermatogonia, among the germ cells and in Sertoli cells (Figure 3B). A very low expression was detected in the interstitium (Figure 3B). We confirmed these data also at protein level by western blot analysis of cell extracts from adult mouse testis fractionated in the different types of germ cells. As shown in Figure 3C, PATZ1 protein (about 60 kDa) was clearly detectable only in spermatogonia and Sertoli cells, whereas a very low signal was visible in the interstitum fraction, in agreement with immunohistochemical and northern blot results.

PATZ1 expression in testes of young mice

We next evaluated *PATZ1* expression during spermatogenesis using total RNA from testes of wild-type mice of different ages (6, 13 and 34 days). As shown in Figure 3D, *PATZ1*-specific transcript was abundant in testes of 6 day-old mice when germinal cells are rich in spermatogonia, still present in those of 13 day-old mice when testis contains mainly spermatocytes, and very low in testes from 34 day-old mice when germinal cells are rich in spermatocytes and spermatids. These results are consistent with the expression of the *PATZ1* gene in the first stages of spermatogenesis.

PATZ1 expression in human normal testis

Next, we investigated the expression of PATZ1 in human testes by immunohistochemistry. Normal human germ cell epithelium showed positive nuclear staining for PATZ1 protein, according to previous work in which PATZ1 was shown to be localized exclusively in the speckled nuclear compartment in transfected NIH-3T3 cells [1]. In particular, the immunoreactivity was observed in the nuclei of spermatogonia, Sertoli cells and in a few Leydig cells (Figure 4A).

PATZ1 expression in the germ cell tumours

Since PATZ1 is expressed in the testis and a previous work has suggested a role for this gene in tumourigenesis [4], we examined samples from 30 patients with different TGCTs by immunohistochemistry. PATZ1 protein was generally expressed in seminomas and non-seminomas tumours (teratomas and

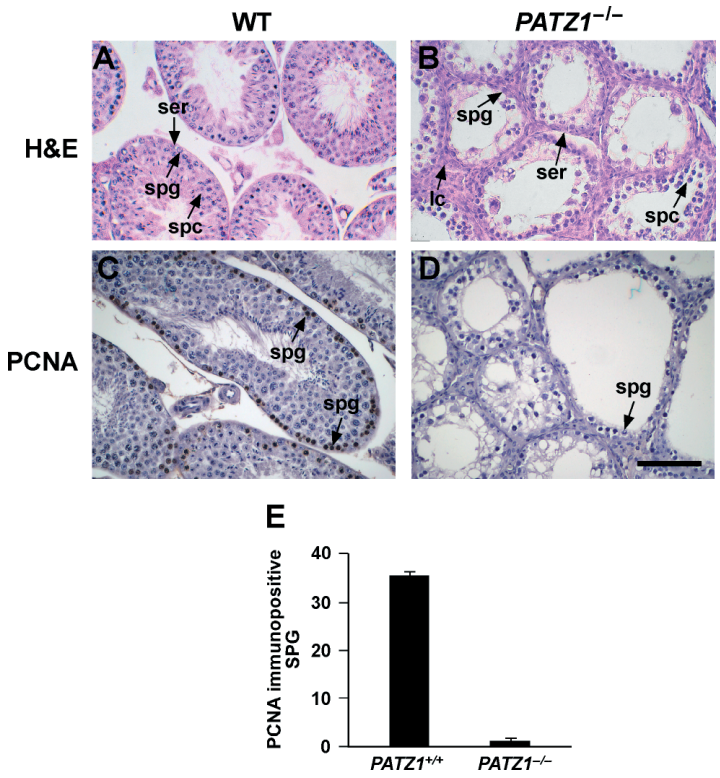

Figure 1. Histological analysis of adult *PATZ1*$^{+/+}$ and *PATZ1*$^{-/-}$ mouse testes. (A) H&E staining for testicular morphology; testis morphology was normal in all adult wild-type animals. (B) In contrast, spermatogenesis is impaired in *PATZ1*$^{-/-}$ testes; many seminiferous tubules of *PATZ1*$^{-/-}$ testis showed only spermatogonia (spg) and Sertoli cells (Ser), and other tubules showed Sertoli cells (ser), degenerating spermatogonia (spg) and spermatocytes (spc); moreover, the interstitial tissue showed an increase of number of Leydig cells (lc). Immunohistochemistry with antibody to PCNA on sections of testes from adult *PATZ1*$^{+/+}$ and *PATZ1*$^{-/-}$. (C) Black arrowheads indicate the spermatogonia (spg) in testis of wild-type, which are PCNA-positive. (D) Degenerating tubules in testis of *PATZ1*$^{-/-}$ mice lack PCNA-positive spermatogonia (spg) (bar = 100 μm). (E) Evaluation of the PCNA immunopositive spermatogonia in the testes of adult *PATZ1*$^{+/+}$ and *PATZ1*$^{-/-}$. Three randomly chosen sections/testis/mouse of each genotype have been evaluated. Values represent the mean ± SE of number of PCNA-positive spermatogonia/total spermatogonia counted/section, multiplied by 100. Significance of differences has been evaluated at $p < 0.01$

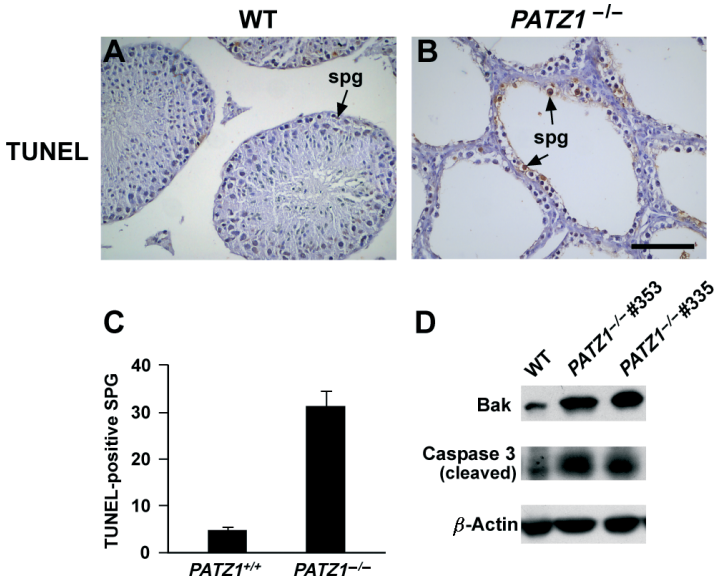

Figure 2. Apoptosis analysis in adult *PATZ1*$^{+/+}$ and *PATZ1*$^{-/-}$ mouse testes. (A) Spontaneous apoptosis in wild-type littermate testis and (B) in *PATZ1*$^{-/-}$ mouse testis. Cells with dark-stained nuclei are apoptotic cells and are indicated by arrowheads (bar = 100 μm). (C) Evaluation of apoptotic cells as measured by TUNEL-positive spermatogonia in the testes of adult *PATZ1*$^{+/+}$ and *PATZ1*$^{-/-}$. Three randomly chosen sections/testis/mouse of each genotype have been evaluated. Values represent the mean ± SE of a number of TUNEL-positive spermatogonia/total spermatogonia counted/section, multiplied by 100. Significance of differences has been evaluated at $p < 0.01$. (D) Western blot analysis of apoptotic molecular markers in the testes of adult *PATZ1*$^{+/+}$ and *PATZ1*$^{-/-}$. In total, 40 μg of total proteins were resolved on 10% SDS–PAGE, transferred onto nitrocellulose filters and western-blotted with anti-Bak and caspase 3 polyclonal antibodies. Antibodies to β-actin served as a loading control

J Pathol 2008; **215**: 39–47 DOI: 10.1002/path

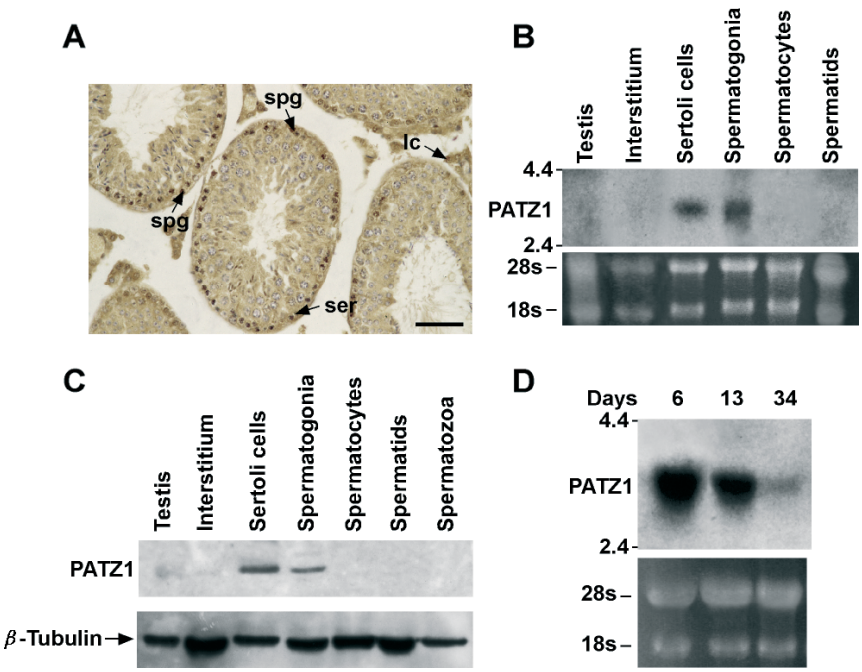

Figure 3. PATZ1 expression in adult mouse testis. (A) Localization of the PATZ1 protein in sections of adult mouse testis by immunohistochemistry. A representative seminiferous tubule showing staining in the nuclei of spermatogonia (spg), Sertoli cells (ser) and Leydig cells (lc) (bar = 100 μm). (B) Expression of *PATZ1* mRNA in mouse testis. Northern blot analysis of *PATZ1* mRNA in adult mouse testis (lane 1), interstitial tissue (lane 2) and normal freshly isolated testicular cell populations (lanes 3–6). Each lane contained 20 μg total RNA. All blots were probed with *PATZ1* cDNA. The integrity and relative abundance of RNA samples were determined by ethidium bromide staining of the filter (lower panel). (C) Distribution of PATZ1 protein in mouse testicular cells. Western blot analysis of PATZ1 protein in mouse adult testis (lane 1), interstitium (lane 2), Sertoli cells (lane 3) and normal mouse germ cells (lanes 4–7) (40 μg/lane). Whole lysates were detected by western blotting with anti-PATZ1 polyclonal serum. Antibodies to β-tubulin served as a loading control. (D) Expression of *PATZ1* mRNA in mouse testes of 6, 13 and 34 day-old mice (lanes 1–3). Each lane contained 20 μg total RNA. All blots were probed with *PATZ1* cDNA. The integrity and relative abundance of RNA samples were determined by ethidium bromide staining of the filter (lower panel)

embryonal carcinomas). In particular, PATZ1 expression was higher in the cytoplasm than in the nucleus in both seminomas and non-seminomas. PATZ1 staining was intense in 12/14 seminomas examined and in all six *in situ* carcinomas examined (Figure 4B, C; Table 1). There was a strong PATZ1 signal also in all the eight teratomas examined and in seven of eight embryonal carcinomas (Figure 4D, E; Table 1).

These observations have been confirmed by Western blot analysis of tissues obtained from a different set of patients. As shown in Figure 5A, PATZ1 is barely detectable in hypertrophic testis and is highly expressed in the TGCTs. In addition, further analysis of the cytoplasmic and nuclear protein fractions from these samples indicated that PATZ1 protein is more abundant in the cytoplasmic fraction compared to the nuclear in TGCTs (Figure 5B); these results are in agreement with the immunohistochemical observations.

Discussion

Testicular development and normal spermatogenesis require specialized transcriptional mechanisms that ensure stringent stage-specific gene expression to form male gametes [27,28]. In the present work, we have studied the expression of PATZ1 in the testis, showing that it is expressed among the germ cells exclusively in spermatogonia. Previous studies have shown that PATZ1 may function as a novel androgen receptor coregulator [7]. In particular, PATZ1 does not directly influence the androgen response, but it acts by attenuating the coactivator activity of RNF4/SNURF [7]. Although it is not clear whether AR is expressed in germ cells, spermatogenesis is essentially dependent on the action of androgens, and Sertoli cells may represent a main site of AR production in the testis [29]. We found that, among the testicular somatic cells, PATZ1 is expressed in Sertoli cells, consistently with a specific role in mediating the androgen response [29]. In particular, the absence of *PATZ1* gene could have a crucial role in the altered regulation of AR machinery essential for the right germ cells maturation inducing the activation of apoptotic pathways. It is important to note that preliminary data, obtained by analysing a limited number of animals do not show significant difference in the serum content of FSH and LH between *PATZ1*-null mice and normal mice. In contrast, an increase in testosterone and oestradiol-17β serum levels was observed in *PATZ1* $^{-/-}$ males in comparison with wild-type mice (data not shown). Studies are in progress in order to confirm these results analysing a large number of animals. In addition, it is interesting to note that, among the germ cells, PATZ1 is exclusively

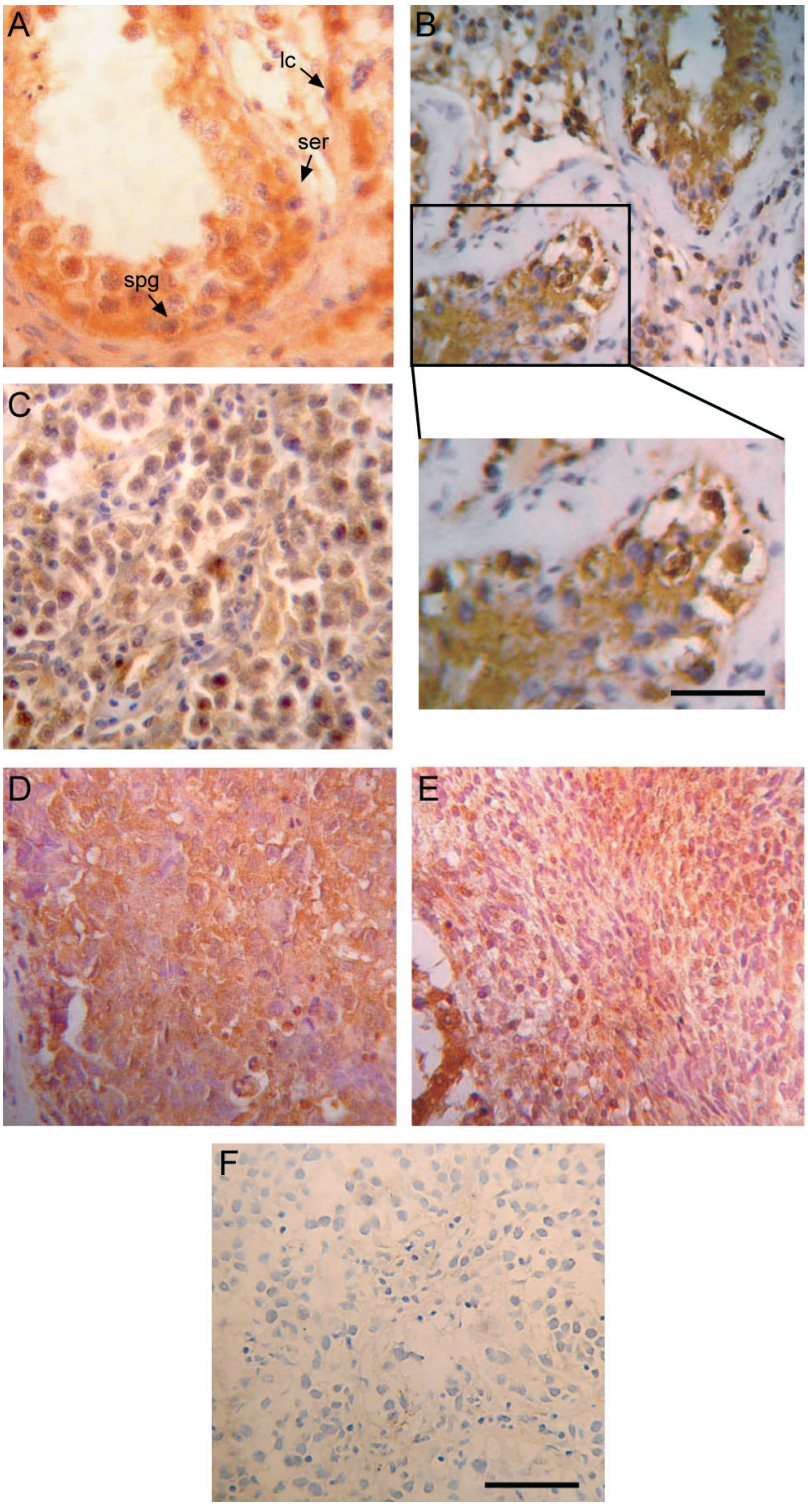

Figure 4. Immunohistochemical analysis of PATZ1 expression in human normal testis, *in situ* carcinoma and testicular germ cell tumors. (A) PATZ1 expression in human normal testis in which a nuclear positivity was observed in spermatogonia (spg), Sertoli cells (ser) and Leydig cells (lc). (B) PATZ1 expression in *in situ* carcinoma, in which an intense cytoplasmic positivity and absence of nuclear positivity were observed; (insert) high magnification of *in situ* carcinoma cells. (C) Classic seminoma with an intense and diffuse cytoplasmic PATZ1 positivity. (D) Embryonal carcinoma with an intense cytoplasmic PATZ1 positivity. (E) Immature teratoma with mesenchymal component, showing an intense cytoplasmic PATZ1 positivity. (F) Control section of a classic seminoma by using the antibody preadsorbed with the cognate peptide (10^{-6} M). In (A–F), bar = 25 μm; insert of (B), bar = 15 μm

expressed in spermatogonia, in which it could exert the role of transcriptional repressor to maintain the stem cell pool. Recently, studies by Buaas and colleagues [30] and Costoya and colleagues [31] have shown that the *Plzf* gene, belonging, like PATZ1, to the POK (POZ and Kruppel) family of transriptional repressors, regulates the mechanisms required for the self-renewal of spermatogonial stem cells. *PATZ1*-null

and *Plzf*-null mice show similar defects in sperm production, suggesting that PATZ1 also influences the ability of spermatogonial self-renewal. However, we observed PATZ1 and PLZF coexpression only in rare spermatogonia (data not shown).

Previous studies have shown that PATZ1 interacts through its POZ-AT hook-zinc finger with HMGA1 and with RNF4 [1,32], both of which are expressed in the testis [8,26,33], showing a restricted expression pattern during spermatogenesis. The *PATZ1* gene is expressed as multiple mRNA variants that give rise to different protein isoforms [4]. Although it cannot be excluded that antibodies used in this study have a different ability to recognize the different PATZ1 isoforms, by comparing protein and mRNA sizes (60 kDa and 3.0 kb, respectively) our data suggest that only PATZ1 variant 3 is expressed in the testis.

To establish whether *PATZ1* gene expression is crucial for testis maturation, we also analysed the testes of *PATZ1* $^{-/-}$, which do not produce spermatids and spermatozoa and in which most spermatogonia and spermatocytes have an abnormal morphology. These mice are unfertile and their testes show few spermatogonia exiting from the mitotic cycle. Moreover, residual postmitotic spermatocytes did not undergo the meiotic divisions required to generate spermatids and, consequently, haploid gametes. Therefore, *PATZ1*

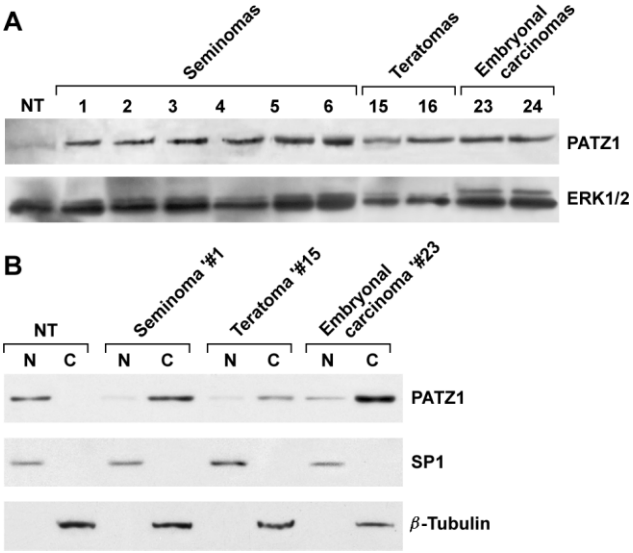

Figure 5. (A) Western blot analysis of PATZ1 expression in human normal and neoplastic testis. 40 μg total proteins were resolved on 10% SDS–PAGE, transferred onto nitrocellulose filters and western-blotted with anti-PATZ1 polyclonal serum. Lane NT, normal testis; lanes 2–7, seminomas (cases 1–6); lanes 8 and 9, teratomas (cases 15 and 16); lanes 10 and 11, embryonal carcinomas (cases 23 and 24). Antibodies to ERK1/2 served as a loading control. (B) Western blot analysis with anti-PATZ1 polyclonal serum on cytoplasmic and nuclear extracts in: normal testis (NT); seminoma (case 1); teratoma (case 15); embryonal carcinoma (case 23); SP1 and β-tubulin were used as controls of fractionated proteins. N, nuclear extracts; C, cytoplasmic extracts

Table 1. Immunohistochemical analysis of PATZ1 in TGCTs

Case	Age	Diagnosis	IHC
1	25	Seminoma	C^{+++}, N^{-}
2	22	Seminoma	C^{++}, N^{-}
3	24	Seminoma	C^{++}, N^{+}
4	27	Seminoma	C^{++}, N^{-}
5	36	Seminoma	C^{++}, N^{-}
6	47	Seminoma	C^{+++}, N^{+}
7	40	Seminoma	C^{++}, N^{-}
8	33	Seminoma	C^{++}, N^{-}
9	33	Seminoma	C^{++}, N^{-}
10	35	Seminoma	C^{+++}, N^{-}
11	30	Seminoma	C^{++}, N^{-}
12	33	Seminoma	C^{++}, N^{-}
13	44	Seminoma	C^{+++}, N^{-}
14	31	Seminoma	C^{+++}, N^{-}
15	34	Teratoma	C^{++}, N^{+}
16	24	Teratoma	C^{+++}, N^{-}
17	27	Teratoma	C^{+++}, N^{-}
18	30	Teratoma	C^{+++}, N^{+}
19	23	Teratoma	C^{++}, N^{-}
20	20	Teratoma	C^{++}, N^{-}
21	22	Teratoma	C^{++}, N^{-}
22	27	Teratoma	C^{+++}, N^{-}
23	22	Embryonal carcinoma	C^{+++}, N^{+}
24	22	Embryonal carcinoma	C^{+++}, N^{-}
25	26	Embryonal carcinoma	C^{+++}, N^{-}
26	24	Embryonal carcinoma	C^{+++}, N^{+}
27	77	Embryonal carcinoma	C^{++}, N^{-}
28	28	Embryonal carcinoma	C^{++}, N^{-}
29	43	Embryonal carcinoma	C^{++}, N^{-}
30	29	Embryonal carcinoma	C^{+++}, N^{-}

N, nuclear localization; C, cytoplasmic localization.
+++, very high intensity; ++, moderate intensity; +, mild intensity; −, no reactivity.

seems to be involved in the network that regulates the first mitotic steps of development of the germ cells. We hypothesize that PATZ1 protein, by interacting with other nuclear proteins, such as RNF4 or HMGA1, regulates the expression of testis-specific proteins that are required for spermatogenic mitotic proliferation. The analysis of the genes expressed in normal and *PATZ1* $^{-/-}$ testes might lead to the identification of other factors involved in the regulation of process of germinal epithelium proliferation. Previous studies have suggested a tumour suppressor role for the *PATZ1* gene [4]. In addition, it has been shown that RNF4 expression is down-regulated in TGCTs [8], while HMGA1 is over-expressed in seminomas and embryonal carcinomas [34]. Therefore, we investigated PATZ1 expression in human TGCTs. Despite its suggested tumour suppressor role, we observed an increase of the PATZ1 protein in these tumours compared to normal testes but, interestingly, PATZ1 protein was mainly delocalized in the cytoplasm. Cytoplasmic sequestration of nuclear proteins in tumours has been identified only recently as a mechanism whereby cancer cells promote carcinogenesis in humans [35,36]. This has been well described for $p27^{kip1}$ that is delocalized in the cytoplasm of different human tumour cells including prostate, thyroid, ovarian and breast carcinomas [35,36]. The data shown here on TGCTs led us to consider PATZ1 to function in carcinogenesis with a mechanism similar

to $p27^{kip1}$, even though some questions still remain opened. First, it should be addressed whether mislocalization of PATZ1 observed in these tumours merely contributes to abrogate its function (transcriptional regulation) or also induces PATZ1 to acquire new 'cytoplasmic' functions. Moreover, it will be interesting to investigate whether PATZ1 shuttling between the nucleus and the cytoplasm represents a regulatory mechanism that also operates in normal cells. The potential involvement of PATZ1 in cancer brings additional importance to its identification as a regulator of stem cell differentiation. Understanding the molecular programmes controlling stem cell self-renewal will have an additional impact on development of anticancer therapies.

In conclusion, here we demonstrate that PATZ1 is expressed in a stage-specific manner in the mouse germinal epithelium, and that impairment of *PATZ1* gene function results in disruption of the testis cytoarchitecture and block of spermatogenesis. In addition, we show that PATZ1 is up-regulated and mislocalized in TGCTs compared to human normal testes. This opens the intriguing possibility that PATZ1 function could be impaired in these tumours, according to its previously suggested tumour suppressor role or, alternatively, that it may acquire some new cytoplasmic function related to cellular transformation.

Acknowledgements

This study was supported by the Associazione Italiana per la Ricerca sul Cancro (AIRC) and the Lance Armstrong Foundation. We thank Fabrizio Fiorbianco (www.studiociotola.it) for skilful technical assistance with the artwork.

References

1. Fedele M, Benvenuto G, Pero R, Majello B, Battista S, Lembo F, *et al*. A novel member of the BTB/POZ family, PATZ, associates with the RNF4 RING finger protein and acts as a transcriptional repressor. *J Biol Chem* 2000;**275:**7891–7901.
2. Galili N, Nayak S, Epstein JA, Buck CA. Rnf4, a RING protein expressed in the developing nervous and reproductive systems, interacts with *Gsc1*, a gene within the DiGeorge critical region. *Dev Dyn* 2000;**218:**101–111.
3. Lingsø C, Bouiteiller G, Damgaard CK, Ryom D, Sanchez-Munoz S, Norby PL, *et al*. Interaction between the transcription factor SPBP and the positive cofactor RNF4. An interplay between protein binding zinc fingers. *J Biol Chem* 2000;**275:**26141–26149.
4. Mastrangelo T, Modena P, Tornielli S, Bullrich F, Testi MA, Mezzelani A, *et al*. A novel zinc finger gene is fused to EWS in small round cell tumor. *Oncogene* 2000;**19:**3791–3804.
5. Bilic I, Koesters C, Unger B, Sekimata M, Hertweck A, Maschek R, *et al*. Negative regulation of CD8 expression via Cd8 enhancer-mediated recruitment of the zinc finger protein MAZR. *Nat Immunol* 2006;**7:**391–400.
6. Kobayashi A, Yamagiwa H, Hoshino H, Muto A, Sato K, Morita M, *et al*. A combinatorial code for gene expression generated by transcription factor Bach2 and MAZR (MAZ-related factor) through the BTB/POZ domain. *Mol Cell Biol* 2000;**20:**1731–1746.
7. Pero R, Lembo F, Palmieri EA, Vitiello C, Fedele M, Fusco A, *et al*. PATZ attenuates the RNF4-mediated enhancement of androgen receptor-dependent transcription. *J Biol Chem* 2002;**277:**3281–3285.
8. Pero R, Lembo F, Di Vizio D, Boccia A, Chieffi P, Fedele M, *et al*. RNF4 is a growth inhibitor expressed in germ cells but not in human testicular tumors. *Am J Pathol* 2001;**159:**1221–1230.
9. Morii E, Oboki K, Kataoka TR, Igarashi K, Kitamura Y. Interaction and cooperation of *mi* transcription factor(MITF) and c-Myc-associated zinc-finger protein-related factor (MARZ) for transcription of mouse mast cell protease 6 gene. *J Biol Chem* 2002;**277:**8561–8571.
10. Mitchelmore C, Kjaerulff KM, Pedersen HC, Nielsen JV, Rasmussen TE, Fisker MF, *et al*. Characterization of two novel nuclear BTP/POZ domain zinc finger isoforms. Association with differentiation of hippocampal neurons, cerebellar granule cells, and macroglia. *J Biol Chem* 2002;**277:**7591–7609.
11. Oosterhuis JW, Looijenga LH. Testicular germ-cell tumors in a broader perspective. *Nat Rev Cancer* 2005;**5:**211–222.
12. Chieffi P. Molecular targets for the treatment of testicular germ cell tumors. *Mini-Rev Med Chem* 2007;**7:**751–59.
13. Houldsworth J, Reuter V, Bosl GJ, Chaganti RSK. Aberrant expression of cyclin D2 is an early event in human male germ cell tumorigenesis. *Cell Growth Diff* 1997;**8:**291–299.
14. Looijenga LH, de Munnik H, Oosterhuis JW. A molecular model for the development of germ cell cancer. *Int J Cancer* 1999;**83:**801–814.
15. Looijenga LH, Oosterhuis JW. Pathogenesis of testicular germ cell tumours. *Rev Reprod* 1999;**4:**91–100.
16. Lothe RA, Peltomaki P, Tommerup N, Fossa SD, Stenwing AE, Stewing AL, *et al*. Molecular genetic changes in human male germ cell tumors. *Lab Invest* 1995;**73:**601–614.
17. Bergthorsson JT, Agnarsson BA, Gudbjartsson T, Magnusson K, Thoroddsen A, Palsson B, *et al*. A genome-wide study of allelic imbalance in human testicular germ cell tumors using microsatellite markers. *Cancer Genet Cytogenet* 2006;**164:**1–9.
18. Viglietto G, Romano A, Maglione D, Rambaldi M, Paoletti I, Lago CT, *et al*. Neovascularization in human germ cell tumors correlates with a marked increase in the expression of the vascular endothelial growth factor but not in the placenta-derived growth factor. *Oncogene* 1996;**13:**571–587.
19. Meng X, de Rooij DG, Westerdahl K, Saarma M, Sariola H. Promotion of seminomatous tumors by targeted overexpression of glial cell line-derived neurotrophic factors in mouse testis. *Cancer Res* 2001;**61:**3261–3271.
20. Di Vizio D, Cito L, Boccia A, Chieffi P, Insabato L, Pettinato G, *et al*. Loss of tumour suppressor gene *PTEN* marks the transition from intratubular germ cell neoplasias (ITGCN) to invasive germ cell tumors. *Oncogene* 2005;**24:**1881–1894.
21. Rossi P, Dolci, S, Albanesi C, Grimaldi P, Ricca R, Geremia R. Follicle-stimulating hormone induction of steel factor (SLF) mRNA in mouse Sertoli cells, and stimulation of DNA synthesis in spermatogonia by soluble SLF. *Dev Biol* 1993;**155:**61–74.
22. Meistrich ML. Separation of spermatogenic cells and nuclei from rodent testes. *Methods Cell Biol* 1997;**15:**11–54.
23. Sette C, Barchi M, Bianchini A, Conti M, Rossi P, Geremia R. Activation of the mitogen-activated protein kinase Erk1 during meiotic progression of mouse pachytene spermatocytes. *J Biol Chem* 1999;**124:**2261–2274.
24. Chen WS, Manova K, Weinstein DC, Duncan SA, Plump AS, Prezioso VR, *et al*. Disruption of the *HNF-4* gene, expressed in visceral endoderm, leads to cell death in embryonic ectoderm and impaired gastrulation of mouse embryo. *Genes Dev* 1994;**8:**2461–2477.
25. Sambrook J, Fritsch EF, Maniatis T. *Molecular Cloning: A Laboratory Manual*, 2nd edn. Cold Spring Harbor Laboratory Press: Cold Spring Harbor, NY, 1989.
26. Chieffi P, Battista S, Barchi M, Di Agostino S, Pierantoni GM, Fedele M, *et al*. HMGA1 and HMGA2 protein expression in mouse spermatogenesis. *Oncogene* 2002;**21:**3541–3550.
27. McCarrey JR. Development of germ cell. In *Cell and Molecular Biology of the Testis*, Desjardins C, Ewing LL (eds). Oxford University Press: New York, 1993; 51–89.
28. Eddy EM. Regulation of gene expression during spermatogenesis. *Semin Cell Dev Biol* 1998;**9:**451–457.

29. Suarez-Quian CA, Martinez-Garcia F, Nistal M, Regadera J. Androgen receptor distribution in the adult human testis. *J Clin Endocrinol Metab* 1991;**84:**351–358.
30. Buaas WF, Kirsh AL, Sharma M, McLean DJ, Morris JL, Griswold MD, *et al*. Plzf is required in adult male germ cells for stem cell self-renewal. *Nat Genet* 2004;**36:**641–652.
31. Costoya JA, Hobbs RM, Barna M, Cattoretti G, Manova K, Sukhwani M, *et al*. Essential role of Plzf in maintenance of spermatogonial stem cells. *Nat Genet* 2004;**36:**651–659.
32. Chiariotti L, Benvenuto G, Fedele M, Santoro M, Simeone A, Fusco A, *et al*. Identification and characterization of a novel RING-finger gene (*RNF4*) mapping at 4p16.3. *Genomics* 1998;**47:**251–265.
33. Pero R, Lembo F, Chieffi P, Del Pozzo G, Fedele M, Fusco A, *et al*. Translational regulation of a novel testis-specific *RNF4* transcript. *Mol Reprod Dev* 2003;**66:**1–7.
34. Franco R, Esposito F, Fedele M, Liguori G, Pierantoni MG, Botti G, *et al*. Detection of high mobility group proteins A1 and A2 represents a valid diagnostic marker in post-pubertal testicular germ cell tumours. *J Pathol* 2008;**214:**51–64.
35. Viglietto G, Motti ML, Bruni P, Melillo RM, D'Alessio A, Califano D, *et al*. Cytoplasmic relocalization and inhibition of the cyclin-dependent kinase inhibitor p27Kip1 by PKB/Akt-mediated phosphorylation in breast cancer. *Nat Med* 2002;**8:**1131–1144.
36. Viglietto G, Motti ML, Fusco A. Understanding p27(kip1) deregulation in cancer: down-regulation or mislocalization. *Cell Cycle* 2002;**1:**391–400.

APPENDIX II

Stra8 (stimulated by retinoic acid 8) encodes a protein crucial for mammalian germ cells entering into premeiotic stages but its molecular functions are still unknown. In collaboration with the group of dott. Donatella Farini "*Department of Public Health and Cell Biology, University of Rome "Tor Vergata"* we studied its cellular localization in several cell types demonstrating that STRA8 can exert important functions in the nucleus rather than in the cytoplasm as believed previously, likely depending on the cell type and regulated by its nuclear-cytoplasmic shuttling.

THE JOURNAL OF BIOLOGICAL CHEMISTRY VOL. 284, NO. 51, pp. 35781–35793, December 18, 2009

STRA8 Shuttles between Nucleus and Cytoplasm and Displays Transcriptional Activity*[S]

Received for publication, August 16, 2009, and in revised form, September 22, 2009 Published, JBC Papers in Press, October 5, 2009, DOI 10.1074/jbc.M109.056481

Marianna Tedesco, Gina La Sala, Federica Barbagallo, Massimo De Felici, and Donatella Farini[1]

From the Department of Public Health and Cell Biology, University of Rome "Tor Vergata," 00173 Rome, Italy

Stra8 **(stimulated by retinoic acid 8) encodes a protein crucial for mammalian germ cells entering into premeiotic stages. Here, to elucidate the still unknown STRA8 molecular functions, we studied the cellular localization of the protein in several cell types, including premeiotic mouse germ cells and stem cell lines. We reported distinct STRA8 localization in germ and stem cell types and a heterogeneous protein distribution in the cytoplasm and nucleus of such cells suggesting that the protein can shuttle between these two compartments. Moreover, we identified specific protein motifs determining its nuclear import/export. Furthermore, we demonstrated that in transfected cell lines the nuclear import of STRA8 is an active process depending on an N-terminal basic nuclear localization signal. Moreover, its nuclear export is mainly mediated by the Exportin1 (XPO1) recognition of a nuclear export signal. Significantly, we also demonstrated that STRA8 associates with DNA and possesses transcriptional activity. These observations strongly suggest that STRA8 can exert important functions in the nucleus rather than in the cytoplasm as believed previously, likely depending on the cell type and regulated by its nuclear-cytoplasmic shuttling.**

Germ cells play a unique role as the carriers of genetic information between generations. They are the only cells able to divide meiotically and to halve their genetic material generating haploid cells. In the mouse ovary, oocytes begin meiosis during fetal development around 13.5 days post-coitum (dpc)[2] (1), whereas in the testis the onset of meiosis is delayed until after birth (2).

Recent findings indicate that despite the different timing for the meiotic entry, male and female germ cells might share an identical meiotic initiation pathway in which retinoic acid (RA) induces *Stra8* (stimulated by retinoic acid 8) gene expression in premeiotic germ cells (3–6). The *Stra8* gene encodes a predicted 393-amino acid protein and was originally identified in a gene screening to detect genes that are up-regulated in P19 embryonal carcinoma cells in response to RA (7). A subsequent study reported that *Stra8* is expressed in embryonic stem and germ cells and male germ cells of embryonic and adult mice (8). By using *in situ* hybridization analysis, Menke *et al.* (9) demonstrated that *Stra8* is expressed in embryonic ovaries in an anterior-to-posterior wave that spans ~4 days, from 12.5 to 16.5 dpc. In male gonads, *Stra8* is expressed in premeiotic postnatal germ cells (5, 6) rather than in embryonic germ cells (8). $Stra8^{-/-}$ female and male mice are infertile due to severe gametogenesis impairment (11–13). In particular, in female embryos lacking *Stra8*, the initial mitotic development of germ cells is normal, but they fail to undergo premeiotic DNA replication and meiotic chromosome condensation. In male mutant mice, the premeiotic DNA replication is conserved (11, 13), and germ cells are able to partly condense chromosomes and initiate meiotic recombination. They fail, however, to regularly continue over the leptotene stage of prophase I (13). Although all these studies reinforce the importance of *Stra8* in gametogenesis and perhaps in stem cell physiology, the molecular functions of this protein remain unknown.

Intracellular localization and its dynamics represent important information to identify protein functions. Apart from the study by Oulad-Abdelghani *et al.* (8), in which STRA8 was localized in the cytoplasmic fraction of P19 stem cells, no clear information is available on the intracellular localization of this protein and its dynamics, in particular in premeiotic and meiotic germ cells.

Movement of ions, metabolites, and other small molecules through the nuclear pore complex occurs via passive diffusion, but the translocation of cargoes larger than ~40 kDa generally requires specific transport receptors (14). These transport receptors are central to the nuclear import and export steps of recognizing signal-bearing cargoes, interacting with the nuclear pore complex, and delivering the cargo to its destination compartment. The largest group of transport receptors includes structurally related members of the karyopherin-β/importin-β (Kapβ/Impβ) protein family (importins, exportins, or transportins) that usually bind to specific signals within the cargo protein termed nuclear localization signals (NLS) or nuclear export signals (NES), respectively. These have classically been defined as primary amino acid motifs that are both necessary and sufficient for transport. Importin-α recognizes the NLS and forms a ternary complex with importin-β to enter into the nucleus, whereas exportins recognize the NES in the cargo protein, and the complex is exported from the nucleus by binding with the GTP-bound form of the guanine nucleotide-binding protein Ran

* This work was supported by Italian Ministry of Work and Welfare Grant 1650.
[S] The on-line version of this article (available at http://www.jbc.org) contains supplemental Figs. S1–S4.
[1] To whom correspondence should be addressed: Dept. of Public Health and Cell Biology, University of Rome "Tor Vergata," Via Montpellier 1, 00173 Rome, Italy. Tel.: 39-06-72596152; Fax: 39-06-72596172; E-mail: donatella.farini@uniroma2.it.
[2] The abbreviations used are: dpc, days post-coitum; HLH, helix-loop-helix; NLS, nuclear localization signal; NES, nuclear export signal; XPO1, chromosome region maintenance 1; PGC, primordial germ cell; ATRA, all-*trans*-retinoic acid; GAL4-DBD, GAL4 DNA binding domain; LMB, leptomycin B; WT, wild type; PBS, phosphate-buffered saline; aa, amino acid; GFP, green fluorescent protein; RA, retinoic acid.

(RanGTP) (15). The classical NES sequence, a short leucine-rich motif, is specifically bound by the exportin known as exportin 1 (XPO1 or CRM1) (16).

XPO1 binds export cargo proteins and RanGTP in the nucleus to form an export complex that is subsequently translocated to the cytoplasm where it dissociates by the RanGTPase-activating protein action (16–18). Nuclear-cytoplasmic shuttling plays an important role in regulating the activity of several proteins involved in cell proliferation, transformation and tumorigenesis, and signal transduction (19, 20). For example, numerous transcription factors are held inactive in the cytoplasm until adequate signals trigger their import to the nucleus and allow activation or repression of their respective target genes. Moreover, the nuclear export machinery also counteracts the slow but steady leakage of cytoplasmic proteins into the nuclear compartment.

It was hypothesized that in germ cells and stem cells the regulation of nuclear transport of transcription factors and machinery components could represent an important driver for differentiation (21). For example, importin proteins show a distinct localization pattern through ovary and testis development (22), and it has been shown that Importin13 (*Ipo13*), a member of importin-β gene family, plays a stage-specific role in nuclear-cytoplasmic translocation of cargoes that accompanies meiotic differentiation of the mouse germ cells (23).

STRA8 protein has a predicted 46-kDa mass and from the cytoplasmic compartment could passively enter the nucleus. Here, however, we show that this in not the case. In fact, we describe for the first time distinct cellular localizations of this protein in female and male premeiotic germ cells and in embryonic stem and embryonic carcinoma cell lines and identified specific protein motifs regulating its nuclear import/export. The observation that STRA8, previously described as a prevalently cytoplasmic protein, may actually shuttle between the cytoplasm and nucleus with apparent different dynamics in the cell types analyzed suggests that this protein can exert distinct functions in different cellular compartments. Interestingly, we found that STRA8 can be efficiently cross-linked to DNA, and after binding to DNA, it shows robust transcriptional capability.

EXPERIMENTAL PROCEDURES

Localization of STRA8 in Primordial Germ Cells (PGCs), Spermatogonia, ESD3, and ECF9 cells—For immunocytochemical studies, PGCs were obtained from testes and ovary of 13.5 dpc CD-1 mouse embryos following MiniMACS immunomagnetic cell sorter method (PGCs purity >90%) (24). Spermatogonia were obtained from 7 days postpartum CD-1 mice, as reported previously (25). Mouse embryonic stem cells (ESD3, ATCC) were cultured in the presence of mouse embryonic fibroblasts in Dulbecco's modified Eagle's medium (Invitrogen) supplemented with 15% fetal calf serum (Invitrogen), 1 mM sodium pyruvate, 1× nonessential amino acids, 10^{-4} M 2-mercaptoethanol (Sigma), and 1000 units/ml leukemia inhibitory factor (Immunological Science, Naples, Italy) on gelatin-coated dishes. When indicated, leukemia inhibitory factor was substituted with 1 μM all-*trans*-retinoic acid (ATRA) for 24 h. Mouse F9 embryonic carcinoma cells (ECF9, ATCC) were grown in Dulbecco's modified Eagle's medium supplemented with 10% fetal calf serum. PGCs and spermatogonia were left to adhere to poly-L-lysine-coated slides before fixation. All cell types were fixed by 4% paraformaldehyde in PBS for 10 min at room temperature and then permeabilized for 10 min in 0.1% Triton X-100 in PBS. After a 1-h block in 5% bovine serum albumin in PBS, rabbit IgG or a polyclonal antibody against STRA8 (Abcam) was added at a 1:250 dilution in 0.5% bovine serum albumin in PBS and incubated overnight at 4 °C. A goat anti-rabbit secondary antibody (Alexa Fluor 488 or 568, Molecular Probes) was added to the samples for 1 h, and nuclei were labeled with Hoechst 33349 (1 μg/ml). Samples were visualized under a Leica CTR600 microscope.

TABLE 1
Primers used in this study

Oligonucleotide	Sequence 5′ to 3′
1) GFP-STRA8-up	AGGAATTCTATGGCCACCCCTGGA
2) myc-STRA8 up	AGGAATTCATGGCCACCCCTGGAG
3) GFP-STRA8-dw	AGGTCGACTTACAGATCGTCAAAG
4) GFP-myc-HLH-dw	AGGTCGACCTTATCCAGCTTTCTTCC
5) GFP-ΔHLH-up	AGGAATTCTCCCAACAGCTTAGAGGAG
6) GFP-NES1-up	AGGAATTCTCTGTCACAGGCCCGCCAT
7) GFP-NES1-dw	AGGTCGACcggcaacagagtggagga
8) GFP-NES2-up	AGGAATTCTGGTGAAGAGAGAGAGGTA
9) GFP-NES2-dw	AGGTCGACCTCCTCTGGATTTTCTGA
10) GFP-NES3-up	AGGAATTCTAAGCAGACCATGGACCTC
11) pBINDSTRA8up	AGGGATCCATCCGGAATTCATG
12) pBIND-COOH	AGGGATCCATGACCTCATGGAATTTGAA

DNA Constructs—The coding region of mouse *Stra8* (GenBank™ accession number NM 0092921) was amplified by reverse transcription-PCR from 1 μg of total RNA obtained from 13.5 dpc ovaries using primers 1–3 and 2–3 listed in Table 1. Plasmids expressing the fusion protein GFP-STRA8 and myc-STRA8 were constructed by subcloning the coding sequence of mouse *Stra8* to the C terminus of pEGFP-C1 (Clontech) and pCDNA3-N2myc (Stratagene) using restriction enzymes EcoRI and SalI. GFP-HLH-STRA8 and myc-HLH-STRA8 (aa 1–84), GFP-ΔHLH-STRA8 (aa 99–393), GFP-NES1 (aa 34–207), GFP-NES2 (aa 174–348), and GFP-NES3 (aa 219–393) fragments were amplified by PCR by using pEGFP-C1-STRA8 as template and primers indicated in Table 1 (1–4, 2–4, 5–3, 6–7, 8–9, and 10–3, respectively) and subcloned in pEGFP-C1 and pCDNA3-N2myc. For the GAL4 binding assay, we constructed the pBIND-STRA8-WT (aa 1–393), pBIND-HLH-STRA8 (aa 1–84), pBIND-NH_2-STRA8 (aa 1–207), and pBIND-COOH-STRA8 (aa 209–393) vectors. The STRA8 fragments were amplified by PCR using primers listed in Table 1 (primers 11–3, 11–14, 11–7, and 12–3), digested with BamHI and SalI, and inserted into the pBIND vector (Promega) to express fusion protein with GAL4 DNA binding domain (GAL4-DBD). The sequences of cDNAs were verified by DNA sequencing (BMR Genomics, Padova, Italy). The plasmid encoding yellow fluorescent protein-XPO1 (YFP-XPO1) was generously provided by Dr. J. A. Rodrìguez (University of Basque Country).

Localization of Recombinant Wild-type (WT) STRA8 and Mutant STRA8 in GC-1 and HEK293 Cells—GC-1 and HEK293 cells (ATCC), were grown in Dulbecco's modified

Eagle's medium with 10% fetal calf serum. 2.5×10^5 cells were transfected with 1.5 μg of pEGFP-STRA8 constructs (WT or mutants) or empty vector (pEGFP-C1) or pCDNA3-N2-myc-STRA8 constructs using TransFast transfection reagent (Promega) according to the manufacturer's protocol. Twenty four hours after transfection, the cells were fixed with 4% (v/v) paraformaldehyde for 10 min. For myc-STRA8 detection, cells were permeabilized with 0.1% Triton X-100 in PBS for 5 min at room temperature. Following a blocking step with 10% goat serum in PBS for 45 min, the c-Myc antibody (1:500; 9E10, Santa Cruz Biotechnology) was applied for 1 h at room temperature. After washing with PBS, cells were incubated with goat anti-mouse secondary antibody (Alexa Fluor 568, Molecular Probes) for 45 min. Nuclei were labeled as above. In the case of leptomycin B (LMB) treatment, at 24 h after transfection, the cells were treated with 6 ng/ml LMB for 3 h at 37 °C before fixation. Three samples each of about 100 fluorescent cells were counted and scored for subcellular localization in three independent experiments.

Identification and Mutation of Putative STRA8 NLS and NES—The WoLF PSORT program (26) was used to identify sequences in murine *Stra8* containing highly charged basic amino acid residues (Fig. 5*A,* indicated in *boldface*) that could potentially function as NLS. For generation of basic amino acid mutation (Arg to Ala) of pEGFP-STRA8 (Fig. 5*B, GFP-STRA8-NLSmut*), a QuickChange site-directed mutagenesis kit (Stratagene) was used according to the manufacturer's protocol with specific primers as follows: NLSR28A_R31A, 5′-tgcagaagcttgagcctgcggtggtcgccgcagccctgtcacaggcccg-3′, and NLSR28A_R31A_antisense, 5′-cgggcctgtgacagggctgcggc-gaccaccgcaggctcaagcttctgca-3′.

NES motif prediction was achieved by using a Web-based NES motif predictor, NES Finder 0.2 (see Fig. 6*B*). A QuickChange site-directed mutagenesis kit was also used for generation of hydrophobic amino acids mutation to Ala of pEGFP-STRA8 (GFP-STRA8-NES1mut, GFP-STRA8-NES2mut, GFP-STRA8-NES3mut, Fig. 7*A*) with specific primers as follows: NES1F92A_L94A, 5′-ttgctgaagctcaaagcatccgccaacgcgcaagatggg-aatcccaacag-3′, and NES1F92A_L94A_antisense, 5′-ctgttgggattc-ccatcttgcgcgttggcggatgctttgagcttcagcaa-3′; NES2L216A_F218A, 5′-acctcatggaatttgaacggtatgccaacgcttacaagcagaccatggacctc-3′, and NES2L216A_F218A_antisense, 5′-gaggtccatggtctgct-tgtaagcgttggcataccgttcaaattccatgaggt-3′; NES3:I356A_F358A, 5′-ggagaaatttcagctctacatacaggccattgaggctttcaaaagccttggct-gtgttaac-3′, and NES3:I356A_F358A_antisense, 5′-gttaac-acagccaaggcttttgaaagcctcaatggcctgtatgtagagctgaaatttctcc-3′. The DNA sequence of all mutants was confirmed at BMR Genomics.

Cell Fractionation and Western Blot Analysis—Total lysates were obtained from freshly isolated PGCs and spermatogonia. ESD3 and ECF9 cells were treated with ATRA (1 μM) for 24 h before lysis. GC-1 or HEK293 cells were lysed 24 h after transfection. Protein cellular extraction was performed in Lysis buffer (50 mM HEPES (pH 7.9), 15 mM $MgCl_2$, 150 mM NaCl, 10% glycerol, 1% Triton X-100, 0.1% SDS, 0.5 mM dithiothreitol, 10 μg/ml phenylmethylsulfonyl fluoride, and protease inhibitor mix (Sigma)) for 30 min on ice. Insoluble material was removed by centrifugation at 13,000 rpm for 10 min. For cellular protein fractionation, 24 h after transfection cells were lysed in buffer A (10 mM HEPES (pH 7.9), 1.5 mM $MgCl_2$, 10 mM KCl, 0.5 mM dithiothreitol, 10 μg/ml phenylmethylsulfonyl fluoride, and protease inhibitor mix (Sigma)). The homogenates were centrifuged for 10 min at 3,000 rpm to pellet nuclei. The supernatants were collected and used as cytosolic fractions. Nuclear fractions were extracted with buffer C (20 mM HEPES (pH 7.9), 1.5 mM $MgCl_2$, 600 mM NaCl, 0.5 mM dithiothreitol, 10 μg/ml phenylmethylsulfonyl fluoride, and protease inhibitor mix), followed by centrifugation for 15 min at 21,000 $\times$ *g*. Equal cellular amounts of each fraction were used for Western blot analysis. The indicated antibodies were diluted in TBST buffer (5% nonfat dry milk, 50 mM Tris-HCl, 150 mM NaCl (pH 7.5), 0.1% (v/v) Tween 20) and added to the polyvinylidene difluoride membranes for 1 h at room temperature or overnight at 4 °C followed by incubation with the appropriate horseradish peroxidase-conjugated secondary antibodies (Amersham Biosciences) for 45 min at room temperature. All proteins were detected with ECL Plus detection reagents (Amersham Biosciences) and visualized by chemiluminescence.

Immunoprecipitation—GC-1 cells cultured 24 h after transfection with pCDNA3-N2 myc-STRA8 were washed with cold PBS and lysed (20 min at 4 °C) in buffer containing 50 mM Tris-HCl (pH 7.6), 150 mM NaCl, 2 mM EDTA, 1% Nonidet P-40, 3% glycerol, 10 μg/ml phenylmethylsulfonyl fluoride, and protease inhibitor mix (Sigma). Immunoprecipitation was carried with 1 μg of c-Myc antibody (9E10, Santa Cruz Biotechnology) or mouse IgG for 2 h at 4 °C. After washing, precipitates were analyzed by Western blotting using anti-XPO1 (BD Transduction Laboratories) or anti c-Myc mouse monoclonal antibodies.

Cross-Linking Experiment—ECF9 and ESD3 cells were cultured in 60-mm dishes in the presence of 1 μM ATRA, and 5×10^5 HEK293 cells were transiently transfected with 3 μg of pEGFP-STRA8. After 24 h, cells were treated or not for 10 min with 1% formaldehyde in the culture medium to cause molecular cross-linking according to a standard protocol. Cells were then collected by centrifugation and resuspended in 1 ml of TRIzol solution (Invitrogen). Following the protocol described in Ref. 27, the aqueous phase that contains RNAs was discarded, and DNA (with or without cross-linked proteins) and protein fractions were recovered in the interphase and phenol phase, respectively, after sequential precipitation following the manufacturer's instruction. To isolate DNA-bound proteins, the DNA fraction was resuspended in TE (10 mM Tris, 1 mM EDTA) and treated with 30 μg/ml DNase for 30 min at 37 °C and sonicated. Total and DNA-bound protein fractions were then diluted in SDS-sample buffer for Western blot analysis with either anti-ERK42/44 (Santa Cruz Biotechnology) or anti-STRA8 antibodies.

One-hybrid Transcription Activation Assay—4×10^4 HEK 293 cells were seeded in 24 wells and co-transfected with 200 ng of GAL4 reporter plasmid (pG5-luc, Fig. 9*B*), 200 ng of each pBIND fusion construct, and 200 ng of pCDNA-3 to make final 600 ng of DNA. For positive control experiments, cells were transfected with 200 ng of pACT-myoD containing the VP16 activation domain and 200 ng of pBIND-Id control vector of CheckMate™ mammalian two-hybrid sys-

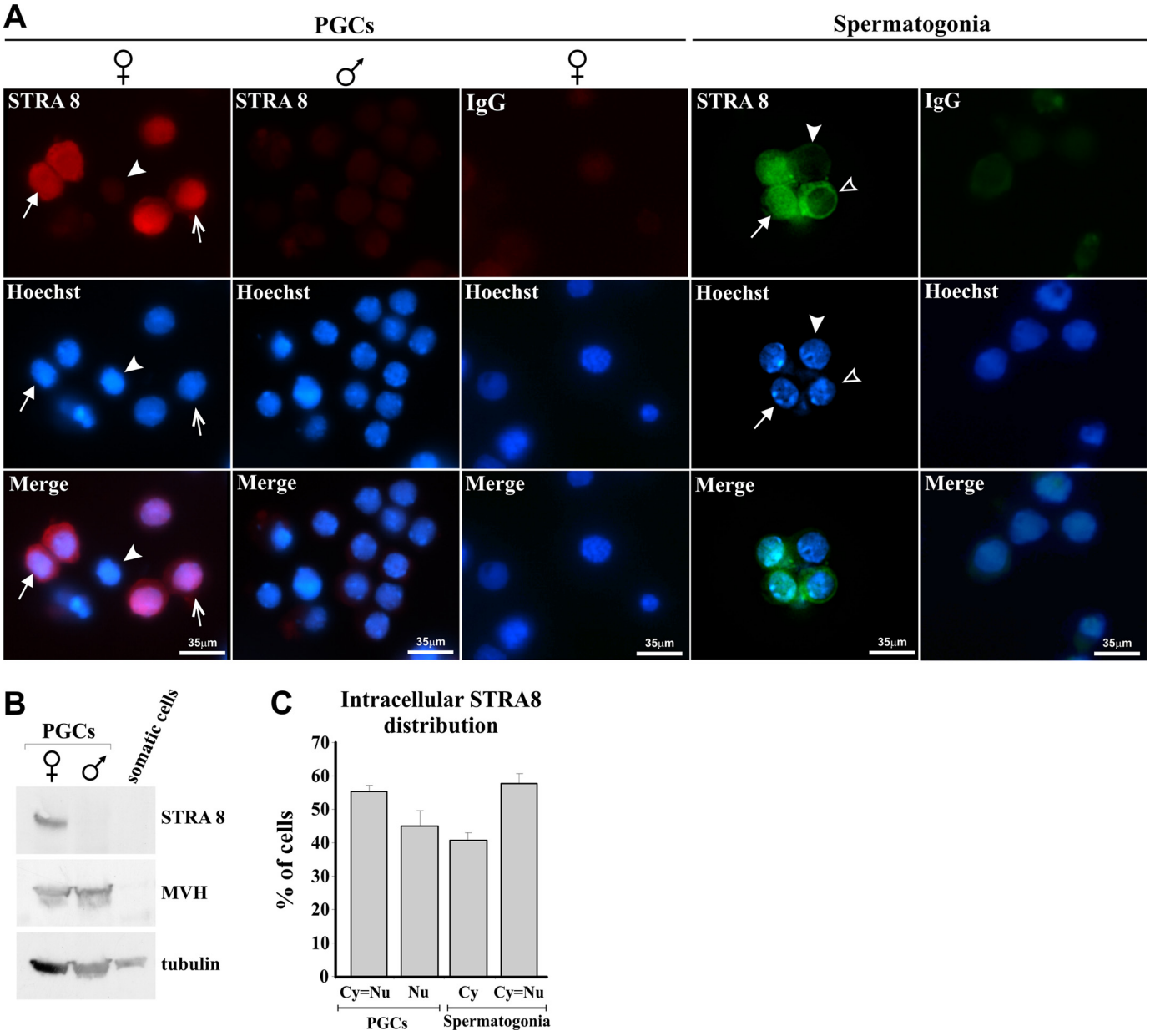

FIGURE 1. **STRA8 immunolocalization in PGCs and spermatogonia.** *A,* immunostaining of STRA8 in PGCs from 13.5 ovaries (♀) and testes (♂) and in 7 ddp spermatogonia. Nuclei were stained with Hoechst. Negative somatic cells (identified by different nuclear morphology and Hoechst staining) are indicated (▲). Note in female PGCs, the localization of STRA8 was in the nucleus and cytoplasm or in the nucleus only (↑). In the spermatogonia population, there are cells in which STRA8 is only present in the cytoplasm (Δ). Rabbit IgG was used as the antibody-negative control (IgG). *B,* immunoblotting for STRA8 in total cell lysates prepared from 20 ovaries (♀) or testes (♂) obtained from 13.5 dpc mice. Lysates were applied to SDS-PAGE followed by immunoblotting with anti-STRA8, anti-Mouse Vasa Homolog (MVH), a PGC-specific marker (45), and anti-β-tubulin as loading control. *C,* quantification of different patterns of STRA8 localization in female PGCs and spermatogonia. At least 100 cells/field were scored for cytoplasmic (*Cy*), nuclear (*Nu*), or diffuse (*Cy=Nu*) STRA8 localization (mean ± S.D. from three experiments).

tem (Promega) instead of pBIND vector. Each well also received 10 ng of a pRL-TK vector (Promega) to normalize for transfection efficiency. At 48 h after transfection, cells were washed three times with PBS and scraped in 100 μl of reporter lysis buffer (Promega). Luciferase activity in 20 μl of the cell extracts was quantified using the Dual-Luciferase reporter assay system (Promega). Protein concentration was determined using a BCA protein assay kit (Pierce). Each extract was assayed three times with a Fluoroskan Ascent FL luminometer. The *Firefly* luciferase activity was divided by the *Renilla* luciferase activity, and transcriptional activity was expressed as fold increase over the pBIND (GAL4-DBD alone) control group.

RESULTS

Intracellular Immunolocalization of STRA8—Cellular immunolocalization showed positivity for STRA8 in about 30% of PGCs freshly isolated from 13.5-dpc ovaries, whereas male PGCs of the same age were immunonegative. Somatic cells of both sexes were STRA8-negative (Fig. 1*A*). These observations are consistent with the notion that at this age female PGCs are entering into meiosis, whereas male PGCs are undergoing a

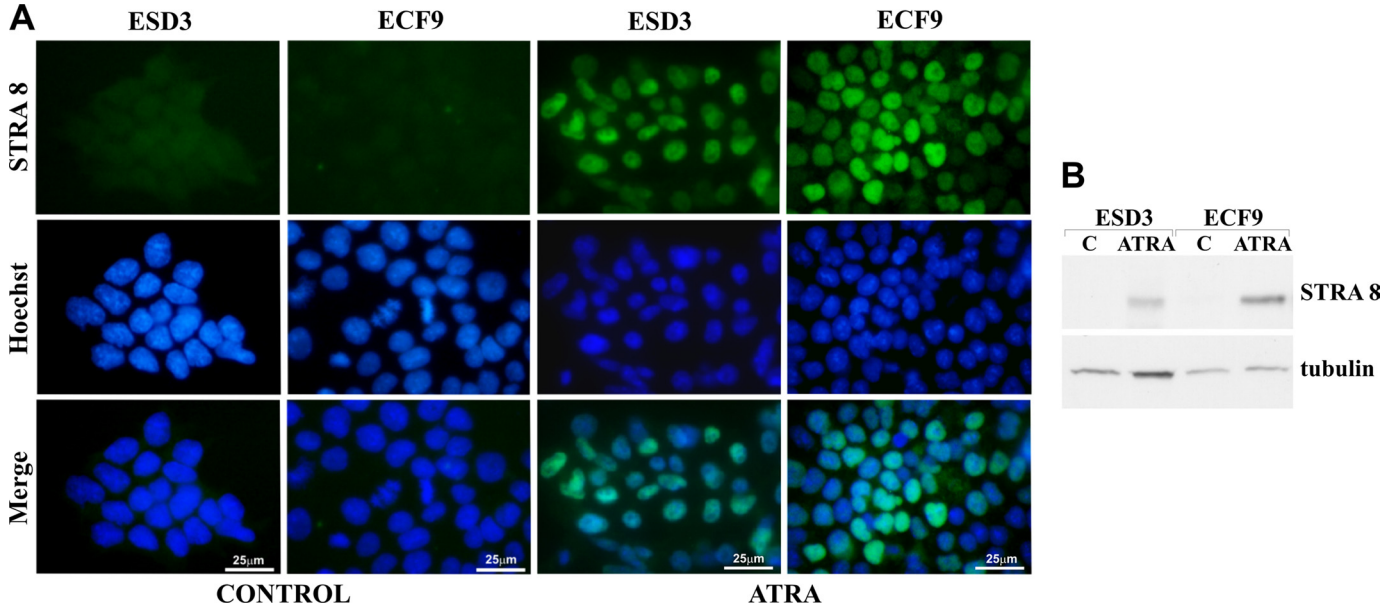

FIGURE 2. **Localization of ATRA-stimulated STRA8 in embryonic stem and embryonic carcinoma cell lines.** *A,* ESD3 and ECF9 cells were cultured with (*ATRA*) or without (*control*) 1 μM ATRA for 24 h before immunostaining. Nuclei were visualized with Hoechst. Note the nuclear STRA8 immunopositivity in ESD3 cells and F9EC cells treated with ATRA. *B,* total lysates from ESD3 and F9EC cells after 24 h with or without ATRA treatment were subjected to immunoblotting with STRA8 antibody. Anti-β-tubulin was used as loading control (*C*).

mitotic block in G_0/G_1 (2). Although in about 55% of the STRA8-positive PGCs, STRA8 was evenly localized in the cytoplasm and nucleus (Fig. 1, *A, upper panel,* and *C*), the protein appeared prevalently nuclear in the rest of the cells (Fig. 1, *A, upper panel,* and *C*). The specificity of the antibody was confirmed by immunoblotting (Fig. 1*B*).

In 7 days postpartum spermatogonia, distinctive STRA8 immunolocalization was observed (Fig. 1, *A, lower panel,* and *C*). About 70% of spermatogonia in the whole population were STRA8-positive, and of these 41% showed the protein immunopositivity exclusively in the cytoplasm, whereas in the remaining a diffuse distribution both in the cytoplasmic and the nuclear compartment was detected. No STRA8 immunopositivity in somatic cells was observed.

Because STRA8 protein was first identified as a retinoic acid-responsive protein in various stem cell types (8), we performed intracellular immunolocalization of the protein also in ESD3 and ECF9 cells cultured for 24 h in the absence or presence of 1 μM ATRA. As expected, STRA8 protein was immunodetectable only when cells were stimulated with ATRA (Fig. 2, *A* and *B*). In both ECF9 and ESD3 cells, STRA8 was exclusively nuclear, and prolonged ATRA incubation for 48 or 72 h did not change the protein localization (data not shown).

STRA8 Can Shuttle between Nucleus and Cytoplasm—To verify whether STRA8 can shuttle between nucleus and cytoplasm and to identify the localization signals, we produced a GFP-STRA8 fusion protein and transiently expressed the construct in different cell types. In GC-1 cells, the only available germ cell line (SV40 T-large antigen immortalized spermatogonia-like cells (28)), in which no STRA8 expression was detectable (data not shown), we observed that GFP-STRA8 localization was heterogeneous with a prevalent presence in the cytoplasm (45%) or throughout the cytoplasm and nucleus (38%) and with the 17% of the transfected cells showing the protein exclusively in the nucleus (Fig. 3, *A* and *B*). A similar heterogeneous GFP-STRA8 compartmentalization was observed in other transfected non-germ cell types (Fig. 3*B*). Immunoblotting of transfected GC-1 cell cytoplasmic and nuclear fraction lysates probed with anti-GFP antibody (Fig. 3*C*) and anti-STRA8 antibody (data not shown) confirmed the heterogeneous distribution of STRA8 in such cells.

Because the fusion with GFP may change the biological function of STRA8 because of larger molecular mass (70 kDa instead 46 kDa) and the fusion with a tag could affect the localization of several proteins (29), we constructed N-terminal Myc-tagged STRA8 expression vector and transfected the construct into both GC-1 cells and HEK293 cells (cells showing very high transfection efficiency). Immunolocalization (supplemental Fig. S1) and immunoblotting analysis (data not shown) gave results comparable with those obtained with the GFP-STRA8 construct.

Nuclear Localization of STRA8 Is Mediated by HLH Domain—The N-terminal HLH domain is a well conserved region of the *Stra8* sequence (NCBI GeneID 20899, aa 17–84; see also supplemental Fig. S2 and supplemental Fig. S3 in Ref. 12. This domain allows protein-protein interaction (30) and may include functional sequences for nucleus-cytoplasm shuttling of proteins (31), for example in Id2 (32) or in the steroid receptor co-activator 3 (SRC-3) (33). To investigate whether the HLH region of STRA8 plays a functional role in its localization, we generated an N-terminal mutant construct deleted in the HLH domain (aa 1–84) and fused to GFP (GFP-ΔHLH-STRA8, schematic representation in Fig. 4*A*). The correct expression of the mutant protein was verified by immunoblotting with anti-GFP antibody in the total cell lysates obtained from transfected GC-1 cells after 24 h of culture (supplemental Fig. S3). As shown in supplemental Fig. S3, we observed a remarkably higher steady-state level of this STRA8 mutant protein (ΔHLH)

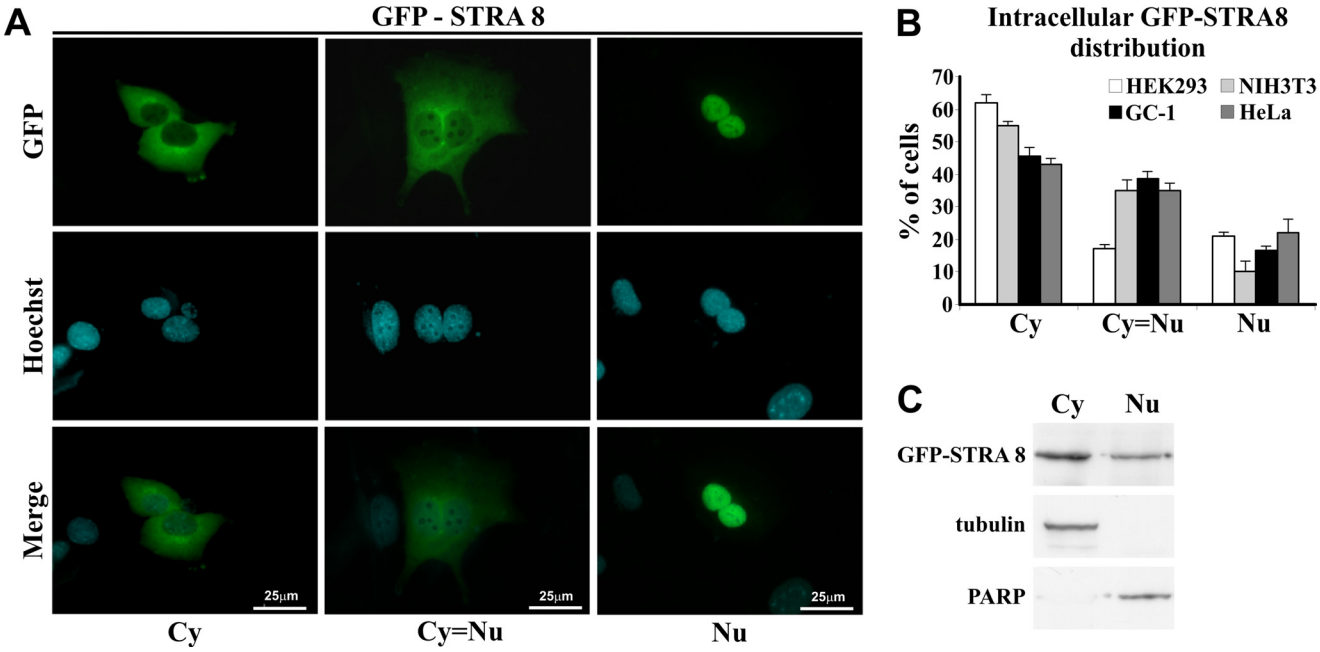

FIGURE 3. **GFP-STRA8 shuttles between the nucleus and cytoplasm in transfected cell lines.** *A,* localization of GFP-STRA8 in GC-1 cells transfected with pEGFP-STRA8 vector. *B*, quantification of the different pattern of STRA8 localization in four types of transfected cells. *Nu,* nuclear; *Cy=Nu,* diffuse; *Cy,* cytoplasmic (mean ± S.D. from three experiments). At least 100 cells were analyzed in each experiment. *C,* immunoblotting for STRA8 in subcellular fraction of GC-1 cells. Cells (2×10^6) were harvested and fractionated into cytoplasmic (*Cy*) or nuclear (*Nu*) fractions as described under "Experimental Procedures." Equal amounts of the two fractions were resolved by SDS-PAGE and analyzed by immunoblotting with anti-GFP (*top*), anti-β-tubulin (a marker for cytoplasmic fraction), and anti-poly(ADP-ribose) polymerase (*PARP*) antibodies (a marker for nuclear fraction).

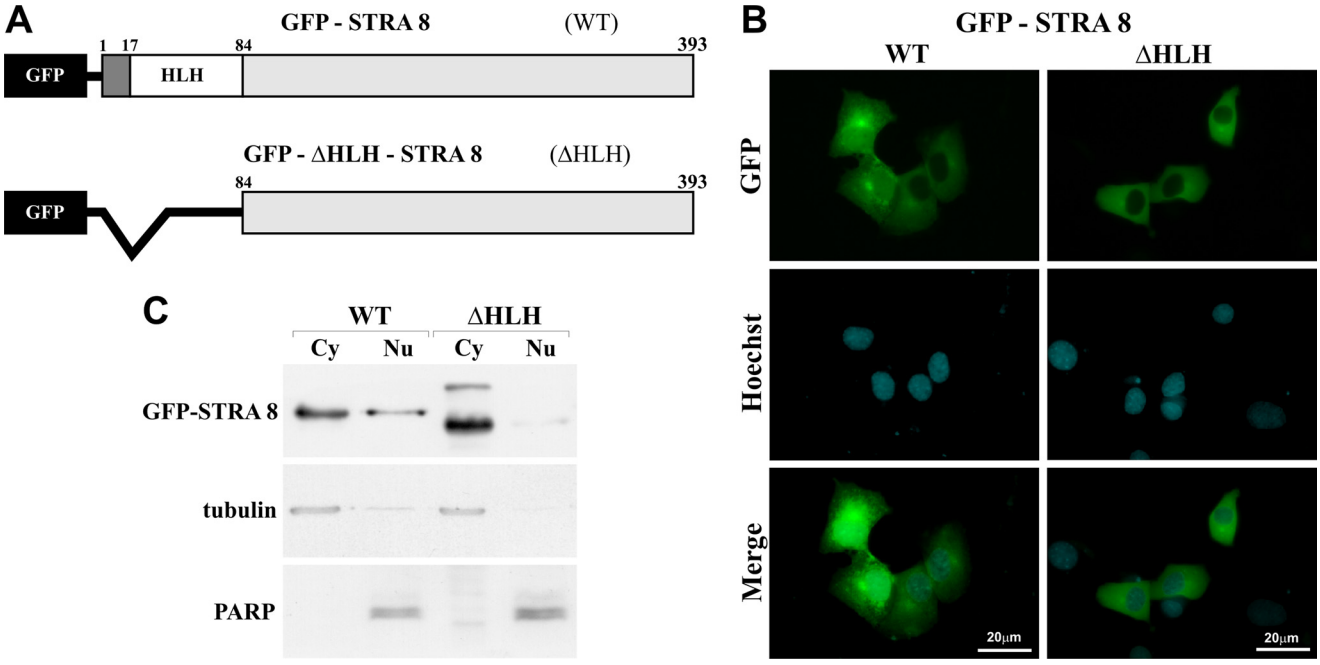

FIGURE 4. **N-terminal HLH domain deletion restrains STRA8 localization in the cytoplasm.** *A*, schematic representation of the GFP-STRA8 fusion protein (*WT*) and HLH deletion mutant (*ΔHLH*). *B,* representative pictures of the localization of the fusion proteins in GC-1 cells transiently expressing WT or ΔHLH STRA8 constructs after 24 h of culture. Note the different nuclear and cytoplasmic localization of WT STRA8 and exclusive cytoplasmic localization of ΔHLH mutant. *C*, cellular compartmentalization of the fusion proteins. After 24 h from transfection with WT or ΔHLH constructs, GC-1 cells were lysed, and aliquots of the cytoplasmic (*Cy*) and nuclear (*Nu*) fractions were subjected to SDS-PAGE followed by immunoblotting using anti-GFP antibody. The blot was reprobed with poly(ADP-ribose) polymerase (*PARP*) and β-tubulin antibodies to mark the nuclear and the cytoplasmic fraction, respectively.

than of the WT STRA8 when equal amounts of plasmid DNA were transfected into the cells. Moreover, an additional higher molecular weight band in the ΔHLH mutant lysates, probably corresponding to a covalent structural modification of the STRA8 protein, was observed. Similar results were obtained in HEK293 and HeLa cell lines (data not shown). When GFP-ΔHLH-STRA8 was transfected in GC-1 cells, a prevalent cytoplasmic localization of the mutant protein in all transfected cells was observed (Fig. 4*B*). A similar result was obtained in HEK293 and HeLa cell lines (data not shown). This distinctive

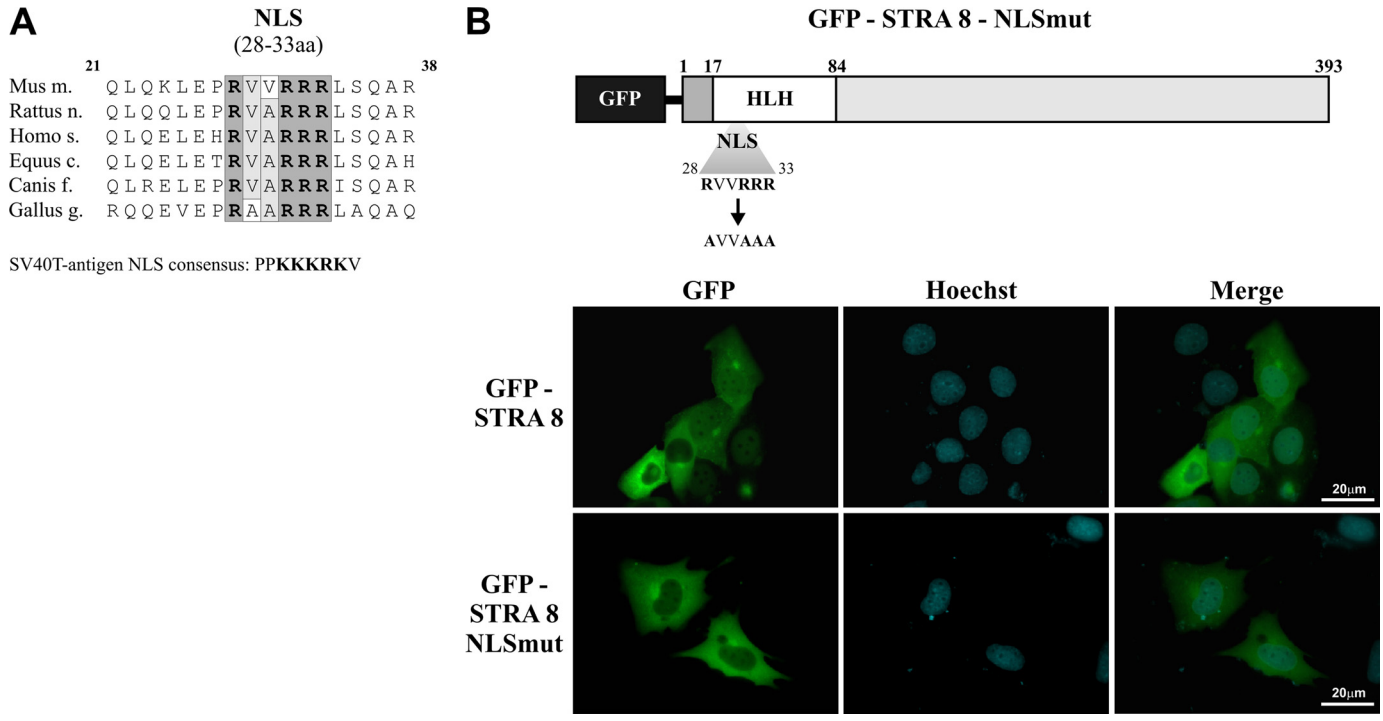

FIGURE 5. **NLS in the HLH domain mediates STRA8 nuclear localization.** *A,* NLS sequence (*boxed*) with the basic amino acids (*boldface*) is conserved in the STRA8 protein from different vertebrate species. The monopartite basic NLS consensus present in SV40-Large Antigen was shown (34). *B, top,* schematic representation of the GFP-STRA8-NLS mutant fusion protein. Basic amino acids (arginine) were muted in alanine. *Bottom,* subcellular localization of GFP-STRA8 or GFP-STRA8-NLSmut in GC-1 cells after 24 h of transfection as determined by fluorescence microscopy. The mutated NLS protein is clearly localized prevalently in the cytoplasm in comparison with WT STRA8.

localization of the ΔHLH mutant in comparison with the WT, confirmed by Western blot analysis using anti-GFP antibody (Fig. 4*C*), suggests that the HLH domain contains a signal that facilitates its nuclear localization or that is necessary to mediate an interaction of STRA8 with an unknown protein promoting its nuclear translocation.

Putative Nuclear Localization Sequences in HLH Domain of STRA8—In the aim to discriminate between the possibilities reported above, we used the WoLF PSORT program (26), which allows us to identify sequences in proteins containing highly charged, basic amino acid residues that could potentially function as NLS. Canonical NLS consist of two classes, including monopartite NLS, composed of a single stretch of basic amino acids (34), and bipartite NLS, consisting of two basic residues, a spacer of ~10 amino acids, and a second region consisting of at least three out of five basic residues (35). We identified a putative nuclear localization signal located at the N-terminal region (amino acid residues ^{28}**R**VV**RRR**) and occurring within the HLH domain. This sequence is a monopartite cluster, and the basic amino acids are conserved among different STRA8 homologs (Fig. 5*A*). We first examined the subcellular localization of the GFP fusion protein containing only the HLH domain of STRA8, and we observed that the protein was uniformly distributed in both cytoplasm and nucleus (data not shown). To check if the failed accumulation into the nuclear compartment of the fusion protein was due to the proximity of GFP to the putative NLS sequence, we transfected GC-1 cells with myc-HLH-STRA8. The immunolocalization of the fusion protein with anti-Myc antibody showed that myc-HLH-STRA8 was exclusively present in the nucleus of the cells (supplemental Fig. S4) indicating that in the HLH domain, a functional NLS is present. To test whether the NLS in the HLH domain is also necessary to induce nuclear import of STRA8, we converted all the basic arginine residues in the sequence (Arg-28 and Arg-31 to Arg-33) to alanine (schematic representation in Fig. 5*B*) and analyzed the distribution of the GFP-STRA8-NLS mutant in transiently transfected GC-1 and HEK293 cells. The correct expression of the mutant protein was verified by immunoblotting with anti-GFP antibody in the total cell lysates obtained from transfected GC-1 cells after 24 h of culture (data not shown). As shown in Fig. 5*B, lower panel*, the GFP-STRA8-NLS mutant localized exclusively in the cytoplasm, confirming the requirement for the **R**VV**RRR** sequence motif for STRA8 nuclear import.

STRA8 Is Actively Exported from Nucleus through XPO1 Recognition of an NES Sequence—The exit of proteins from the nucleus is mainly regulated via the nuclear export receptors. The XPO1 protein, also known as exportin1 and CRM1, is the most versatile of all export receptors, being involved in the movement of many different classes of proteins (17). For this reason, we tested the effect of the specific XPO1-mediated nuclear export inhibitor LMB (36) on the cellular localization of transiently expressed GFP-STRA8 protein in GC-1 and HEK293 cells. Fluorescence imaging in GC-1 cells showed that as expected LMB treatment (6 ng/ml for 3 h) did not change the diffuse nuclear and cytoplasmic localization of the GFP protein (data not shown). However, LMB caused a marked redistribution of GFP-STRA8 with over 95% of the transfected cells showing an increase in its nuclear localization (Fig. 6*A*). The relocalization of GFP-STRA8 to the nucleus was already evident after

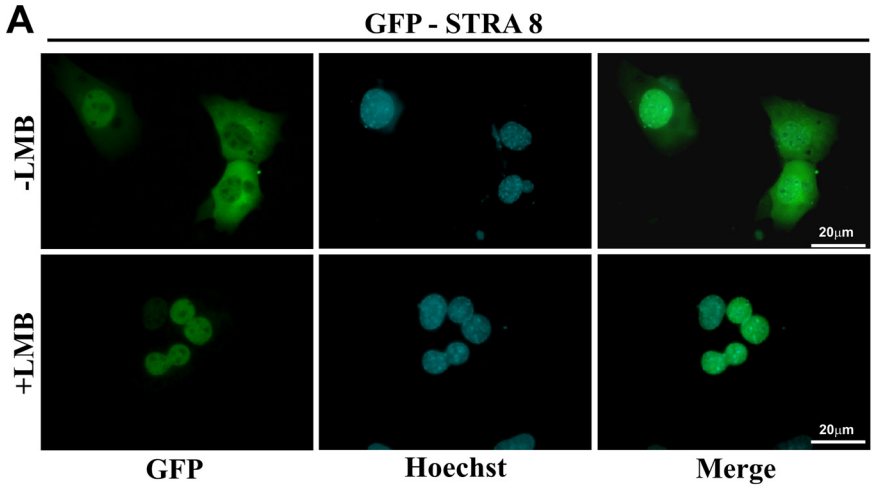

B

	Position (aa)	NES	Type
NES 1	85	LLKLKASFNL	2-3-1
NES 2	209	LMEFERYLNF	2-3-1
NES 3	349	FQLYIQIIEF	3-2-1

NES consensus ΦX(2-3)ΦX(2-3)ΦXΦ
Φ = hydrophobic amino acid
X= any amino acid

RevNES		LQLPPLERLTLD	
APC	68	LLERLKELNLD	78
P53	340	MFRELNEALELK	354
c-Abl	1089	KLRNNLRELQIC	1100
BRCA1	22	LEKPICLEL	30

C

NES 1 (85-94 aa)

	80									98
Mus m.	E	S	L	D	K	L	L	K	L	K	A	S	F	N	L	Q	D	G	N
Rattus n.	I	M	T	L	A	L	V	S	L	I	G	F	F	N	L	Q	D	G	P
Homo s.	Q	T	L	D	N	L	L	K	L	K	A	S	F	N	L	E	D	G	H
Equus c.	Q	T	L	D	N	L	L	K	L	K	E	Y	F	S	L	K	D	G	N
Canis f.	Q	T	L	D	N	L	L	K	L	K	E	S	F	N	L	E	D	G	N
Gallus g.	Q	T	L	S	S	L	L	K	M	K	E	S	F	S	L	E	D	G	N

NES 2 (209-218aa)

	205										220
Mus m.	L	L	P	D	L	M	E	F	E	R	Y	L	N	F	Y	K
Rattus n.	L	L	P	D	L	M	E	F	E	R	Y	L	N	F	Y	K
Homo s.	L	S	P	D	L	M	E	F	E	R	Y	L	N	F	Y	K
Equus c.	L	L	P	D	L	M	E	F	E	R	Y	L	N	F	Y	K
Canis f.	L	L	P	D	L	M	E	F	E	R	Y	L	N	F	Y	K
Gallus g.	S	S	P	D	L	V	E	F	E	R	Y	L	Y	F	Y	K

NES 3 (349-358aa)

	345																	362
Mus m.	P	E	E	K	F	Q	L	Y	I	Q	I	I	E	F	F	K	G	L
Rattus n.	L	E	E	K	F	Q	L	Y	I	Q	I	I	E	F	F	K	G	L
Homo s.	P	E	E	K	F	Q	L	Y	M	Q	I	I	N	F	F	K	G	L
Equus c.	P	E	E	K	F	Q	L	Y	M	Q	I	I	D	F	F	K	G	L
Canis f.	P	E	E	K	F	Q	L	Y	M	Q	I	I	E	F	F	K	G	L
Gallus g.	P	E	D	D	H	R	L	Y	L	Q	I	T	D	F	L	K	S	L

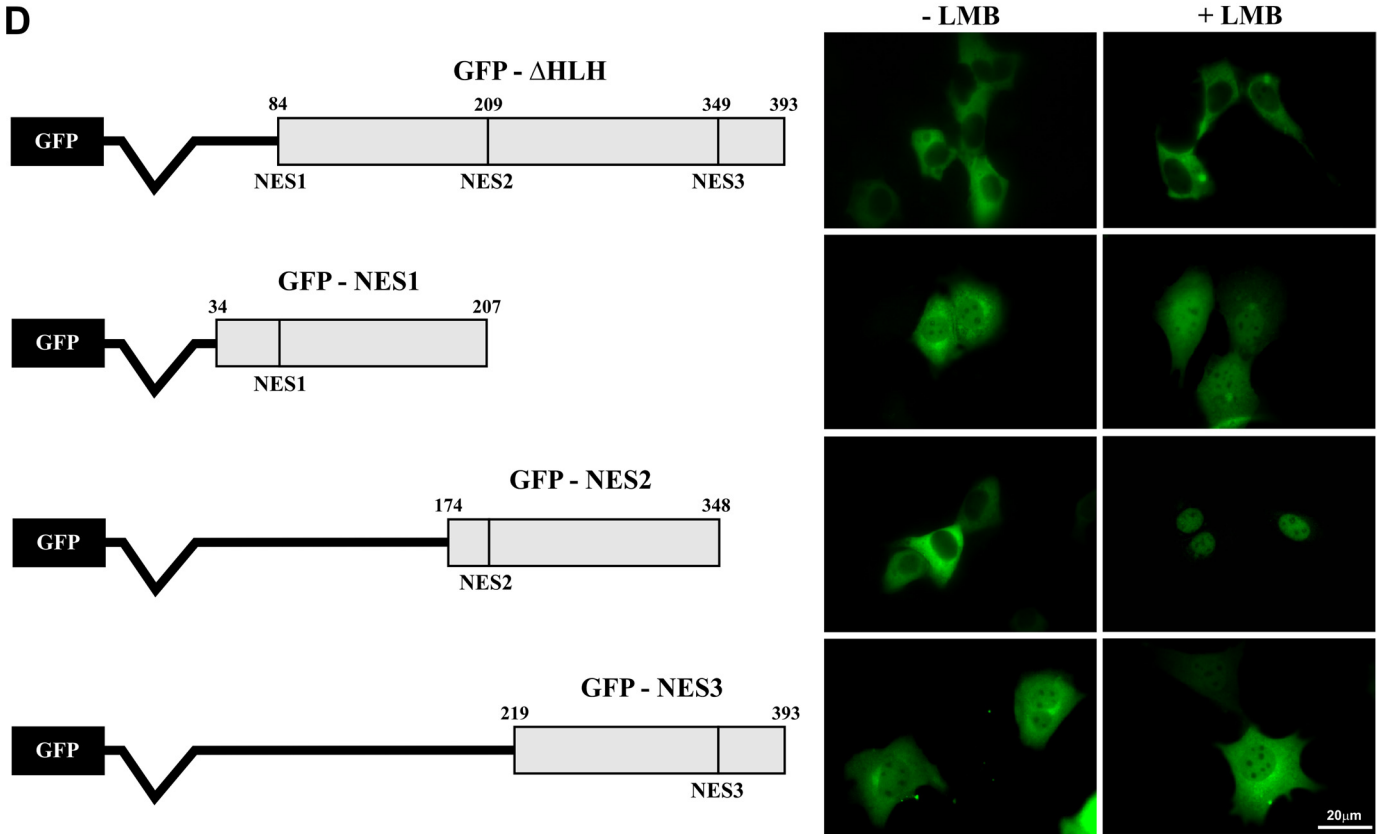

FIGURE 6. **Nuclear export of STRA8 is dependent on XPO1 and NES sequence.** *A,* XPO1-mediated nuclear export inhibitor LMB restrains STRA8 localization in the nucleus. GC-1 cells transiently transfected with GFP-STRA8 plasmid and cultured for 24 h were further incubated without (−*LMB*) or with 6 ng/ml of LMB (+*LMB*) for 3 h. The presence of LMB induced a relocalization of GFP-STRA8 to the nucleus. *B,* identification of STRA8 NES. Three potential NES in *Stra8* sequence was identified with a Web-based NES motif predictor, NES Finder 0.2. In the consensus NES sequence, Φ indicates a large hydrophobic residue, such as leucine, isoleucine, valine, or methionine The RevNES that represents the well characterized NES model and the sequences of other knowing NES in different proteins are shown. *C,* comparison of putative NES in STRA8 homologs of various species. Residues critical to NES activity are indicated in *boldface. D, left,* schematic representation of the GFP-STRA8-NES fusion proteins used for GC-1 cells transfection. *Right*, localization of the corresponding constructs in transfected GC-1 cells treated (+*LMB*) or not (−*LMB*) with LMB for 3 h. Sequences between amino acids 174 and 348 (present in GFP-NES2 construct) were crucial for STRA8 cytoplasmic localization.

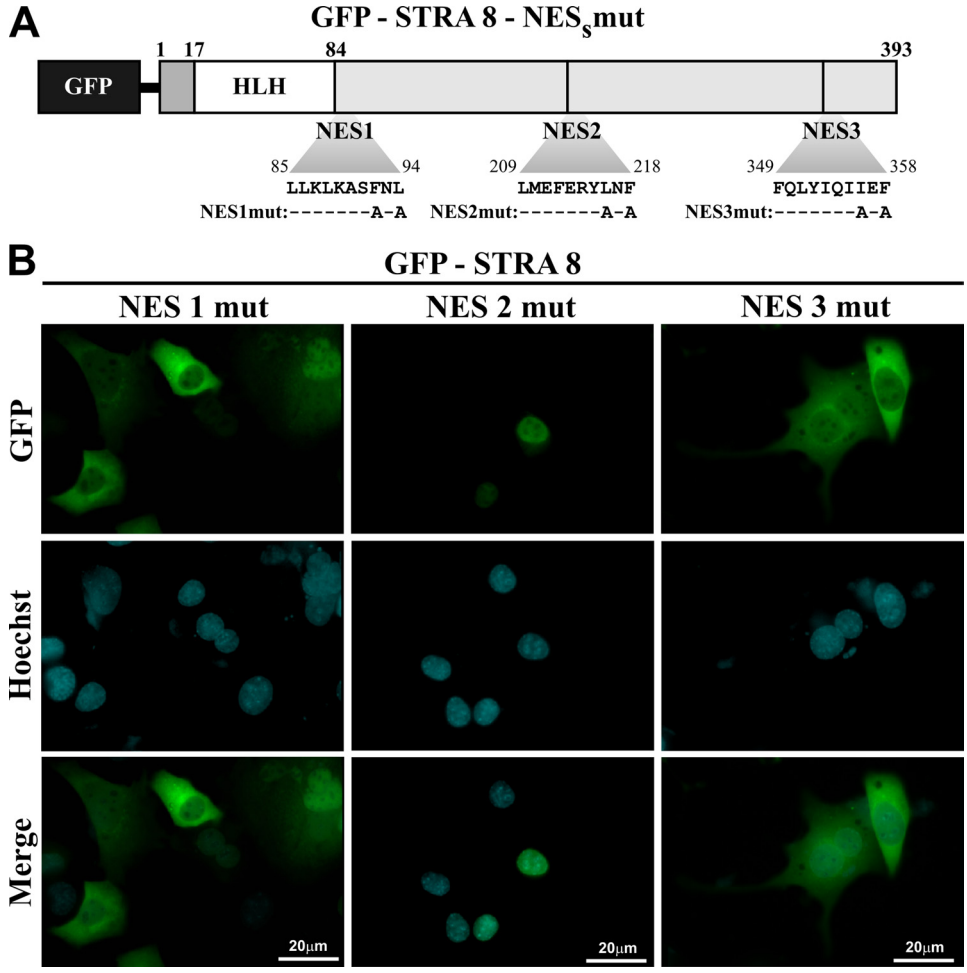

FIGURE 7. **Mutations in NES2 region impair STRA8 nuclear export.** *A*, schematic representation of the three different GFP-STRA8-NES mutants (*NES1*, *NES2*, and *NES3*) in which two of the hydrophobic amino acid were substituted with alanine. *B*, subcellular localization of GFP-STRA8-NES mutants. GFP-STRA8 localizations in GC-1 cells were transfected for 24 h with different plasmids (shown in *A*) as determined by fluorescence microscopy. Only mutagenesis in NES2 sequence induced a severe impairment of STRA8 nuclear export.

30 min of treatment and reached its maximum at 3 h. The kinetics of this LMB response is comparable with that observed for other nuclear shuttling proteins (37), supporting the possibility that STRA8 may be actively exported from the nucleus through an XPO1 pathway. LMB is a *Streptomyces* metabolite that inhibits export of leucine-rich NES-containing proteins preventing the association of XPO1 with such cargoes (36). Therefore, the strong effect of this drug on STRA8 localization suggests that this protein is exported from the nucleus through the XPO1/exportin recognition of an NES sequence. Examination of the mouse *Stra8* sequence for a classical Rev-type NES consensus sequence (38) using NES software revealed the presence of three similar motifs that we refer to as NES1, NES2, and NES3 (Fig. 6*B*, *upper panel*) that display significant similarities to previously identified NES (Fig. 6*B*, *lower panel*) and include hydrophobic residues conserved in different species, suggesting evolutionary significance (Fig. 6*C*).

These sequences are included in the α-helical region of STRA8 protein (supplemental Fig. S2), a common structural characteristic of other well known NES motifs (39). To address the contribution of these sequences to the nuclear export of STRA8, we generated a number of GFP-STRA8 proteins containing only one of the NES sequences as indicated in Fig. 6*D* (*left panel*). GC-1 cells were transfected with the expression plasmids and after 24 h were incubated with or without LMB (6 ng/ml) for 3 h. All these proteins were expressed at the expected size and at similar levels (data not shown). As shown in Fig. 6*D* (*right panel*), GFP-NES2 (aa 174–348) containing only the second NES sequence of STRA8 was distributed prevalently in the cytoplasm, and treatment with LMB caused a marked redistribution in the nucleus. The same result was obtained in HEK293 cells (data not shown). By contrast, GFP-NES1 and GFP-NES3 were uniformly distributed between the cytoplasm and nucleus in GC-1 cells, and they were not affected by LMB, indicating that these sequences do not contribute to STRA8 intracellular distribution. Thus, these experiments indicate that the region included between aa 174 and 348 containing the LMB-sensitive NES2 motif plays a major role in the STRA8 nuclear export. To obtain further support to this notion, various mutant constructs were prepared as GFP-fused forms in which the two conserved large hydrophobic amino acids in the C-terminal end of the motifs were replaced with alanine (Fig. 7*A*). These substitutions are predicted to affect NES function (40). Once again all the proteins were expressed at similar levels with the expected sizes (data not shown). Neither mutations in the NES1 (F92A_L94A) nor in the NES3 (I355A_F358A) sequences affected the cytoplasmic localization of GFP-STRA8, whereas the substitution of the two hydrophobic residues in the NES2 sequence (L216A_F218A) led to nuclear localization of the fusion protein in 95% of the transfected cells (Fig. 7*B*). Therefore, we conclude that the major contribution to the overall process of nuclear export of STRA8 is likely due to the NES2 motif.

The inability of the GFP-ΔHLH-STRA8 and GFP-STRA8-NLSmut containing the NES2 motif to localize within the nucleus of the transfected cells even in the presence of LMB (Fig. 6*D*, *right upper panel*, and data not shown) can be explained by the impossibility of entering into the nucleus and forming a complex with XPO1 rather than by the lack of nuclear retentive capacity. In fact, the GFP-NES2 protein that, because of its small dimension, is likely to enter the nucleus by diffusion is exported through an LMB-sensitive mechanism.

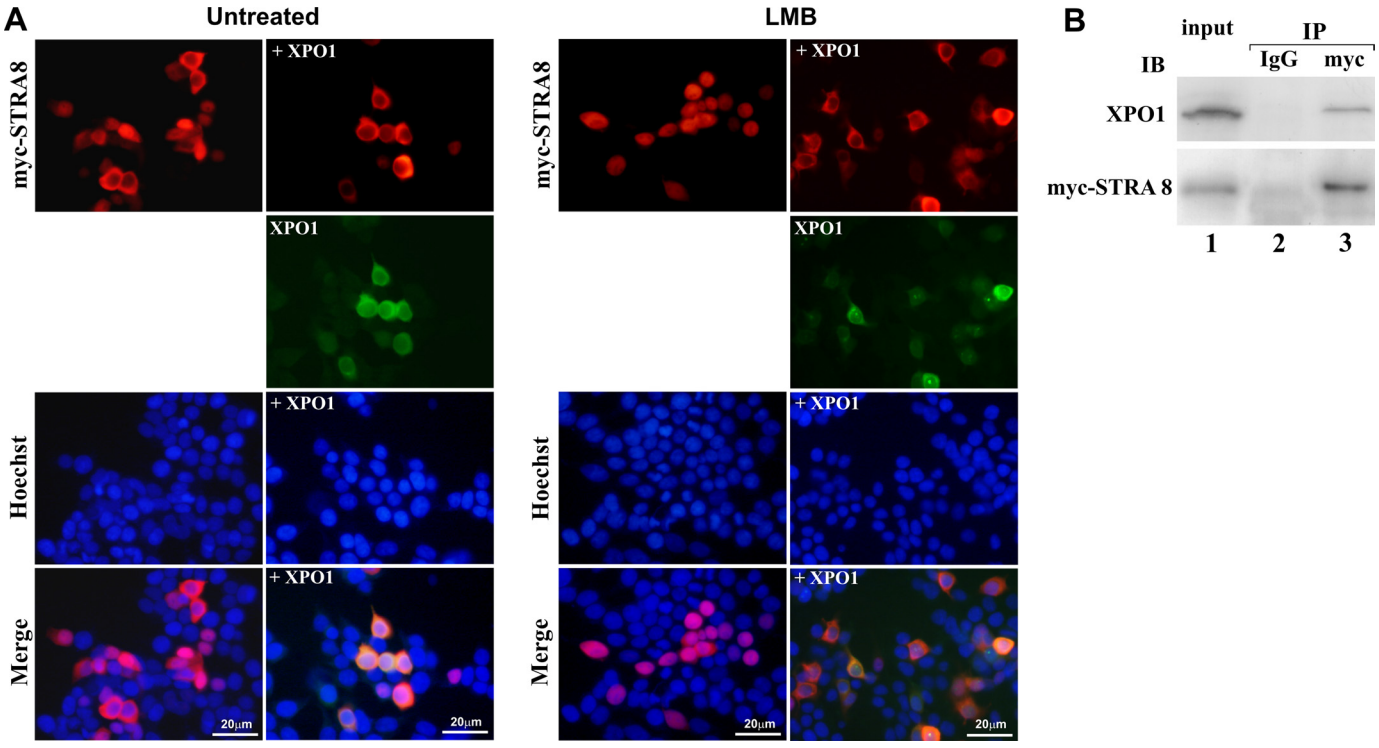

FIGURE 8. *A,* XPO1 overexpression causes STRA8 to accumulate in the cytoplasm. HEK293 cells expressing myc-STRA8 alone or co-transfected with YFP-XPO1 were treated with or without LMB for 3 h, and after 24 h, immunofluorescence analysis was performed with anti-Myc antibody as described under "Experimental Procedures." *Left panel,* in HEK293 cells, which overexpressed YFP-XPO1, myc-STRA8 is completely excluded from the nucleus. *Right panel,* when myc-STRA8 cells were co-expressed with YFP-XPO1, LMBs were not be able to induce its nuclear accumulation. *B,* STRA8 binds XPO1 *in vivo*. Protein from HEK293 cells expressing myc-STRA8 (*lane 1*) were immunoprecipitated (*IP*) with anti-Myc antibody (*lane 3*) or IgG (*lane 2*); STRA8 complexes were resolved, and immunoblots (*IB*) were probed for XPO1 and Myc.

STRA8 Interacts with XPO1 and Its Overexpression Increases STRA8 Nuclear Export—The effects of LMB on STRA8 nuclear export and the nuclear accumulation of STRA8-NES2mut suggest that XPO1 might have a major role in the cytoplasmic localization of this protein. This aspect was further analyzed by overexpressing yellow fluorescent protein-tagged XPO1 in HEK293 cells co-transfected with myc-STRA8. After 24 h of culture, we observed that when expressed alone, myc-STRA8 was distributed both in the cytoplasm and nucleus of HEK293 (Fig. 8*A*, *Untreated, left panel*) and GC-1 cells (data not shown). By contrast, co-expression of YFP-XPO1 caused the exclusive cytoplasmic localization of myc-STRA8 (Fig. 8*A*, *Untreated, right panel*). Moreover, the overexpression of XPO1 in HEK293 cells could also revert the inhibitory effect of LMB on the nuclear localization of myc-STRA8 (Fig. 8*A*, *LMB, right panel*). Finally, to demonstrate physical interaction of STRA8 with XPO1, Myc-tagged full-length STRA8 was transfected into HEK293 cells to determine whether it would co-immunoprecipitate with XPO1 from cell lysates. Recombinant STRA8 expression was verified by SDS-PAGE and Western blotting to the input lysates with an anti-Myc antibody (Fig. 8*B*). The remaining lysates were subjected to immunoprecipitation with the same antibody followed by Western blotting with the XPO1 antibody. As shown in Fig. 8*B*, XPO1 co-immunoprecipitated with myc-STRA8 suggesting that the two proteins can interact and indicating that XPO1 allows regulated export of STRA8 from nucleus to cytoplasm.

STRA8 Associates with DNA and Possesses High Transactivation Activity—To test whether STRA8 can interact with DNA, we performed a protein-DNA cross-link assay. ECF9 and ESD3 cells, expressing endogenous STRA8 in the nucleus following ATRA stimulation and HEK293 cells transfected with GFP-STRA8, were cultured for 24 h, and DNA-protein complexes were fixed by adding 1% formaldehyde in the last 10 min of culture. Total and DNA-bound protein fractions isolated from the cells, as described in detail under "Experimental Procedures," were then analyzed in Western blot for the presence of STRA8. As shown in Fig. 9*A*, both transiently expressed (*upper panel*) and endogenous STRA8 (*lower panel*) were recovered in the DNA-bound protein fractions and in the total protein fractions as well. When cells were not cross-linked, STRA8 was found exclusively in the total proteins fraction.

The nuclear localization of STRA8 and its possible association with DNA suggest that it may possess gene transcription activity. To verify such a possibility, STRA8 was fused to the yeast GAL4-DNA binding domain and transfected into HEK293 cells together with a GAL4 luciferase reporter plasmid containing five GAL4-DBD sites upstream of a TATA box (Fig. 9*B*, *upper panel*). As shown in Fig. 9*B*, WT STRA8 caused a highly significant concentration-dependent increase in GAL4 reporter gene transcription over the GAL4-DBD control. In contrast, STRA8 not fused to the GAL4-DBD had no effect on the luciferase transcription activation. This indicates that its binding to DNA is necessary for allowing transcription of the

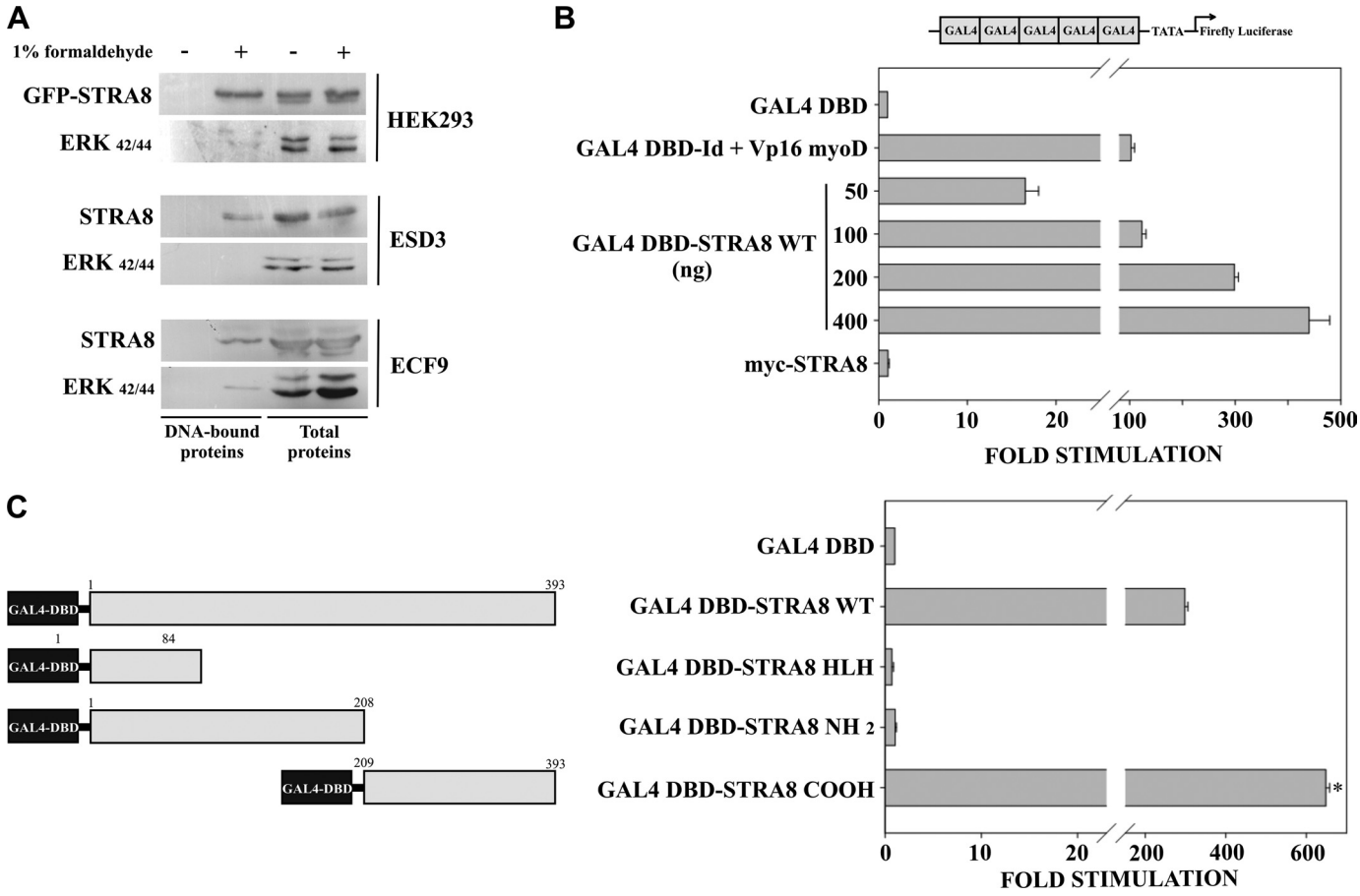

FIGURE 9. **STRA8 can associate with DNA and possess transcriptional activity.** *A*, HEK293 cells transfected with GFP-STRA8 and ESD3 and ECF9 cells treated for 24 h with 1 μM ATRA were either collected at the end of the incubation (−) or cross-linked with 1% formaldehyde for 10 min (+) before collection. After separation of total protein and DNA-bound protein fractions with TRIzol, aliquots (15% of total fraction) were analyzed by Western blot using either the anti-STRA8 or the anti-ERK$_{42/44}$ antibody. *B*, full-length STRA8 was fused to the GAL4-DBD (*GAL4-DBD-STRA8 WT*) and transfected in HEK293 cells at different concentrations. As positive control, cells were transfected with pBIND-Id (*Gal4-DBD-Id*) and pACT-myoD (*VP16-myoD*), which contains the VP16 activation domain. Transfection efficiency was normalized by *Renilla* luciferase, and the results were expressed as fold of stimulation with respect to the pBIND control vector (*GAL4-DBD*) (mean ± S.D. from three experiments). *C*, transactivation domain of STRA8 is located in the C-terminal region. *Left panel*, schematic representation of the different deletion mutants of STRA8 fused to GAL4-DBD. *Right panel*, HEK293 cells were transfected with the different constructs and the GAL4 reporter plasmid. The transcriptional activity was expressed as before. *, $p < 0.01$ *versus* GAL4-DBD-STRA8 WT.

reporter gene. To map the STRA8 domain responsible for the observed transcriptional activity, we fused different portions of STRA8 to the GAL4-DBD (Fig. 9*C*, *left panel*) and tested the ability of these chimeric proteins to activate the transcription of the GAL4-dependent reporter luciferase gene. We verified by Western blot analysis the expression of these fusion proteins (data not shown). As shown in Fig. 9*C* (*right panel*), the GAL4-C-terminal region of STRA8 potently stimulated the activity of the GAL4-dependent reporter gene, and its effect is 2-fold the full-length STRA8 fusion protein. On the contrary, both the HLH and N-terminal region of STRA8 did not affect transcriptional activity.

DISCUSSION

Despite its essential role in germ cell development, it is not known how STRA8 controls the crucial decision of such cells to engage meiotic division. Similarly unknown is the role of STRA8 in retinoic acid-induced differentiation of stem cell lines. In general, a key characteristic of proteins, which can begin to elucidate their possible function, is their subcellular localization. In this study, we show for the first time that around 13.5 dpc when germ cells meiosis is beginning in the ovary, a subpopulation (about 30%) of female PGCs express STRA8, whereas male PGCs are negative for the protein. In about 55% of the STRA8-positive germ cells, the protein is present both in the nuclear and cytoplasmic compartments (Fig. 1, *A* and *C*), and in the remaining it accumulates prevalently in the nucleus. We speculate that the distribution of STRA8 in such cells may depend on distinct cellular conditions (for example, PGCs that have already entered the meiotic division or not) and reflect a different rate of movement through the nuclear envelope or a different retention activity by the two cellular compartments. Besides the nuclear-cytoplasmic localization, a restricted localization of STRA8 in the cytoplasm was observed in a relevant portion (about 40%) of the spermatogonial population obtained from 7 day-old testes (Fig. 1, *A* and *C*). At this age, spermatogonial cells consist of type A1–A4, intermediate and type B spermatogonia, and a minority of spermatogonial stem cells, whereas germ cells in the meiotic prophase are virtually absent (41). Because of such heterogeneity and the lack of specific markers for each cell type, we were unable to associate this distinctive STRA8 localization to a particular type of spermatogonia. Because, however, the same pattern of STRA8 distribu-

tion is present in cells showing various morphologies, we favor the possibility that the different STRA8 localizations in such a spermatogonial population are related to different functional activities rather than to a specific cell type. The prevalent nuclear distribution of endogenous ATRA-induced STRA8 is evident in the stem cell lines examined such as ECF9 and ESD3 (Fig. 2) and could be associated with an early differentiation stimulus (endoderm and neuronal, respectively, for a review see Ref. 42) induced in such cells by retinoic acid.

The heterogeneous intracellular distribution of STRA8 in germ cells is indicative of its capacity to shuttle between the two compartments and probably of a different cell-dependent interaction with molecules that determine its final steady-state localization. Cell type-specific differences in terms of intracellular localization are common with a number of proteins, especially transcription factors, and in many cases are determined by a specific mechanism of regulation of cytoplasmic/nuclear shuttling. For example, specific phosphorylation is an efficient and potentially rapidly responsive mean of modulating NLS or NES accessibility (43).

To investigate the molecular mechanisms that determine the nuclear-cytoplasmic distribution of STRA8, we used epitope-tagged constructs of the protein and cell line transient transfection experiments. We demonstrated heterogeneous distribution of transfected GFP-STRA8 in the spermatogonia-like GC-1 cells and in other cell lines. Moreover, we identified NLS and NES sequences present in the STRA8 structure. The N-terminal region of STRA8 is predicted from sequence analysis to contain a well conserved HLH domain (Fig. 5*A* and supplemental Fig. S2). Our data reveal that this region is necessary and sufficient for the nuclear import of the protein. In fact, an NLS sequence is present in this domain that when mutated or deleted impairs the STRA8 movement into the nucleus. We do not know, however, if the HLH domain, normally important for protein-protein interaction, mediates the direct binding of importins to NLS or other protein(s) that could indirectly lead nuclear STRA8 localization. The transfection experiments also showed that STRA8 is able to interact with XPO1 and that it accumulates in the nucleus when the XPO1-dependent export pathway is blocked with LMB. Moreover, its nuclear exclusion increases when XPO1-tagged protein is co-expressed in the cell (Fig. 8), thus indicating that the cytoplasmic presence of STRA8 is an active process and not a default localization of a cytoplasm-synthesized protein. The central region of the protein (aa 209–218) is important for the presence of a functional leucine-rich NES homolog to classical XPO1-bounded Rev-NES (38, 40). When fused to GFP, this region is able to locate the recombinant protein in the cytoplasm (Fig. 6*D*). In addition, disruption of this NES sequence by alanine substitution of hydrophobic leucine and phenylalanine residues (GFP-STRA8-NES2mut) abolishes the cytoplasmic localization of STRA8 in 95% of the transfected cells and induces its nuclear accumulation (Fig. 7). The other two putative NES motifs (aa 85–94 and 349–358) that we identified in the STRA8 sequence were nonfunctional. In fact, they were not able to cause the relocation of the protein when fused to GFP, and their mutation does not change the STRA8 intracellular distribution.

The active import of STRA8 into the nucleus raises the little considered possibility that this protein may act as transcription factor or cooperate with transcription factors in regulating specific gene activities. We actually obtained evidence strongly supporting such a possibility. In the stem cell lines in which endogenous STRA8 is prevalently nuclear and in transiently transfected cells showing heterogeneous GFP-STRA8 localization, we found that STRA8 associates with DNA when the cells are exposed to formaldehyde. Because this treatment cross-links both protein-DNA and protein-protein, it is possible that STRA8 can interact with DNA in an indirect manner. Such a possibility is supported by the observation that STRA8 does not possess a canonical basic DNA binding region next to its HLH domain (NCBI GeneID 20899, aa 17–84; see also supplemental Fig. S2 and supplemental Fig. 3 in Ref. 12). However, the presence of the basic NLS sequence in the first helical region of the HLH domain could mediate the direct DNA binding of STRA8. Finally, in the one-hybrid transcription activation assay, STRA8 fused to a DNA binding domain showed a surprisingly high capability to activate DNA transcription, and the C-terminal region seemed to be important for this action. In conclusion, we stress that the novel shuttling ability of STRA8 reported here may be a relevant mechanism underlying the regulation of its biological functions. Moreover, its ability to transactivate a reporter gene strongly suggests the intriguing possibility that STRA8 may act as a transcription factor or transcriptional co-regulator. The functional consequences of the shuttling activity of STRA8 and its specific target gene(s) remain to be established. STRA8 is indispensable for meiotic entry in embryonal female and postnatal male germ cells. Different STRA8 localization integrating different signals from the cytoplasmic and nuclear compartments could be important to coordinate nuclear and/or cytoplasmic events in the shift between mitosis and meiosis. STRA8 function seems, however, not restricted to meiosis because it is expressed also in stem cell lines following stimulation with RA, a well known differentiating agent, and in testicular germ cell cancer.[3] There is no information on the function(s) of STRA8 in these cell types in which meiotic events do not represent the normal differentiation pathway. An interesting possibility is that in such cells STRA8 might be involved in differentiation and cell cycle processes requiring spatial and temporal localization of the protein different from them involving STRA8 during the premeiotic stage. In this regard, it is interesting to note that the *Stra8* promoter is expressed by neuronal cells (44) that represent a common RA-induced cell type in embryonic stem cells. Further studies are needed to clarify and dissect the molecular functions of STRA8 in premeiotic germ cells and in the RA-induced differentiating stem cells.

Acknowledgments—We are grateful to Dr. Rodriguez for the generous gift of YFP-XPO1; to Prof. C. Sette and Dr. A. Di Florio for fruitful discussions; to Dr. S. Di Siena and Dr. F. Barrios for the spermatogonial cell preparation; to Mr. G. Bonelli for the images preparation; and to Dr. I. Moscatelli for critical reading of the paper.

[3] D. Farini, unpublished observations.

REFERENCES

1. Speed, R. M. (1982) *Chromosoma* **85,** 427–437
2. Hilscher, B., Hilscher, W., Bülthoff-Ohnolz, B., Krämer, U., Birke, A., Pelzer, H., and Gauss, G. (1974) *Cell Tissue Res.* **154,** 443–470
3. Bowles, J., Knight, D., Smith, C., Wilhelm, D., Richman, J., Mamiya, S., Yashiro, K., Chawengsaksophak, K., Wilson, M. J., Rossant, J., Hamada, H., and Koopman, P. (2006) *Science.* **312,** 596–600
4. Koubova, J., Menke, D. B., Zhou, Q., Capel, B., Griswold, M. D., and Page, D. C. (2006) *Proc. Natl. Acad. Sci. U.S.A.* **103,** 2474–2479
5. Zhou, Q., Li, Y., Nie, R., Friel, P., Mitchell, D., Evanoff, R. M., Pouchnik, D., Banasik, B., McCarrey, J. R., Small, C., and Griswold, M. D. (2008) *Biol. Reprod.* **78,** 537–545
6. Zhou, Q., Nie, R., Li, Y., Friel, P., Mitchell, D., Hess, R. A., Small, C., and Griswold, M. D. (2008) *Biol. Reprod.* **79,** 35–42
7. Bouillet, P., Oulad-Abdelghani, M., Vicaire, S., Garnier, J. M., Schuhbaur, B., Dollé, P., and Chambon, P. (1995) *Dev. Biol.* **170,** 420–433
8. Oulad-Abdelghani, M., Bouillet, P., Décimo, D., Gansmuller, A., Heyberger, S., Dollé, P., Bronner, S., Lutz, Y., and Chambon, P. (1996) *J. Cell Biol.* **135,** 469–477
9. Menke, D. B., Koubova, J., and Page, D. C. (2003) *Dev. Biol.* **262,** 303–312
10. Deleted in proof
11. Anderson, E. L., Baltus, A. E., Roepers-Gajadien, H. L., Hassold, T. J., de Rooij, D. G., van Pelt, A. M., and Page, D. C. (2008) *Proc. Natl. Acad. Sci. U.S.A.* **105,** 14976–14980
12. Baltus, A. E., Menke, D. B., Hu, Y. C., Goodheart, M. L., Carpenter, A. E., de Rooij, D. G., and Page, D. C. (2006) *Nat. Genet.* **38,** 1430–1434
13. Mark, M., Jacobs, H., Oulad-Abdelghani, M., Dennefeld, C., Féret, B., Vernet, N., Codreanu, C. A., Chambon, P., and Ghyselinck, N. B. (2008) *J. Cell Sci.* **121,** 3233–3242
14. Cook, A., Bono, F., Jinek, M., and Conti, E. (2007) *Annu. Rev. Biochem.* **76,** 647–671
15. Askjaer, P., Jensen, T. H., Nilsson, J., Englmeier, L., and Kjems, J. (1998) *J. Biol. Chem.* **273,** 33414–33422
16. Hutten, S., and Kehlenbach, R. H. (2007) *Trends Cell Biol.* **17,** 193–201
17. Fornerod, M., Ohno, M., Yoshida, M., and Mattaj, I. W. (1997) *Cell* **90,** 1051–1060
18. Stade, K., Ford, C. S., Guthrie, C., and Weis, K. (1997) *Cell* **90,** 1041–1050
19. Fried, H., and Kutay, U. (2003) *Cell. Mol. Life Sci.* **60,** 1659–1688
20. Gama-Carvalho, M., and Carmo-Fonseca, M. (2001) *FEBS Lett.* **498,** 157–163
21. Yasuhara, N., Shibazaki, N., Tanaka, S., Nagai, M., Kamikawa, Y., Oe, S., Asally, M., Kamachi, Y., Kondoh, H., and Yoneda, Y. (2007) *Nat. Cell Biol.* **9,** 72–79
22. Hogarth, C. A., Jans, D. A., and Loveland, K. L. (2007) *Dev. Dyn.* **236,** 2311–2320
23. Yamaguchi, Y. L., Tanaka, S. S., Yasuda, K., Matsui, Y., and Tam, P. P. (2006) *Dev. Biol.* **297,** 350–360
24. Pesce, M., and De Felici, M. (1995) *Dev. Biol.* **170,** 722–725
25. Rossi, P., Dolci, S., Albanesi, C., Grimaldi, P., Ricca, R., and Geremia, R. (1993) *Dev. Biol.* **155,** 68–74
26. Horton, P., Keun-Joon, P., Takeshi, O., Naoya, F., Hajime, H., Adams-Collier, C. J., and Nakai, K. (2007) *Nuclear Acids Res.* **35,** W585–W587
27. Di Agostino, S., Fedele, M., Chieffi, P., Fusco, A., Rossi, P., Geremia, R., and Sette, C. (2004) *Mol. Biol. Cell.* **15,** 1224–1232
28. Hofmann, M. C., Narisawa, S., Hess R. A., and Millán, J. L. (1992) *Exp. Cell Res.* **201,** 417–435
29. Birbach, A., Bailey, S. T., Ghosh, S., and Schmid, J. A. (2004) *J. Cell Sci.* **117,** 3615–3624
30. Norton, J. D. (2000) *J. Cell Sci.* **113,** 3897–3905
31. Black, B. E., Holaska, J. M., Rastinejad, F., and Paschal, B. M. (2001) *Curr. Biol.* **11,** 1749–1758
32. Kurooka, H., and Yokota, Y. (2005) *J. Biol. Chem.* **280,** 4313–4320
33. Li, C., Wu, R. C., Amazit, L., Tsai, S. Y., Tsai, M. J., and O'Malley, B. W. (2007) *Mol. Cell. Biol.* **27,** 1296–1308
34. Kalderon, D., Roberts, B. L., Richardson, W. D., and Smith, A. E. (1984) *Cell.* **39,** 499–509
35. Robbins, J., Dilworth, S. M., Laskey, R. A., and Dingwall, C. (1991) *Cell.* **64,** 615–623
36. Kudo, N., Wolff, B., Sekimoto, T., Schreiner, E. P., Yoneda, Y., Yanagida, M., Horinouchi, S., and Yoshida, M. (1998) *Exp. Cell Res.* **242,** 540–547
37. Taagepera, S., McDonald, D., Loeb, J. E., Whitaker, L. L., McElroy, A. K., Wang, J. Y., and Hope, T. J. (1998) *Proc. Natl. Acad. Sci. U.S.A.* **95,** 7457–7462
38. Fischer, U., Meyer, S., Teufel, M., Heckel, C., Lührmann, R., and Rautmann, G. (1994) *EMBO J.* **13,** 4105–4112
39. la Cour T., Kiemer, L., Mølgaard, A., Gupta, R., Skriver, K., and Brunak, S. (2004) *Protein Eng. Des. Sel.* **17,** 527–536
40. Wen, W., Meinkoth, J. L., Tsien, R. Y., and Taylor, S. S. (1995) *Cell.* **82,** 463–473
41. Pellegrini, M., Grimaldi, P., Rossi, P., Geremia, R., and Dolci, S. (2003) *J. Cell Sci.* **116,** 3363–3372
42. Soprano, D. R., Teets, B. W., and Soprano, K. J. (2007) *Vitam. Horm.* **75,** 69–95
43. Jans, D. A., and Hübner, S. (1996) *Physiol. Rev.* **76,** 651–685
44. Giuili, G., Tomljenovic, A., Labrecque, N., Oulad-Abdelghani, M., Rassoulzadegan, M., and Cuzin, F. (2002) *EMBO Rep.* **3,** 753–759
45. Toyooka, Y., Tsunekawa, N., Takahashi, Y., Matsui, Y., Satoh, M., and Noce, T. (2000) *Mech. Dev.* **93,** 139–149

ACKNOWLEDGEMENTS

Ecco, sono arrivata alla parte più difficile della tesi: i ringraziamenti! Vorrei non scordare nessuno, ma se accadesse vi prego di perdonarmi (comincio ad avere una certa età anche io).

Ringrazio il mio Papi e la mia Mami perché continuano a credere in me. Anche se siete andati a vivere da soli lo so che non l'avete fatto per colpa mia. Vi amo, sarete sempre il mio faro. Fratè grazie anche a te, perché lo so che in fondo mi vuoi bene (anche se non ti strappo mai un abbraccio).

Grazie al mio amore, Marco, perché dopo tanto tempo ancora sopporta i miei cambiamenti d'umore e in questo periodo più che mai. Fiocchi che dire di te?solo questo… il papà…. Grazie per le lacrime di gioia. Telli a te farò un monumento, grazie di esserci sempre!Tu e Dani siete il pepe della mia vita …continuate così. Un pensiero va alla mia amica Nina… tesoro abbiamo fatto quasi tutte le cose in contemporanea ma con il matrimonio mi hai proprio spiazzato. Hai vinto!

Un doveroso grazie a Claudio perché ha avuto pazienza e perché molto di quello che ho imparato lo devo a lui. Grazie a tutti i professori di Anatomia in particolare al prof.Geremia.

Un abbraccio speciale ad Alessia e Enri, a Roby, al vulcano di Pamela, a Claudia che è appena arrivata ma già ha conquistato un posto nel mio cuore, a chi è andato e a chi è tornato. Grazie a tutte le ragazze del II piano Ed. E-Nord stanze 263/259/255.

Questa tesi la dedico a te nonna Valeria. Mi manchi, spero di fare bene e di non deluderti mai.